Acta Cryst C STRUCTURAL CHEMISTRY
ISSN 2053-2296

Synthesis, crystal structures, antiproliferative activities and reverse docking studies of eight novel Schiff bases derived from benzil

Xue-Jie Tan,[a,b]* Di Wang,[a] Xiao-Ming Hei,[a,b] Feng-Cun Yang,[a] Ya-Ling Zhu,[a] Dian-Xiang Xing[a,b] and Jian-Ping Ma[c]

[a]School of Chemistry and Pharmaceutical Engineering, Qilu University of Technology (Shandong Academy of Sciences), Jinan, Shandong Province 250353, People's Republic of China, [b]Key Laboratory of Pulp and Paper Science & Technology of Ministry of Education/Shandong Province, Qilu University of Technology (Shandong Academy of Sciences), Jinan, Shandong Province 250353, People's Republic of China, and [c]College of Chemistry, Chemical Engineering and Materials Science, Collaborative Innovation Centre of Functionalized Probes for Chemical Imaging, Key Laboratory of Molecular and Nano Probes, Ministry of Education, Shandong Normal University, Jinan 250014, People's Republic of China. *Correspondence e-mail: tanxuejie@163.com

Received 5 June 2019
Accepted 19 November 2019

Edited by F. A. Almeida Paz, University of Aveiro, Portugal

Keywords: antiproliferative activity; Schiff base; benzil; indole; reverse docking; crystal structure; quantum chemistry.

CCDC references: 1966764; 1966763; 1966762; 1966761; 1966760; 1966759; 1966758; 1018144

Supporting information: this article has supporting information at journals.iucr.org/c

Eight novel Schiff bases derived from benzil dihydrazone (**BDH**) or benzil monohydrazone (**BMH**) and four fused-ring carbonyl compounds (3-formylindole, **FI**; 3-acetylindole, **AI**; 3-formyl-1-methylindole, **MFI**; 1-formylnaphthalene, **FN**) were synthesized and characterized by elemental analysis, ESI–QTOF–MS, ^{1}H and ^{13}C NMR spectroscopy, as well as single-crystal X-ray diffraction. They are (1*Z*,2*Z*)-1,2-bis{(*E*)-[(1*H*-indol-3-yl)methylidene]hydrazinylidene}-1,2-diphenylethane (**BDHFI**), $C_{32}H_{24}N_6$, (1*Z*,2*Z*)-1,2-bis{(*E*)-[1-(1*H*-indol-3-yl)ethylidene]hydrazinylidene}-1,2-diphenylethane (**BDHAI**), $C_{34}H_{28}N_6$, (1*Z*,2*Z*)-1,2-bis{(*E*)-[(1-methyl-1*H*-indol-3-yl)methylidene]hydrazinylidene}-1,2-diphenylethane (**BMHMFI**) acetonitrile hemisolvate, $C_{34}H_{28}N_6\cdot 0.5CH_3CN$, (1*Z*,2*Z*)-1,2-bis{(*E*)-[(naphthalen-1-yl)methylidene]hydrazinylidene}-1,2-diphenylethane (**BDHFN**), $C_{36}H_{26}N_4$, (*Z*)-2-{(*E*)-[(1*H*-indol-3-yl)methylidene]hydrazinylidene}-1,2-diphenylethanone (**BMHFI**), $C_{23}H_{17}N_3O$, (*Z*)-2-{(*E*)-[1-(1*H*-indol-3-yl)ethylidene]hydrazinylidene}-1,2-diphenylethanone (**BMHAI**), $C_{24}H_{19}N_3O$, (*Z*)-2-{(*E*)-[(1-methyl-1*H*-indol-3-yl)methylidene]hydrazinylidene}-1,2-diphenylethanone (**BMHMFI**), $C_{24}H_{19}N_3O$, and (*Z*)-2-{(*E*)-[(naphthalen-1-yl)methylidene]hydrazinylidene}-1,2-diphenylethanone (**BMHFN**) $C_{25}H_{18}N_2O$. Moreover, the *in vitro* cytotoxicity of the eight title compounds was evaluated against two tumour cell lines (A549 human lung cancer and 4T$_1$ mouse breast cancer) and two normal cell lines (MRC-5 normal lung cells and NIH 3T3 fibroblasts) by MTT assay. The results indicate that four (**BDHMFI**, **BDHFN**, **BMHMFI** and **BMHFN**) are inactive and the other four (**BDHFI**, **BDHAI**, **BMHFI** and **BMHAI**) show severe toxicities against human A549 and mouse 4T$_1$ cells, similar to the standard cisplatin. All the compounds exhibited weaker cytotoxicity against normal cells than cancer cells. The Swiss Target Prediction web server was applied for the prediction of protein targets. After analyzing the differences in frequency hits between these active and inactive Schiff bases, 18 probable targets were selected for reverse docking with the Surflex-dock function in *SYBYL-X* 2.0 software. Three target proteins, *i.e.* human ether-á-go-go-related (hERG) potassium channel, the inhibitor of apoptosis protein 3 and serine/threonine-protein kinase PIM1, were chosen as the targets. Finally, the ligand-based structure–activity relationships were analyzed based on the putative protein target (hERG) docking results, which will be used to design and synthesize novel hERG ion channel inhibitors.

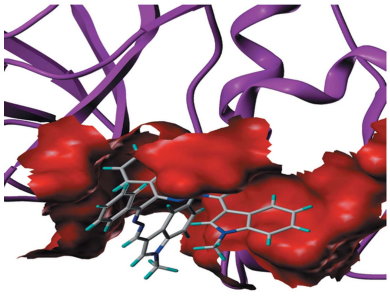

1. Introduction

Schiff bases are important compounds in chemistry and biochemistry due to their flexibility (Mayans *et al.*, 2018; Pramanik *et al.*, 2018), easy preparation (Erxleben, 2018;

Ganguly *et al.*, 2014), exceptional chelating ability (Malik *et al.*, 2018; Vardhan *et al.*, 2015) and to their broad spectrum of biological and pharmaceutical activities, such as antimicrobial (Anush *et al.*, 2018; Unver & Bektas, 2018; Bharathi *et al.*, 2018; Carreño *et al.*, 2018), anti-inflammatory (Venkatesan *et al.*, 2018; Farag *et al.*, 2017; Bano *et al.*, 2017; Khayyat *et al.*, 2015) and anticancer properties (Unver & Bektas, 2018; Santhosh Kumar *et al.*, 2018; Kalaiarasi *et al.*, 2018; Ariyaeifar *et al.*, 2018). Thus, the chemistry of Schiff bases has always been a promising field of research.

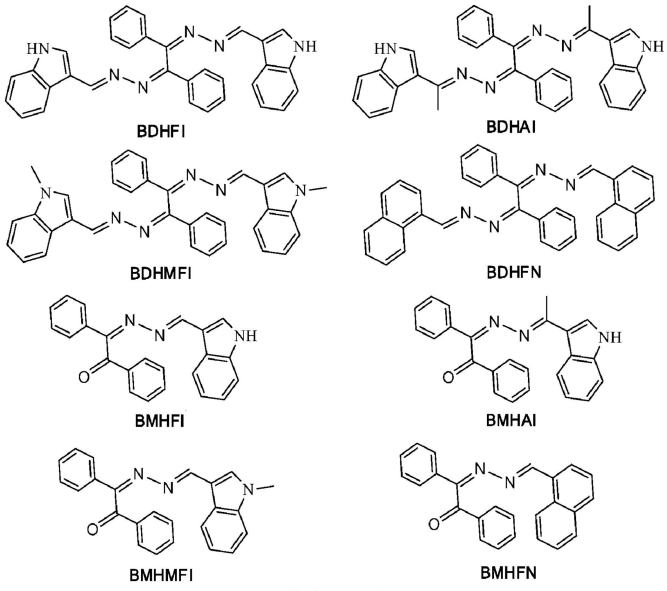

Scheme 1

As an organic helical molecule with a long history (De *et al.*, 2006; Fisher & Stoufer, 1966), benzil dihydrazone (**BDH**) is often used to construct polydentate diazine Schiff bases (Tan *et al.*, 2015), helical coordination complexes (Bai *et al.*, 2012; Drew *et al.*, 2007; Mukherjee *et al.*, 2013) and, more importantly, a leading scaffold for the further design and synthesis of potential anticancer agents (Ke *et al.*, 2013). Here we aimed to use the **BDH** scaffold to construct some novel Schiff bases, especially those containing indole rings. Another set of novel Schiff bases based on benzil monohydrazone (**BMH**) were also constructed for comparison.

As a privileged structure scaffold (de Sá Alves *et al.*, 2009; Evans *et al.*, 1988), indole derivatives play an important role in medicinal chemistry since they frequently exhibit broad and remarkable biological activities. Substituted indole rings have revealed antibacterial (El-Sawy *et al.*, 2010; George *et al.*, 2008), antitumour (Pedada *et al.*, 2016; Fortes *et al.*, 2016; El-Sawy *et al.*, 2012, 2013; Wu *et al.*, 2009; Pojarová *et al.*, 2007; Kamath *et al.*, 2016), antifungal (Bai *et al.*, 2018; Wang *et al.*, 2018; Mishra *et al.*, 2018; Yu *et al.*, 2018), antiviral (Cihan-Üstündağ *et al.*, 2016; Brigg *et al.*, 2016; Zhao *et al.*, 2006; Sellitto *et al.*, 2010; Pu *et al.*, 2017; Atienza *et al.*, 2018), anti-inflammatory (Mandour *et al.*, 2010; Lamie *et al.*, 2016), antioxidant (Estevão *et al.*, 2010; Suzen & Buyukbingol, 2000; Mor *et al.*, 2004), antituberculosis (Naidu *et al.*, 2016; Zhao, 2018; Hong *et al.*, 2017; Akula *et al.*, 2016), analgesic (Fantinati *et al.*, 2017; Bertamino *et al.*, 2018; Ali Khan *et al.*, 2018), anti-convulsant (Saini *et al.*, 2016; Ndagijimana *et al.*, 2013; Ma *et al.*, 2016; Ensch *et al.*, 2018) and many other therapeutic and pharmacological properties. Numerous pharmaceutical molecules with the indole group have been marketed. These include indomethacin, zafirlukast, sumatriptan, indole-3-acetic acid (IAA), serotonin, delavirdine, atevirdine *etc.* There are also large numbers of indole-containing drugs currently going through different clinical phases (Naim *et al.*, 2016). Moreover, the indole nucleus is commonly found in several natural products and displays an indispensable role in therapeutic chemistry (Tzvetkov *et al.*, 2014; Gurer-Orhan *et al.*, 2016; Kumar *et al.*, 2016; Johansson *et al.*, 2013; Blunt *et al.*, 2011; Gul & Hamann, 2005; Sugiyama *et al.*, 2009; Bao *et al.*, 2007; Shaaban *et al.*, 2002; Shaaban & Abdel-Aziz, 2007; Ali Khan *et al.*, 2018; Ndagijimana *et al.*, 2013). Although indole derivatives have been the target of synthetic exploration for many years, more anticancer compounds incorporating the indole scaffold with improved anticancer properties are desired for the systematic study of structure–activity relationships (Hassam *et al.*, 2012; Dai *et al.*, 2016; Singh *et al.*, 2018).

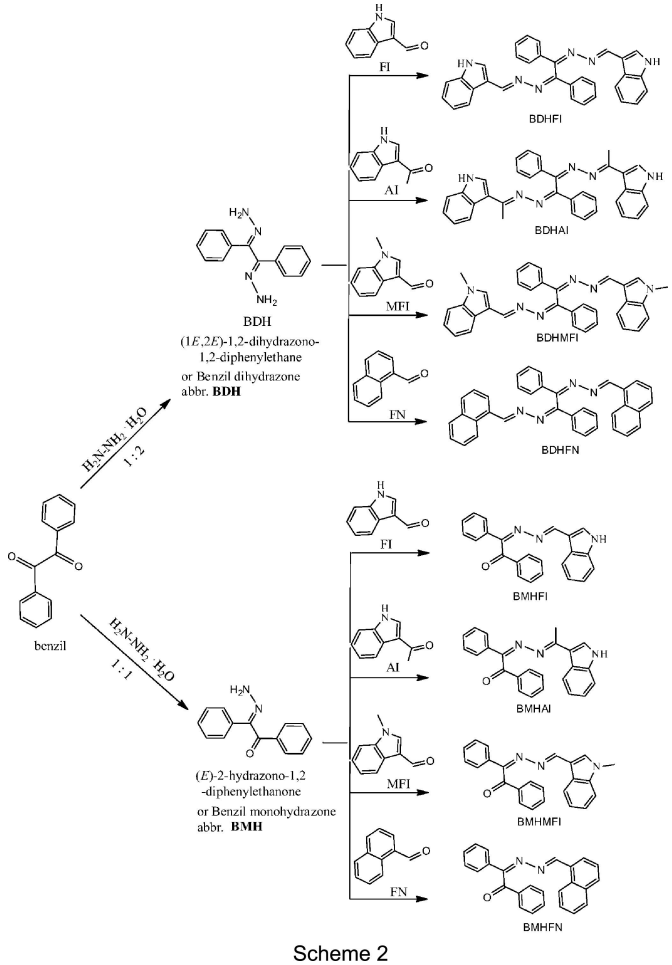

Scheme 2

In order to gain a deeper insight into the antitumour activity of various functionalized indoles, we have been conducting a systematic study on indole derivatives with different scaffolds, for example, novel Schiff bases derived from indole and biphenyl show lung A549 and breast $4T_1$ cancer cell inhibitory activities (IC_{50} = 20.5 and 18.5 μ*M*, respectively) (Bu *et al.*,

2017; Tan *et al.*, 2019). We report here the synthesis, crystal structure and antiproliferative activities of six Schiff bases derived from indole and **BDH**/**BMH**, as well as two comparative compounds derived from naphthalene and **BDH**/**BMH** (see Scheme 1).

2. Experimental

2.1. Materials and measurements

The starting material benzil and related chemicals were purchased from Aladdin Reagent Chemicals and were used without further purification. Elemental (C, H and N) analyses were carried out with a PerkinElmer 2400 microanalyzer. Accurate mass measurements were acquired on an Agilent-6520 quadrupole time-of-flight tandem mass spectrometer. Melting points were determined on a WRS-2A electrothermal digital melting point apparatus (Shanghai Precision & Scientific Instrument Co. Ltd, China). ^{1}H and ^{13}C NMR spectra were recorded on a Bruker Avance 400 MHz instrument. The chemical shifts are reported in parts per million (ppm) relative to tetramethylsilane ($SiMe_4$, δ = 0 ppm), referenced to the chemical shifts of the residual solvent peak [deuterated dimethyl sulfoxide (DMSO-d_6)].

2.2. Synthesis and crystallization

As indicated in Scheme 2, a two-step process was used to synthesize all eight title compounds. In the first step, a mixture of benzil (0.42 g or 2 mmol) and hydrazine hydrate (80%, 0.20 ml or 4 mmol) was added to dry ethanol (20 ml) and the resulting solution refluxed for 3 h. Most of the ethanol was removed by distillation and the resulting solution was cooled to room temperature. Crude benzil dihydrazone (abbreviated as **BDH**) was filtered off, recrystallized from ethanol and dried in a vacuum. Pure **BDH** was obtained as colourless needle-shaped crystals {yield 85%, 0.41 g; m.p. 151.4–152.0 °C [literature m.p. 151–152 (Bach *et al.*, 1982), 150–151.5 (Kim & Yoon, 2004), 149 (Salavati-Niasari & Hassani-Kabutarkhani, 2005), 152 (Chandra *et al.*, 2007), 172 (Singh *et al.*, 2008) and 172 °C (Chauhan *et al.*, 2008)]}. Elemental analysis found (calculated) for $C_{14}H_{14}N_4$ (%): C 70.64 (70.57), H 5.97 (5.92), N 23.63 (23.51). On the other hand, if the molar ratio of benzil and hydrazine hydrate was set at 1:1, benzil monohydrazone (**BMH**) will be obtained in a similar yield. Pure **BMH** was obtained as a colourless crystal (m.p. 138.4–139.2 °C).

In the second step, all eight Schiff bases were readily prepared by a similar method (see Scheme 2). **BDH**/**BMH** and the required carbonyl compounds (**FI**, **AI**, **MFI** and **FN**) were stirred under reflux for 5 h in dry ethanol in a 1:2 (**BDH** *versus* carbonyl compounds) or 1:1 (**BMH** *versus* carbonyl compounds) molar ratio. After the reaction, the solvent was reduced in volume by slow evaporation and crystalline products were usually obtained. Recrystallization can purify the products. Their physical and spectroscopic properties are listed in the following sections. All NMR spectra are available in Figs. S1–S16 of the supporting information.

2.2.1. BDHFI. M.p. 274.0–275.0 °C. Elemental analysis found (calculated) for $C_{32}H_{24}N_6$ (%): C 78.15 (78.03), H 4.98 (4.91), N 17.12 (17.06). HRMS (ESI): *m*/*z* calculated for $C_{32}H_{24}N_6 + H^+$: 493.2141 [$M + H^+$]; found: 493.2142. ^{1}H NMR (DMSO-d_6): 11.637 (*s*, 2H, –NH), 8.757 (*s*, 2H, –N═CH), 7.878–7.825 (*m*, 6H, *J* = 7.2 Hz, Ar-H), 7.587 (*d*, 2H, *J* = 8.0 Hz, Ar-H), 7.450 (*d*, 6H, *J* = 8.0 Hz, Ar-H), 7.330 (*d*, 2H, *J* = 8.0 Hz, Ar-H), 7.076 (*t*, 2H, *J* = 8.0 Hz, Ar-H), 6.851 (*t*, 2H, *J* = 7.2 Hz, Ar-H). ^{13}C NMR (DMSO-d_6): 163.575 (CH═N), 156.485 (CH═N), 136.992 (Ar-C), 135.007 (Ar-C), 132.951 (Ar-C), 130.035 (Ar-C), 128.589 (Ar-C), 126.989 (Ar-C), 124.433 (Ar-C), 122.596 (Ar-C), 122.267 (Ar-C), 120.478 (Ar-C), 112.165 (Ar-C), 111.629 (Ar-C).

2.2.2. BDHAI. M.p. 270.2–271.7 °C. Elemental analysis found (calculated) for $C_{34}H_{28}N_6$ (%): C 78.49 (78.44), H 5.47 (5.42), N 16.21 (16.14). HRMS (ESI): *m*/*z* calculated for $C_{34}H_{28}N_6 + H^+$: 521.2454 [$M + H^+$]; found: 521.2456. ^{1}H NMR (DMSO-d_6): 11.473 (*s*, 2H, –NH), 7.877–7.754 (*m*, 8H, *J* = 6.8 Hz, Ar-H), 7.452–7.271 (*m*, 8H, *J* = 6.8 Hz, Ar-H), 7.020 (*s*, 2H, Ar-H), 6.713 (*s*, 2H, Ar-H), 2.418 (*s*, 6H –CH_3). ^{13}C NMR (DMSO-d_6): 161.007 (CH═N), 136.915 (CH═N), 135.117 (Ar-C), 129.884 (Ar-C), 129.587 (Ar-C), 128.598 (Ar-C), 128.292 (Ar-C), 127.405 (Ar-C), 126.942 (Ar-C), 124.815 (Ar-C), 124.730 (Ar-C), 123.487 (Ar-C), 122.003 (Ar-C), 119.916 (Ar-C), 115.206 (Ar-C), 111.184 (Ar-C), 14.792 (–CH_3).

2.2.3. BDHMFI. M.p. 214.6–215.3 °C. Elemental analysis found (calculated) for $C_{34}H_{28}N_6$ (%): C 78.51 (78.44), H 5.46 (5.42), N 16.19 (16.14). HRMS (ESI): *m*/*z* calculated for $C_{34}H_{28}N_6 + H^+$: 521.2454 [$M + H^+$]; found: 521.2454. ^{1}H NMR (DMSO-d_6): 8.731 (*s*, 2H, –N═CH), 7.874 (*d*, 4H, *J* = 7.2 Hz, Ar-H), 7.789 (*s*, 2H, Ar-H), 7.602 (*d*, 2H, *J* = 7.2 Hz, Ar-H), 7.474–7.373 (*m*, 8H, Ar-H), 7.151 (*t*, 2H, *J* = 7.2 Hz, Ar-H), 6.908 (*t*, 2H, *J* = 7.2 Hz, Ar-H), 3.733 (*s*, 6H –N—CH_3). ^{13}C NMR (DMSO-d_6): 163.813 (CH═N), 155.643 (CH═N), 137.807 (Ar-C), 137.575 (Ar-C), 136.220 (Ar-C), 136.059 (Ar-C), 129.753 (Ar-C), 128.178 (Ar-C), 127.936 (Ar-C), 127.608 (Ar-C), 124.885 (Ar-C), 122.636 (Ar-C), 122.121 (Ar-C), 120.644 (Ar-C), 111.325 (Ar-C), 110.007 (Ar-C), 32.770 (–N—CH_3).

2.2.4. BDHFN. M.p. 203.0–205.0 °C. Elemental analysis found (calculated) for $C_{36}H_{26}N_4$ (%): C 84.08 (84.02), H 5.13 (5.09), N 10.94 (10.89). HRMS (ESI): *m*/*z* calculated for $C_{36}H_{26}N_4 + H^+$: 515.2236 [$M + H^+$]; found: 515.2236. ^{1}H NMR (DMSO-d_6): 8.770 (*s*, 2H, –N═CH), 8.277 (*t*, 4H, *J* = 7.6 Hz, Ar-H), 7.883–7.766 (*m*, 6H, Ar-H), 7.585 (*d*, 2H, *J* = 8.0 Hz, Ar-H), 7.482–7.326 (*m*, 8H, Ar-H), 7.082 (*t*, 2H, *J* = 7.6 Hz, Ar-H), 6.857 (*t*, 2H, *J* = 7.6 Hz, Ar-H). ^{13}C NMR (DMSO-d_6): 163.655 (CH═N), 156.624 (CH═N), 139.670 (Ar-C), 137.877 (Ar-C), 136.970 (Ar-C), 134.977 (Ar-C), 133.068 (Ar-C), 130.076 (Ar-C), 128.623 (Ar-C), 126.980 (Ar-C), 124.391 (Ar-C), 122.620 (Ar-C), 122.270 (Ar-C), 120.504 (Ar-C), 112.123 (Ar-C), 111.655 (Ar-C).

2.2.5. BMHFI. M.p. 197–197.5 °C. Elemental analysis found (calculated) for $C_{23}H_{17}N_3O$ (%): C 77.59 (78.61), H 5.13 (4.88), N 12.22 (11.96). HRMS (ESI): *m*/*z* calculated for $C_{23}H_{17}N_3O + H^+$: 352.1450 [$M + H^+$]; found: 352.1450. ^{1}H

Table 1
Experimental details.

Experiments were carried out with Mo $K\alpha$ radiation using a Bruker SMART CCD area detector. Absorption was corrected by multi-scan methods (*SADABS*; Bruker, 2000). Only H atoms were constrained to ride on their bonding partners, but with freely refined U_{iso} values.

	BDHFI	**BDHAI**	**BDHMFI**	**BDHFN**
Crystal data				
Chemical formula	$C_{32}H_{24}N_6$	$C_{34}H_{28}N_6$	$2C_{34}H_{28}N_6{\cdot}C_2H_3N$	$C_{36}H_{26}N_4$
M_r	492.57	520.62	1082.30	514.61
Crystal system, space group	Monoclinic, $P2_1/c$	Triclinic, $P\overline{1}$	Triclinic, $P\overline{1}$	Monoclinic, $C2/c$
Temperature (K)	293	293	293	298
a, b, c (Å)	13.023 (4), 7.340 (2), 27.762 (9)	10.2585 (4), 11.9610 (5), 12.8232 (6)	11.2710 (6), 11.6944 (7), 12.5164 (6)	26.195 (8), 9.809 (3), 11.806 (4)
α, β, γ (°)	90, 97.693 (5), 90	64.941 (4), 79.573 (3), 76.829 (4)	79.875 (4), 87.701 (4), 64.941 (6)	90, 115.230 (5), 90
V (Å^3)	2630.0 (14)	1381.45 (11)	1470.10 (15)	2744.2 (15)
Z	4	2	1	4
μ (mm^{-1})	0.08	0.08	0.08	0.07
Crystal size (mm)	0.30 × 0.18 × 0.15	0.35 × 0.15 × 0.12	0.35 × 0.20 × 0.15	0.30 × 0.16 × 0.10
Data collection				
T_{min}, T_{max}	0.903, 0.939	0.903, 0.939	0.905, 0.943	0.986, 0.993
No. of measured, independent and observed [$I > 2\sigma(I)$] reflections	13632, 5145, 2852	15195, 5328, 4490	13418, 5640, 4445	6631, 2413, 1197
R_{int}	0.046	0.026	0.029	0.058
(sin $\theta/\lambda)_{max}$ (Å^{-1})	0.617	0.618	0.617	0.595
Refinement				
$R[F^2 > 2\sigma(F^2)]$, $wR(F^2)$, S	0.049, 0.103, 0.88	0.044, 0.129, 1.05	0.049, 0.151, 1.04	0.062, 0.130, 0.95
No. of reflections	5145	5328	5640	2413
No. of parameters	367	392	424	194
No. of restraints	0	0	2	0
$\Delta\rho_{max}$, $\Delta\rho_{min}$ (e Å^{-3})	0.15, −0.22	0.19, −0.19	0.22, −0.17	0.11, −0.10

	BMHFI	**BMHAI**	**BMHMFI**	**BMHFN**
Crystal data				
Chemical formula	$C_{23}H_{17}N_3O$	$C_{24}H_{19}N_3O$	$C_{24}H_{19}N_3O$	$C_{25}H_{18}N_2O$
M_r	351.39	365.42	365.42	362.41
Crystal system, space group	Orthorhombic, $P2_12_12_1$	Tetragonal, $P4_32_12$	Monoclinic, $P2_1/c$	Monoclinic, $P2_1/c$
Temperature (K)	293	293	293	293
a, b, c (Å)	6.8767 (1), 8.3698 (2), 32.6317 (6)	8.3580 (1), 8.3580 (1), 54.6705 (7)	18.6779 (6), 8.6694 (3), 12.7956 (4)	17.2081 (13), 9.4075 (8), 11.9703 (9)
α, β, γ (°)	90, 90, 90	90, 90, 90	90, 106.910 (4), 90	90, 94.814 (7), 90
V (Å^3)	1878.17 (6)	3819.07 (10)	1982.36 (12)	1931.0 (3)
Z	4	8	4	4
μ (mm^{-1})	0.08	0.08	0.08	0.08
Crystal size (mm)	0.35 × 0.1 × 0.09	0.3 × 0.1 × 0.1	0.33 × 0.28 × 0.25	0.40 × 0.40 × 0.16
Data collection				
T_{min}, T_{max}	0.903, 0.939	0.983, 0.998	0.971, 0.987	0.970, 0.989
No. of measured, independent and observed [$I > 2\sigma(I)$] reflections	10418, 3641, 3444	21746, 3759, 3565	9410, 3837, 2964	10556, 3396, 1411
R_{int}	0.023	0.030	0.021	0.078
(sin $\theta/\lambda)_{max}$ (Å^{-1})	0.618	0.618	0.618	0.595
Refinement				
$R[F^2 > 2\sigma(F^2)]$, $wR(F^2)$, S	0.035, 0.096, 1.02	0.041, 0.113, 1.06	0.045, 0.140, 1.03	0.052, 0.083, 0.87
No. of reflections	3641	3759	3837	3396
No. of parameters	262	274	274	272
No. of restraints	0	0	0	0
$\Delta\rho_{max}$, $\Delta\rho_{min}$ (e Å^{-3})	0.15, −0.13	0.16, −0.12	0.16, −0.15	0.15, −0.15
Absolute structure	Not determined because of low anomalous signal	Not determined because of low anomalous signal	–	–
Absolute structure parameter	−1.4 (6)	−1.5 (6)	–	–

Computer programs: *SMART* (Bruker, 2000), *SAINT* (Bruker, 2000), *SHELXS2016* (Sheldrick, 2015*a*), *SHELXTL* (Bruker, 2000), *PLATON* (Spek, 2009), *DIAMOND* (Brandenburg & Putz, 1999), *SHELXL2016* (Sheldrick, 2015*b*) and *WinGX* (Farrugia, 2012).

NMR (DMSO-d_6): 11.800 (*s*, 1H, –NH), 8.800 (*s*, 1H, –N═CH), 7.961–7.928 (*m*, 3H, *J* = 7.2 Hz, Ar-H), 7.767–7.218 (*m*, 10H, Ar-H), 7.087 (*t*, 1H, *J* = 7.6 Hz, Ar-H), 6.789 (*t*, 1H, *J* = 7.6 Hz, Ar-H). ^{13}C NMR (DMSO-d_6): 197.921(C═O), 163.669 (CH═N), 158.076 (CH═N), 137.065 (Ar-C), 135.223 (Ar-C), 134.228 (Ar-C), 134.056 (Ar-C), 132.698 (Ar-C), 131.033 (Ar-C), 130.507 (Ar-C), 129.266 (Ar-C), 129.180 (Ar-C), 128.936 (Ar-C), 128.554 (Ar-C), 128.369 (Ar-C), 127.445 (Ar-C), 126.900 (Ar-C), 124.230 (Ar-C), 122.793 (Ar-C), 121.724 (Ar-C), 120.659 (Ar-C), 111.860 (Ar-C), 111.605 (Ar-C).

2.2.6. BMHAI. M.p. 223.1–224.4 °C. Elemental analysis found (calculated) for $C_{24}H_{19}N_3O$ (%): C 79.24 (78.88), H 6.11 (5.24), N 12.03 (11.50). HRMS (ESI): *m*/*z* calculated for $C_{24}H_{19}N_3O$ + H^+: 366.1606 [*M* + H^+]; found: 366.1606. ^{1}H NMR (DMSO-d_6): 11.644 (*s*, 1H, –NH), 8.028–7.503 (*m*, 11H, *J* = 6.8 Hz, Ar-H), 7.318–7.266 (*q*, 2H, *J* = 8.4 Hz, Ar-H), 7.034–6.998 (*t*, 1H, *J* = 7.2 Hz, Ar-H), 6.649–6.612 (*t*, 1H, *J* = 7.2 Hz, Ar-H), 2.584 (*s*, 3H –CH_3). ^{13}C NMR (DMSO-d_6): 198.911 (C═O), 163.948 (CH═N), 161.192 (CH═N), 136.957 (Ar-C), 134.953 (Ar-C), 134.166 (Ar-C), 133.209 (Ar-C), 131.003 (Ar-C), 130.813 (Ar-C), 129.467 (Ar-C), 129.226 (Ar-C), 129.056 (Ar-C), 128.868 (Ar-C), 126.831 (Ar-C), 124.468 (Ar-C), 122.699 (Ar-C), 122.632 (Ar-C), 122.147 (Ar-C), 121.559 (Ar-C), 121.275 (Ar-C), 120.132 (Ar-C), 114.671 (Ar-C), 111.414 (Ar-C), 14.688 (–CH_3).

2.2.7. BMHMFI. M.p. 220.1–221.3 °C. Elemental analysis found (calculated) for $C_{24}H_{19}N_3O$ (%): C 79.25 (78.88), H 5.65 (5.24), N 11.89 (11.50). HRMS (ESI): *m*/*z* calculated for $C_{24}H_{19}N_3O$ + H^+: 366.1606 [*M* + H^+]; found: 366.1606. ^{1}H NMR (DMSO-d_6): 8.764 (*s*, 1H, –N═CH), 7.927 (*d*, 3H, *J* = 8.4 Hz, Ar-H), 7.749 (*d*, 2H, *J* = 7.6 Hz, Ar-H), 7.665–7.421 (*m*, 8H, Ar-H), 7.239–7.138 (*m*, 1H, Ar-H), 6.834 (*t*, 1H, *J* = 7.2 Hz, Ar-H), 3.799 (*s*, 3H –N—CH_3). ^{13}C NMR (DMSO-d_6): 197.918 (C═O), 163.667 (CH═N), 157.569 (CH═N), 137.675 (Ar-C), 137.549 (Ar-C), 135.209 (Ar-C), 134.066 (Ar-C), 132.680 (Ar-C), 131.044 (Ar-C), 130.126 (Ar-C), 129.975 (Ar-C), 129.298 (Ar-C), 129.261 (Ar-C), 129.179 (Ar-C), 129.055 (Ar-C), 128.564 (Ar-C), 126.840 (Ar-C), 124.658 (Ar-C), 122.873 (Ar-C), 121.838 (Ar-C), 120.960 (Ar-C), 110.576 (Ar-C), 110.261 (Ar-C), 32.950 (–N—CH_3).

2.2.8. BMHFN. M.p. 135.2–136.7 °C. Elemental analysis found (calculated) for $C_{25}H_{18}N_2O$ (%): C 82.18 (82.85), H 5.11 (5.01), N 7.84 (7.73). HRMS (ESI): *m*/*z* calculated for $C_{25}H_{18}N_2O$ + H^+: 363.1497 [*M* + H^+]; found: 363.1497. ^{1}H NMR (DMSO-d_6): 8.770 (*s*, 1H, –N═CH), 8.275 (*t*, 1H, *J* = 7.6 Hz, Ar-H), 8.167 (*t*, 3H, *J* = 7.6 Hz, Ar-H), 7.852 (*q*, 4H, *J* = 7.6 Hz, Ar-H), 7.589–7.320 (*m*, 6H, Ar-H), 7.080 (*t*, 2H, *J* = 7.2 Hz, Ar-H), 6.850 (*t*, 1H, *J* =7.6 Hz, Ar-H). ^{13}C NMR (DMSO-d_6): 196.873 (C═O), 162.531 (CH═N), 156.980 (CH═N), 139.701 (Ar-C), 137.101 (Ar-C), 136.981 (Ar-C), 135.238 (Ar-C), 134.231 (Ar-C), 134.107 (Ar-C), 132.702 (Ar-C), 131.051 (Ar-C), 130.515 (Ar-C), 129.277 (Ar-C), 129.176 (Ar-C), 128.907 (Ar-C), 128.499 (Ar-C), 128.402 (Ar-C), 127.391 (Ar-C), 126.879 (Ar-C), 124.121 (Ar-C), 122.741 (Ar-C), 121.698 (Ar-C), 120.571 (Ar-C), 111.761 (Ar-C), 109.432 (Ar-C).

2.3. Refinement

Crystal data, data collection and structure refinement details are summarized in Table 1. All H atoms in the eight compounds (except for the H atoms on C35 in **BDHMFI**) were found in difference Fourier maps and then allowed to ride on their parent atoms. The location and isotropic displacement parameters of the H atoms on C35 in **BDHMFI** were refined freely.

2.4. Cytotoxicity assays

Human lung carcinoma A549 cells, mouse breast cancer 4T_1 cells, human MRC-5 lung normal cells and normal mouse NIH 3T3 fibroblasts were purchased from the Shanghai Cell Bank, Type Culture Collection Committee, Chinese Academy of Sciences. The cells were cultured in F12K medium supplemented with 10% heat-inactivated fetal bovine serum (FBS), 2 m*M* glutamine, 100 U ml^{-1} penicillin and 100 µg ml^{-1} streptomycin, and maintained at 310 K in a humidified atmosphere of 5% CO_2.

The cells (8000 cells) were seeded on 96-well microtiter plates in F12K medium with 10% FBS and incubated overnight. The cell culture medium was replaced by different doses of the compound solution, *i.e.* 1, 5, 10, 30, 50, 100 and 150 µ*M*, and then the cells were cultured for another 72 h. The MTT reagent was added to the cell supernatant for a final concentration of 0.5 mg ml^{-1} of MTT. After 3 h, the cell culture medium was removed. Formazan crystals in adherent cells were dissolved in dimethyl sulfoxide (DMSO, 200 µl) and the absorbance of the formazan solution was measured. Each compound was tested in triplicate and the experiments were repeated three times.

Generally, the operations from cell culture to MTT assay for cell proliferation are the same as we reported before (Cheng *et al.*, 2016; Bu *et al.*, 2017; Tan *et al.*, 2019).

2.5. Molecular docking and quantum chemistry calculations

Molecular docking studies of all eight Schiff bases with 18 potential target proteins were performed using the *SYBYL*/Surflex-dock (Tripos, 2012) in order to screen the potential targets and illustrate the binding modes between proteins and ligands. All solvent molecules except those within 5 Å around the natural ligand were removed from the protein structure. The molecular structures of the ligands were first extracted from the single-crystal X-ray structure and then optimized by employing density functional theory (DFT) at the B3LYP/6-311+G(d,p) level (Becke, 1993; Lee *et al.*, 1988; McLean & Chandler, 1980; Krishnan *et al.*, 1980). The default parameters were used regarding charges, bonds order and geometrical flexibility with no other constraints.

Except for the aforementioned structural optimizations, quantum chemistry calculations were also used to explore intermolecular interactions in the **BMHFI** crystal (see §3.1.5). Two methods, *i.e.* MP2/6-31G(d,p) and DFT/B3LYP/6-311G+(d,p), were used (Møller & Plesset, 1934; Rassolov *et al.*, 2001; Frisch *et al.*, 1984). The standard counterpoise method was applied to correct interaction energies for the basis set

superposition error (BSSE) (Boys & Bernardi, 1970). All geometries are extracted from the interacting pairs in the crystal of **BMHFI** without any structural relaxation.

All calculations were carried out using the *GAUSSIAN03* program package (Frisch *et al.*, 2004) on a Sunway BlueLight MPP supercomputer housed at the National Supercomputer Center in Jinan, China.

3. Results and discussion

3.1. X-ray structures of the eight title compounds

The identities of the conformations of the eight title compounds have been established through X-ray structure determinations, which clearly show the similarities and differences.

3.1.1. BDHFI. The monomeric structure of **BDHFI** is shown in Fig. 1(*a*), which indicates that the molecule contains a pair of linkage arms (the connection point is the C1—C8 bond axis). The pair of linkage arms crosses each other in an X-shape; each arm has a similar conformation, *i.e.* the two C═N double bonds adopt the same *Z*,*E* conformations in both arms. In fact, the other three di-Schiff bases (**BDHAI**, **BDHMFI** and **BDHFN**) reported in this article are X-shaped molecules and the two X-shaped arms in **BDHFN** are exactly the same (see §3.1.4).

Both arms in **BDHFI** are rather flat. One arm consists of atoms C1–C7/N1/N2/C24–C31/N6/C32 and all 19 non-H atoms are essentially coplanar, with an average r.m.s. deviation of only 0.0811 Å and the largest r.m.s. deviation of −0.1435 Å occurring for atom N6. In another arm, all 19 non-H atoms are slightly less coplanar, with an average r.m.s. deviation of 0.1742 Å (the largest r.m.s. deviation of 0.3027 Å occurs for atom N5). The dihedral angle between the planes of these two arms is about 89.3°.

In the packing structure of **BDHFI**, three kinds of dominant noncovalent interactions (NCIs), including hydrogen bond **a** (Fig. 1*b*), C—H$\cdots\pi$ interaction **b** (Fig. 1*b*) and π–π packing **c** (Fig. 1*c*), can be found with the help of *PLATON* (Tables S1–S3 in the supporting information). The *CrystalExplorer17* program (Hirshfeld, 1977; Turner *et al.*, 2017) was used to

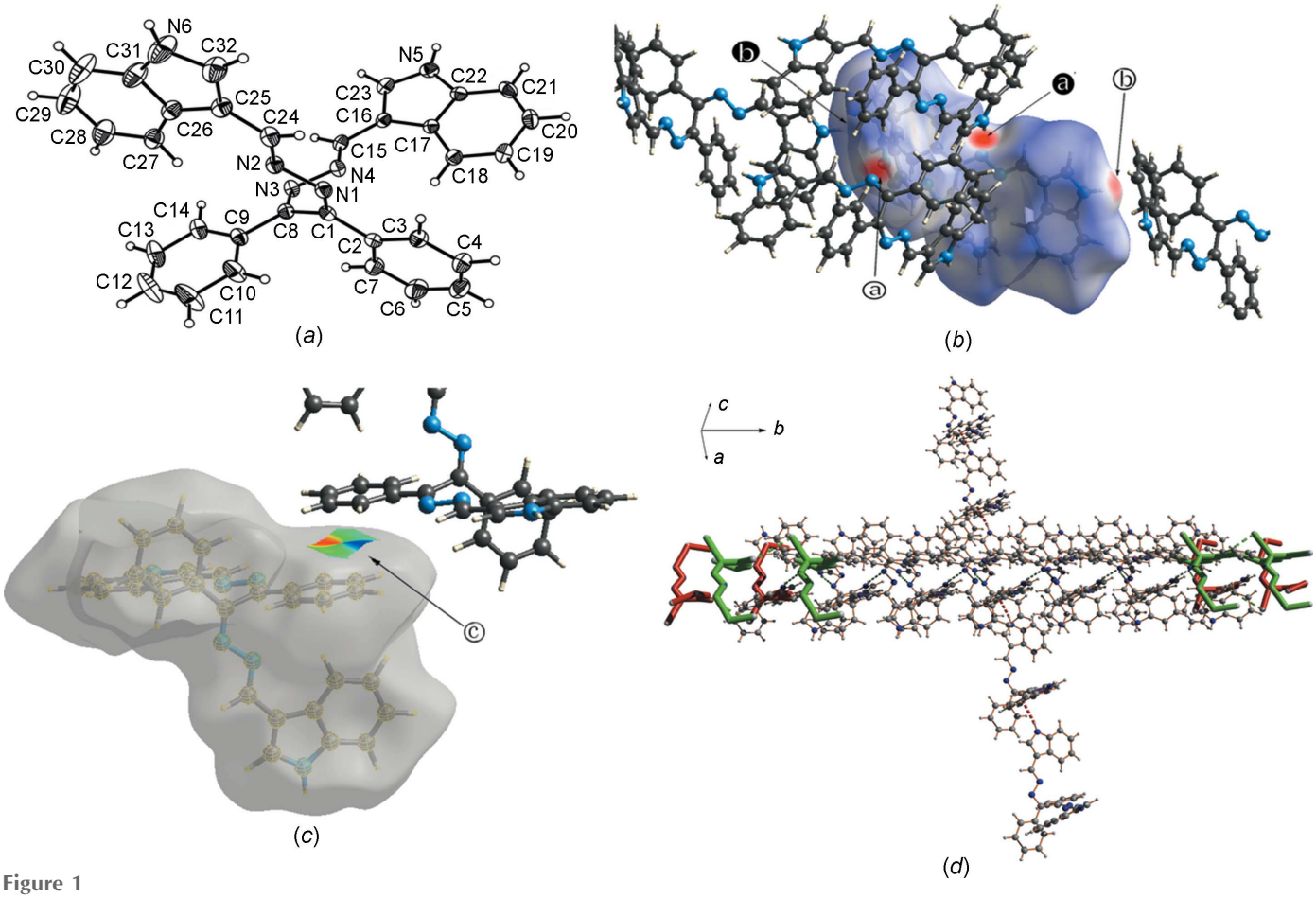

Figure 1
(*a*) The molecular structure of **BDHFI**, showing the atom-labelling scheme, with displacement ellipsoids for non-H atoms drawn at the 30% probability level at 293 K. (*b*) The Hirshfeld surface for **BDHFI**, mapped over d_{norm} (−0.10 to 1.40 Å, same throughout this article). Four red spots correspond to N5—H35$\cdots$N1($-x+2$, $y+\frac{1}{2}$, $-z+\frac{1}{2}$) (marked **a**) and N6—H36$\cdots\pi$ (marked **b**) interactions, respectively. (*c*) The shape-index surface of **BDHFI**, identifying π–π stacking interactions (marked **c**). Only red and blue triangles on the surface are shown for clarity. (*d*) Hydrogen bonds **a** (green dashed lines) and **b** (red dashed lines) link molecules into infinite 1D chains parallel to the crystallographic *b* and *a* axes, respectively, viewed along the crystallographic [8, $\bar{1}$, 17] direction. Eight molecules are illustrated by the simplified structure (centre of gravity) for clarity and the two colours (red and green) represent two different orientations.

verify the strength of these NCIs. It is worth noting that the geometries of all NCIs, including these very weak ones, calculated by *PLATON* are listed in the supporting information for all eight compounds reported in this article (Tables S1–S21 in the supporting information). But only those strong NCIs that can be verified by *CrystalExplorer17* will be analysed. For the convenience of description, different kinds of strong NCIs are simplified into various notations (the first column in Tables S1–S21 in the supporting information). These weak intermolecular NCIs and all intramolecular NCIs are not coded because they make less contribution to the packing structure. For example, the C3—H3···N3(x, $y-1$, z) hydrogen bond (Table S1 in the supporting information) is not coded because its role is not apparent in the Hirshfeld surface analysis (Fig. 1*b*). In rare cases, some 'strong' interactions verified by *CrystalExplorer17* have not been suggested by *PLATON*, for example, N3—H25···N2($x+\frac{1}{2}$, $-y+\frac{1}{2}$, $-z+\frac{1}{4}$) and C24—H24*A*···O1($x+1$, y, z) in Fig. 6(*b*) (see §3.1.6), and C11—H11···N1(x, $-y-\frac{1}{2}$, $z-\frac{1}{2}$) in Fig. 7(*b*) (see §3.1.7). Their roles will not be analysed.

Hydrogen bonds **a** and **b** link **BDHFI** molecules into one-dimensional (1D) chains parallel to the *b* and *a* axes, respectively (Fig. 1*d*), while π–π interaction **c** links two molecules into a dimer. These chains and dimers serve as the main building blocks for the three-dimensional (3D) structures with the aid of other kinds of NCIs, such as van der Waals.

It should be mentioned that all the molecules in **BDHFI** adopt two relative orientations, which are highlighted with red and green colours, respectively (Fig. 1*d*). If these two relatively small arene rings in one molecule are omitted, the X-shaped molecule can be regarded as a V-shaped one. These V-shaped molecules open towards entirely opposite directions: the red

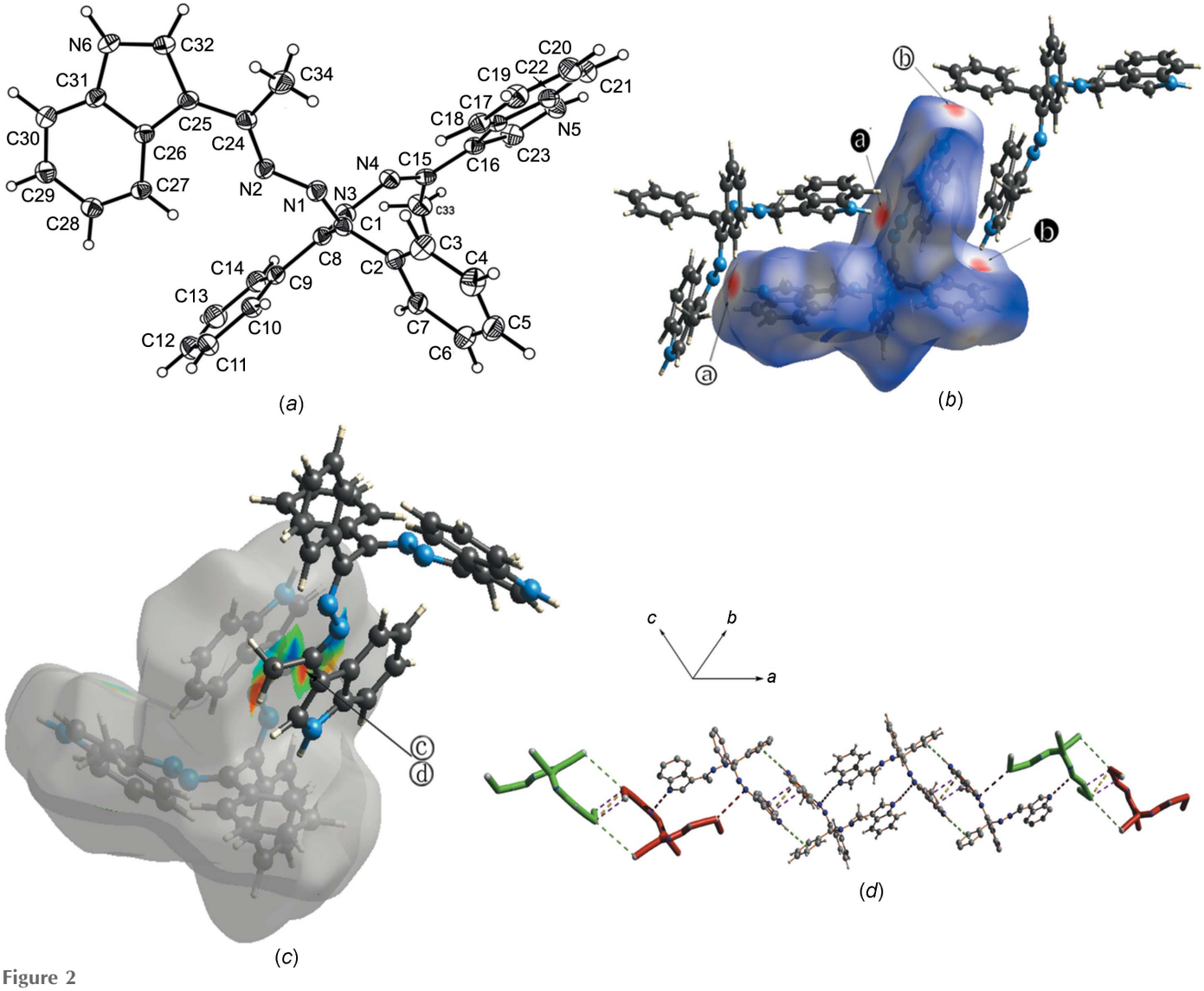

Figure 2
(*a*) The molecular structure of **BDHAI**, showing the atom-labelling scheme, with displacement ellipsoids for non-H atoms drawn at the 30% probability level at 293 K. (*b*) The Hirshfeld surface for **BDHAI**, mapped over $d_{\rm norm}$. Four red spots correspond to N6—H36···N4($-x$, $-y+1$, $-z+1$) (marked **a**) and N5—H35···π (marked **b**) interactions, respectively. (*c*) The shape-index surface of **BDHAI**, identifying π–π stacking interactions (marked **c** and **d**). Only red and blue triangles on the surface are shown for clarity. (*d*) Four kinds of NCIs, *i.e.* **a**, **b**, **c** and **d** (shown with red, green, purple and yellow dashed lines, respectively), link **BDHAI** molecules into an infinite 1D chain extending roughly along the [11$\bar{1}$] direction, viewed along the [7, $\bar{3}$, 7] direction.

ones are directed toward the positive half of the *c* axis, while the green ones are directed toward the negative half (both roughly). Interestingly, the molecules in the other three di-Schiff bases have two similar orientations, so there also exist red and green highlighted molecules in Figs. 2, 3 and 4. While molecules in the four mono-Schiff bases (**BMHFI**, **BMHAI**, **BMHMFI** and **BMHFN**) have four or eight orientations, mostly because of the two apparently asymmetrical arms (see §3.1.5 to §3.1.8).

3.1.2. BDHAI. Similar to **BDHFI**, **BDHAI** is an X-shaped molecule with both arms being somewhat flat. But the coplanarity is worse than in **BDHFI**. In one arm, consisting of atoms C1–C7/N1/N2/C24–C31/N6/C32/C34, the average r.m.s. deviation is 0.3698 Å and the largest r.m.s. deviation of 0.8308 Å occurs for atom C7. In another arm, all 20 non-H atoms have an average r.m.s. deviation of 0.2542 Å and the largest r.m.s. deviation of 0.4662 Å occurs for atom N5. The dihedral angle between the planes of the two arms is about 98.0° (Fig. 2*a*).

In the packing structure of **BDHAI**, the most important four NCIs link molecules into dimers independently (Tables S4–S6 in the supporting information). Hydrogen bonds **a** link two molecules into a dimer (Figs. 2*b* and 2*d*), while **b**, **c** and **d** link two molecules into another dimer (Figs. 2*b*, 2*c* and 2*d*), whether they are used separately or collectively. But **a**, **b**, **c** and **d** will crosslink molecules into infinite 1D chains if working together (Fig. 2*d*).

3.1.3. BDHMFI. The monomeric structure of **BDHMFI** is depicted in Fig. 3(*a*), which contains one complete **BDHMFI** molecule and a half acetonitrile molecule in the asymmetric unit. The half acetonitrile molecule lies on an inversion centre (atom C35, which resides on a centre of inversion at the origin) and was refined disordered into two parts with the site-occupancy factors being fixed at 0.5. The inversion operator will create two **BDHMFI** molecules and one complete acetonitrile molecule, which are linked together by hydrogen bonds **a** (Fig. 3*b*). By the way, **a** only occurs between **BDHMFI** and acetonitrile (Figs. 3*b* and 3*d*).

These two arms of X-shaped **BDHMFI** have a similar coplanarity to that in **BDHFI**. In one arm, consisting of atoms C1–C7/N1/N2/C24–C31/N6/C32/C34, the average r.m.s. deviation is 0.1063 Å and the largest r.m.s. deviation of 0.1870 Å

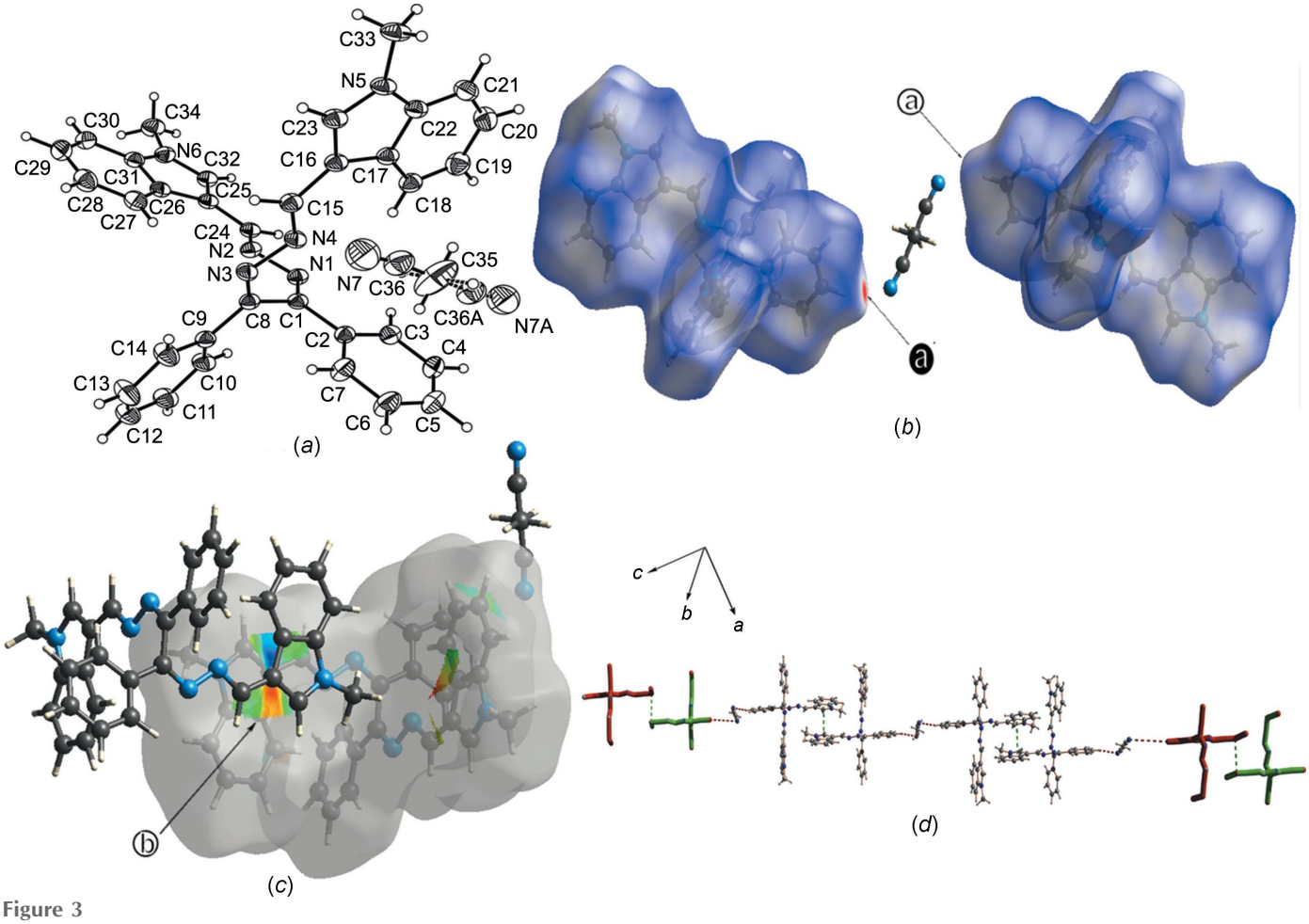

Figure 3
(*a*) The molecular structure of **BDHMFI**, showing the atom-labelling scheme, with displacement ellipsoids for non-H atoms drawn at the 30% probability level at 293 K [symmetry code: (A) $-x+2, -y, -z$]. (*b*) The dimer structure formed by two **BDHMFI** molecules and one disordered acetonitrile molecule through hydrogen bonds **a** (two red spots on the d_{norm} Hirshfeld surface). (*c*) The shape-index surface of **BDHMFI**, identifying π–π stacking interaction **b**. Only red and blue triangles on the surface are shown for clarity. (*d*) NCIs **a** and **b** (shown with red and green dashed lines, respectively) link **BDHMFI** molecules into an infinite 1D chain extending roughly along the $[10\bar{3}]$ direction, viewed along the $[1, 9, \bar{5}]$ direction.

occurs for atom C6. In another arm, all 20 non-H atoms have an average r.m.s. deviation of 0.1964 Å and the largest r.m.s. deviation of 0.4540 Å occurs for atom C33. The dihedral angle between the planes of these two arms is about 90.6°.

Either hydrogen bond **a** or π–π interaction **b** links two adjacent **BDHMFI** molecules into dimers, but they are not the same dimer (Figs. 3*b* and 3*c*). If **a** and **b** collaborate together, 1D chains extending along the crystallographic [24, 1, $\overline{63}$] direction will be formed (Fig. 3*d*).

3.1.4. BDHFN. The molecular structure of **BDHFN** is shown in Fig. 4(*a*), which is the result of a glide reflection along the crystallographic *c* axis. That is to say, the asymmetric unit contains only one half **BDHMFI** molecule, which happened to be one arm of the X-shaped structure. The dihedral angle between the planes of the naphthalene and arene rings is 22.6 (3)° and the dihedral angle between the two symmetry-related arms is 85.1 (4)°.

The only kind of hydrogen bond is intramolecular interactions in the packing structure of **BDHFN** (Table S10 in the supporting information). Besides van der Waals, only one kind of intermolecular π–π interaction **a** plays an important role (Table S11 in the supporting information), which accounts for merely 6.1% of the Hirshfeld surface (Fig. 4*b*). That is to say, it is van der Waals interactions that play a critical role in the crystal molecular assembly. As for π–π interactions **a** (Fig. 4*c*), they help to link **BDHFN** molecules into 1D lines parallel to the crystallographic *c* axis (Fig. 4*d*).

3.1.5. BMHFI. The molecular structure of **BMHFI** is shown in Fig. 5(*a*), which indicates that the molecule still contains a pair of linkage arms, but one arm is shorter than the other because one C═O group has not been converted into a Schiff base. The longer arm has a similar conformation to that in its corresponding di-Schiff base **BDHFI**, *i.e.* these two C═N double bonds adopt the same *Z*,*E* conformations. In fact, all

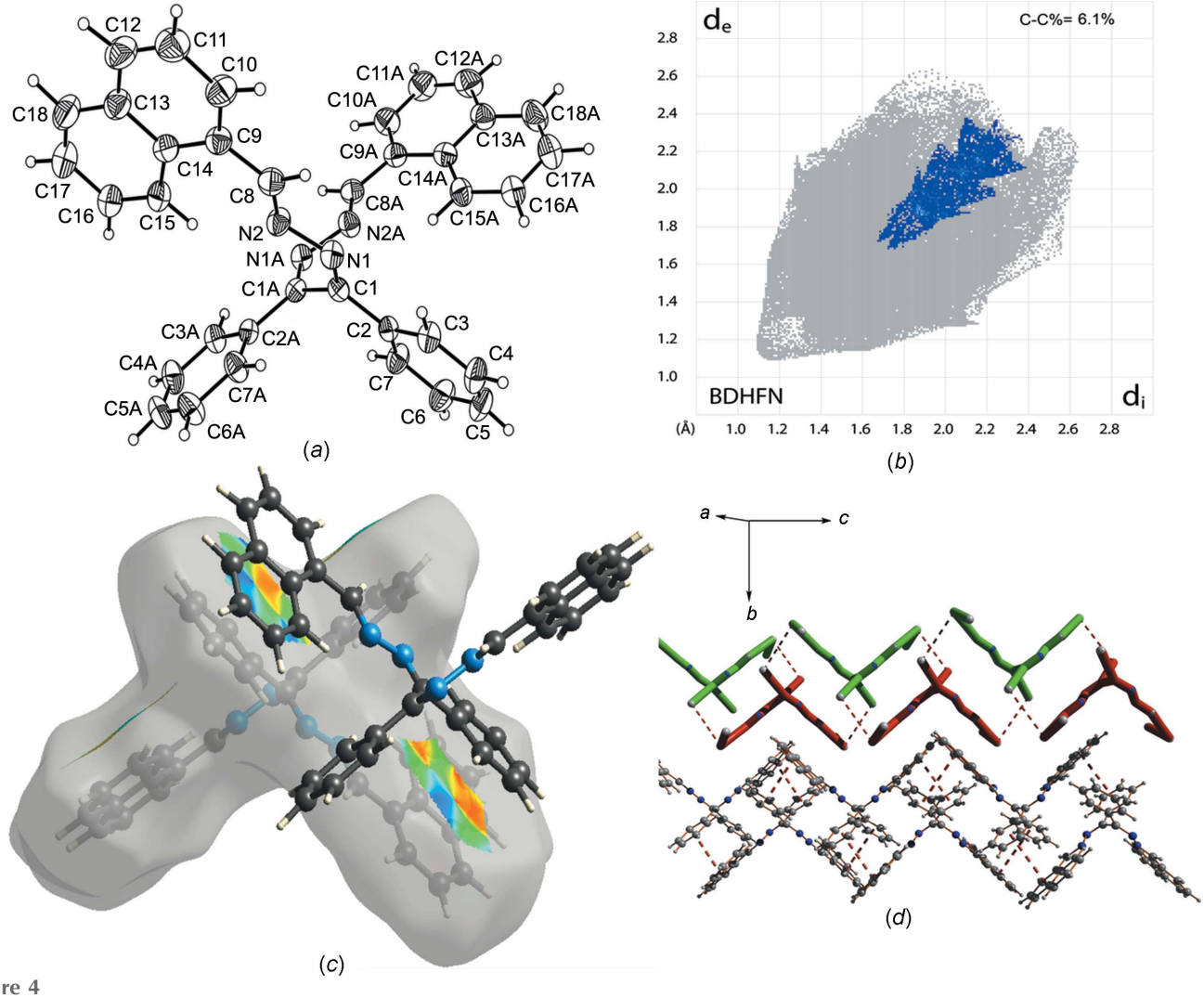

Figure 4
(*a*) The molecular structure of **BDHFN**, showing the atom-labelling scheme, with displacement ellipsoids for non-H atoms drawn at the 30% probability level at 293 K [symmetry code: (A) $-x, y, -z+\frac{1}{2}$]. (*b*) The contribution of C···C contacts in the 2D fingerprints of **BDHFN**, indicating π–π interaction **a**. (*c*) The shape-index surface of **BDHFN**, identifying π–π stacking interaction **a** (not marked as there is only one type of interaction). (*d*) 1D chains formed by π–π stacking interaction **a** (shown with red dashed lines), viewed along the [501] direction. The upper one is illustrated by the simplified structure (centre of gravity).

eight Schiff bases reported in this paper adopt similar *Z*,*E* conformations.

As a whole, both arms in **BMHFI** are flat. The long arm has an average r.m.s. deviation of 0.2242 Å and the largest r.m.s. deviation of −0.3858 Å occurs for N3. The short arm has much better coplanarity, with an average r.m.s. deviation of only 0.0160 Å (the largest r.m.s. deviation of −0.0647 Å occurs for O1). The dihedral angle between the two arms is about 93.8°.

In the packing structure of **BMHFI**, two kinds of intermolecular hydrogen bonds (**a** and **b**) (Table S12 in the supporting information) link molecules into 1D chains parallel to the crystallographic *a* axis, whether they are used separately or collectively. Unlike its corresponding di-Schiff base **BDHFI**, **BMHFI** adopts four relative orientations, which are highlighted in red, green, purple and blue (Figs. 5*c* and 5*d*). It should be noted that the colour intensity of the vivid spot

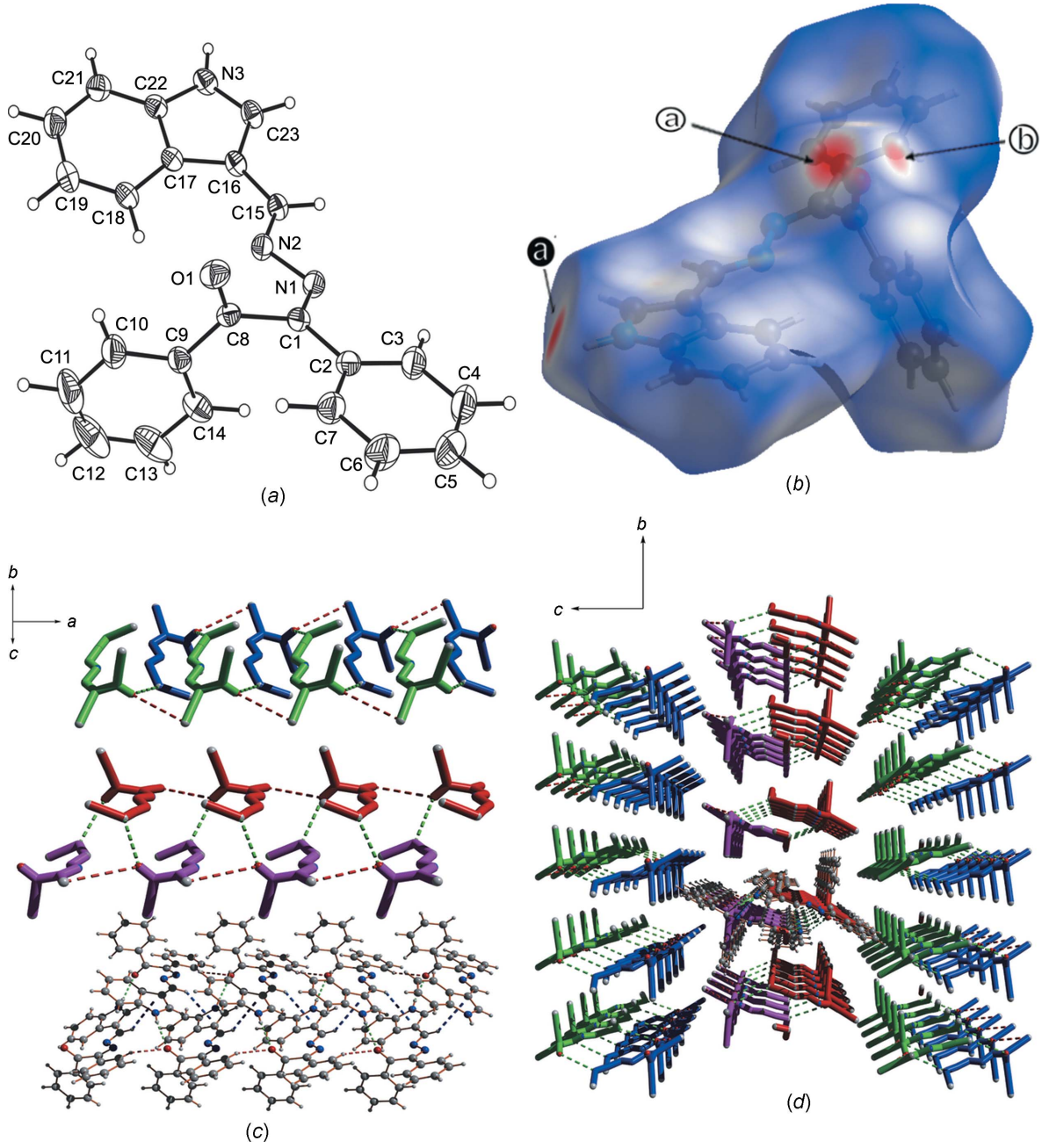

Figure 5
(*a*) The molecular structure of **BMHFI**, showing the atom-labelling scheme, with displacement ellipsoids for non-H atoms drawn at the 30% probability level at 293 K. (*b*) The Hirshfeld surface for **BMHFI**, mapped over $d_{\rm norm}$. Three red spots correspond to N3—H24···O1($x+\frac{1}{2}, -y+\frac{1}{2}, -z$) (marked **a**) and C3—H3···O1($x+1, y, z$) (marked **b**) interactions. (*c*) 1D chains formed by NCIs **a** and **b** (shown with green and red dashed lines, respectively), viewed perpendicular to the extending direction, *i.e.* the *a* axis. The upper two lines are illustrated by the simplified structure (centre of gravity). (*d*) 1D chains formed by the aforementioned NCIs **a** and **b**, viewed along the extending direction, *i.e.* the *a* axis, aiming to show the packing mode of four different orientations (simplified structure with four different colours).

representing hydrogen bond **a** is very high, indicating a strong hydrogen bond. Thus, the intermolecular interaction energy with the BSSE correction has been calculated using the MP2/6-31G(d,p) and B3LYP/6-311G+(d,p) methods on the basis of dimer geometries extracted from the crystal structure. The calculated interaction energies for **a** and **b** are −50.97 and −19.92 kJ mol^{-1} (MP2), and −19.71 and −4.25 kJ mol^{-1} (DFT), respectively, indicating a much stronger favourable binding energy for **a** than that for **b**, which agrees with the colour intensity in the d_{norm} map (Fig. 5*b*).

3.1.6. BMHAI. The 'long arm' in **BMHAI** assumes less coplanarity than that in **BMHFI**, and even less than that in **BDHAI**, which can be deduced from the dihedral angles between the indole and arene rings (Fig. 6*a*). In **BMHFI**, the value is 20.4 (4)°, while in **BDHAI**, the dihedral angles are 23.6 (4) and 39.9 (5)°, but in **BMHAI**, this value is increased to 54.5 (3)°.

There are eight kinds of molecular orientations and one kind of intermolecular hydrogen bond, *i.e.* **a**, in the crystal structure of **BMHAI** (Figs. 6*b* and 6*c*) (Tables S15–S17 in the supporting information). Hydrogen bonds **a** link molecules into two kinds of 1D chains, one is parallel to the crystallographic *a* axis (these molecules are simplified into green, blue, yellow and indigo skeletons in Fig. 6*c*) and the other is parallel to the *b* axis (these molecules are simplified into orange, red, purple and violet skeletons in Fig. 6*c*).

3.1.7. BMHMFI. Both the 'long arm' and the 'short arm' in **BMHMFI** have good coplanarity. The dihedral angle between

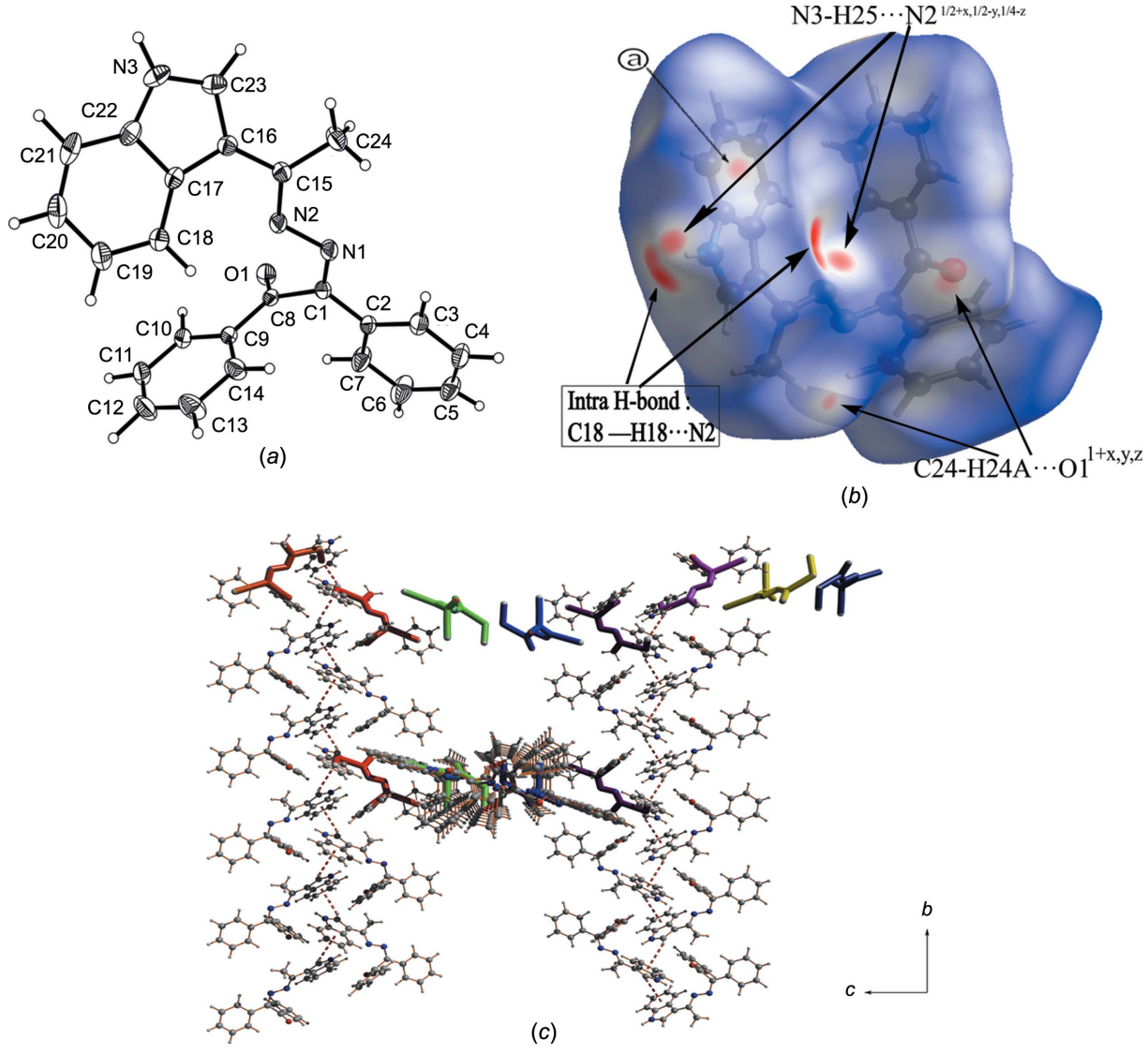

Figure 6
(*a*) The molecular structure of **BMHAI**, showing the atom-labelling scheme, with displacement ellipsoids for non-H atoms drawn at the 30% probability level at 293 K [symmetry code: (A) $-x$, y, $-z+\frac{1}{2}$]. (*b*) The Hirshfeld surface for **BMHAI**, mapped over d_{norm}. Three kinds of intermolecular hydrogen bonds and one kind of intramolecular hydrogen bond can be visualized as red spots, but only hydrogen bond **a** was confirmed by the *PLATON* program (Spek, 2009). (*c*) 1D chains along the *a* and *b* axes formed by the aforementioned hydrogen bonds **a** (shown with red dashed lines), viewed along the *a* axis, aiming to show the packing mode of the eight different orientations as a simplified structure with eight different colours, *i.e.* orange, red, green, blue, purple, violet, yellow and indigo.

the planes of the indole and arene rings in the 'long arm' is only 14.0 (2)°. The long arm has an average r.m.s. deviation of 0.1492 Å and the largest r.m.s. deviation is 0.3816 Å for atom C24; the short arm has an average r.m.s. deviation of only 0.0324 Å and the largest r.m.s. deviation is 0.1135 Å for atom O1. These two arms are roughly perpendicular to each other, with a dihedral angle of 91.1 (3)° (Fig. 7*a*).

The most intense red spots represent a C23—H23···ring(C17–C22)($-x+1, y+\frac{1}{2}, -z+\frac{1}{2}$) interaction, coded as **a** (Fig. 7*b*) (Table S18 in the supporting information), which links molecules into a 1D chain parallel to the *b* axis (Fig. 7*d*). The second intense spot represents a C11—H11···N1($x, -y-\frac{1}{2}, z-\frac{1}{2}$) hydrogen bond (Fig. 7*b*), which was not suggested by *PLATON*. Thus, its role in the packing structure will not be analysed in this article. Two kinds of intermolecular π–π interactions (**b** and **c**) always co-exist (Fig. 7*c*) (Table S19 in the supporting information), and they link two adjacent molecules into a dimer (Fig. 7*d*). The collaboration of **a**, **b** and **c** links molecules into a 2D layer structure (Fig. 7*d*).

3.1.8. BMHFN. The dihedral angle between the planes of the naphthalene and benzene rings in the 'long arm' is 24.2 (5)°. The dihedral angle between the long and short arms is about 81.4 (5)° (Fig. 8*a*).

There are four kinds of molecular orientations and four kinds of intermolecular NCIs (**a**, **b**, **c** and **d**) in the crystal structure of **BMHFN** (Figs. 8*b*, 8*c* and 8*d*) (Tables S20 and S21 in the supporting information). Hydrogen bond **a** links molecules into 1D chains parallel to the crystallographic *b* axis (Figs. 8*b* and 8*d*). Among these three types of π–π stacking interactions, **b** and **d** always co-exist and link molecules into 1D chains parallel to the crystallographic *c* axis (Figs. 8*c* and 8*d*), **c** joins two molecules (red and green, and blue and yellow;

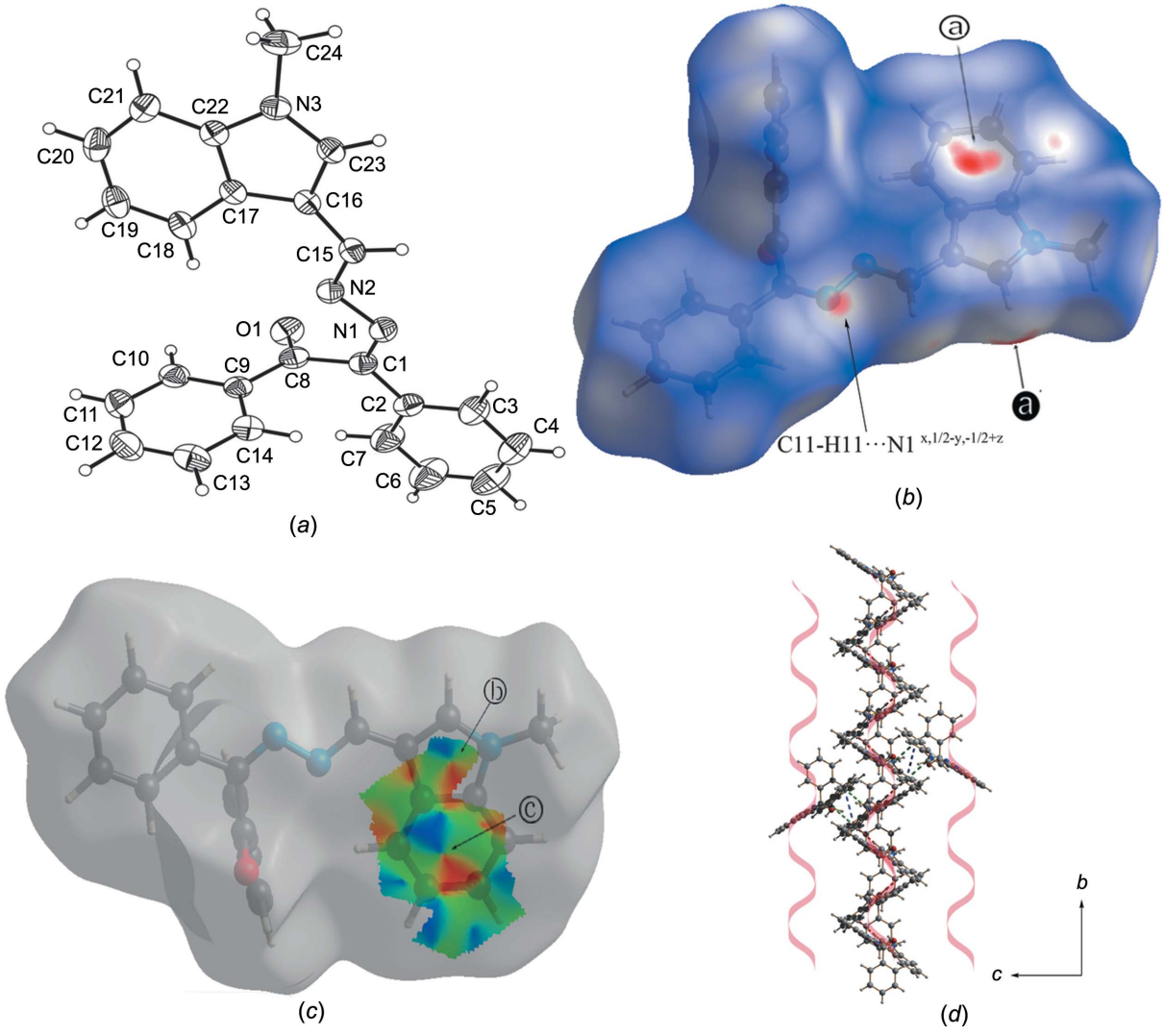

Figure 7
(*a*) The molecular structure of **BMHMFI**, showing the atom-labelling scheme, with displacement ellipsoids for non-H atoms drawn at the 30% probability level at 293 K. (*b*) The Hirshfeld surface for **BMHMFI**, mapped over d_{norm}. The intermolecular hydrogen bonds **a** calculated using *PLATON*, but another kind of hydrogen bond [C11—H11···N1($x, -y-\frac{1}{2}, z-\frac{1}{2}$), which can be found as red spots] was not suggested by *PLATON*. (*c*) The shape-index surface of **BMHMFI**, identifying π–π stacking interactions **b** and **c**. (*d*) 1D chains formed by C—H···π interactions **a** (shown with red dashed lines) can be woven into a 2D layer structure by π–π interactions **b** and **c** (shown with green and blue dashed lines, respectively), viewed along the *a* axis.

Fig. 8*d*) into dimers. The co-operation of all three types of π–π stacking interactions (**b**, **c** and **d**) links molecules into a 2D layer structure extending along the crystallographic (100) plane (Fig. 8*d*). In fact, all four kinds of intermolecular NCIs crosslink molecules into the same infinite 2D layer structure.

3.2. Cytotoxicity assays – inhibition of lung and breast cancer cell growth

To study the growth inhibitory effects of these eight Schiff bases on lung/breast cancer cells, we treated human A549 and mouse $4T_1$ cells with the compounds and examined the growth of cells with an MTT assay. Meanwhile, MRC-5 normal lung cells and NIH 3T3 fibroblasts were also tested using the same method in order to evaluate the selective cytotoxicity of these new compounds. All experiments were carried out with cisplatin (a compound used as a chemotherapy drug to treat many types of cancers) for comparison. The cytotoxic activities as 50% inhibitory concentration (IC_{50}) values are shown in Table 2.

As we can see, both **BDHFI** and **BDHAI** have similar cytotoxic activities to the standard cisplatin for both cancer cell lines. All mono-Schiff bases show slightly weaker inhibi-

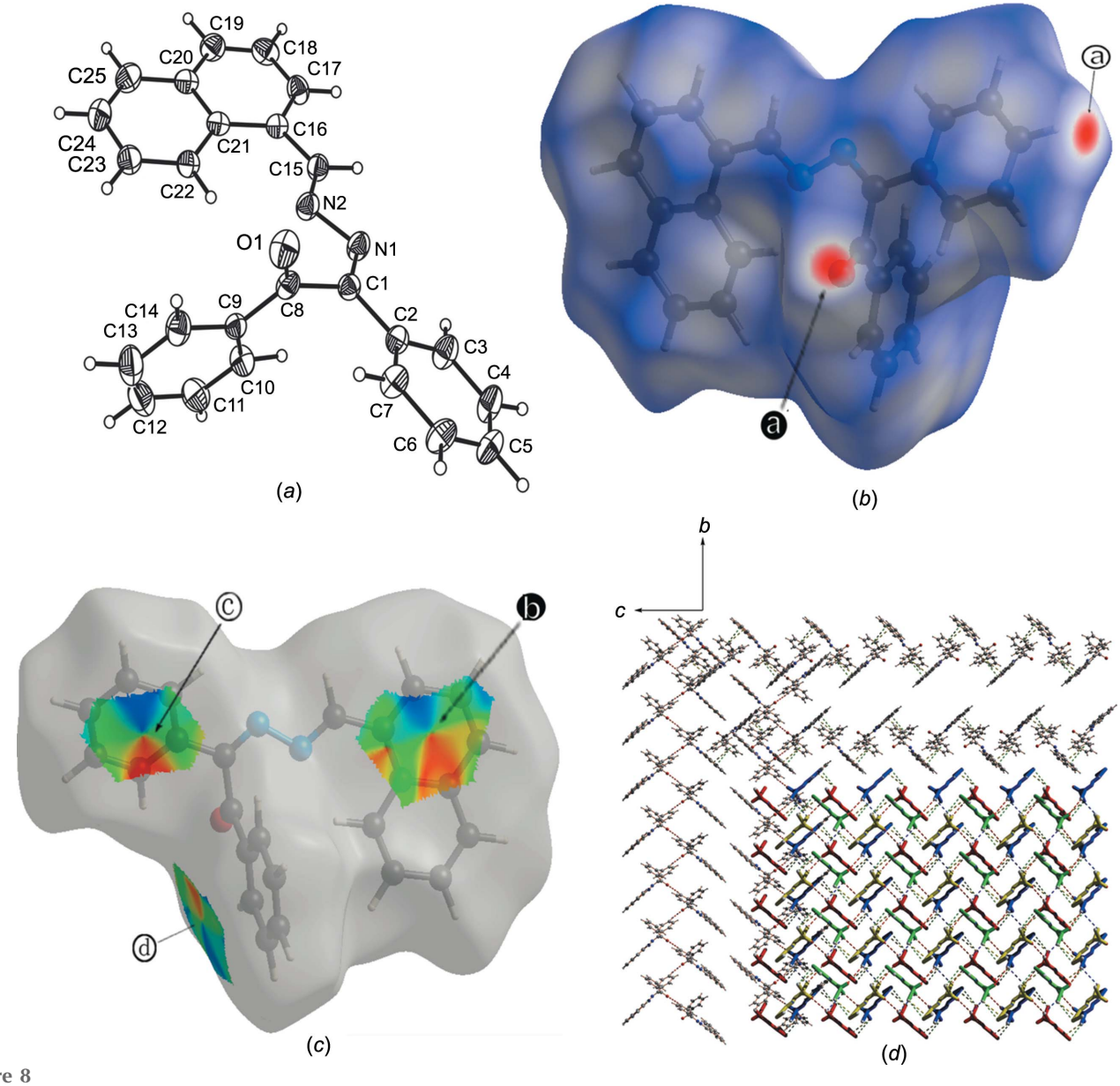

Figure 8
(*a*) The molecular structure of **BMHFN**, showing the atom-labelling scheme, with displacement ellipsoids for non-H atoms drawn at the 30% probability level at 293 K. (*b*) The Hirshfeld surface for **BMHFN**, mapped over d_{norm}. Two red spots correspond to C5—H5···O1($-x+1, y-\frac{1}{2}, -z+\frac{3}{2}$) (marked **a**). (*c*) The shape-index surface of **BMHFN**, identifying π–π stacking interactions **b**, **c** and **d**. Only red and blue triangles on the surface are shown for clarity. (*d*) 2D layer structure formed by NCIs **a** **b**, **c** and **d** (shown with red, green, blue and yellow dashed lines, respectively), viewed along the *a* axis. Four discontinuous lines are shown, the left two (along the *b* axis) are formed by NCI **a** and the top two (along the *c* axis) are formed by NCIs **b** and **d**. Molecules in the bottom right corner are illustrated by the simplified structure (centre of gravity), showing four kinds of orientations.

Table 2
Inhibition of A549, $4T_1$, MRC-5 and NIH 3T3 cell growth by the title compounds compared with cisplatin (μM).

Compound	A549 cells, IC_{50}	$4T_1$ cells, IC_{50}	MRC-5 cells, IC_{50}	NIH 3T3 fibroblasts, IC_{50}
BDHFI	8.0±0.5	7.5±0.5	24.5±1.5	29.5±1.0
BDHAI	8.5±0.6	7.0±0.6	36.5±1.5	43.0±1.5
BDHMFI	125.0±1.0	122.0±1.0	>150.0	>150.0
BDHFN	130.0±1.0	125.0±1.0	>150.0	>150.0
BMHFI	46.5±0.5	32.5±0.5	88.0±1.5	85.0±1.5
BMHAI	43.0±0.5	30.0±0.5	83.0±1.5	76.0±1.5
BMHMFI	148.0±1.2	141.0±1.0	>150.0	>150.0
BMHFN	150.0±1.2	148.0±1.0	>150.0	>150.0
Cisplatin	6.5 ± 0.5	0.5 ± 0.1	22.5 ± 1.5	21.0 ± 1.0

tory activity of A549 and $4T_1$ compared with their corresponding di-Schiff bases. Incorporating a CH_3 group at the N—H position in the indole ring proved detrimental for anticancer activity (**BDHMFI** and **BMHMFI**), while substitution on the imine C atom has little effect (**BDHAI** and **BMHAI**). This might be due to the availability of enough space to accommodate a methyl group at this particular site of the inhibitor binding pocket, or the N—H group favours combination with the hydrogen-bonding pocket. In one word, for **BDHFI**, **BDHAI**, **BMHFI** and **BMHAI**, the normal indole rings should contribute greatly to their cytotoxicities. When indole rings are changed into 1-methylindole or naphthalene, the cytotoxicity is greatly decreased.

As for the selective cytotoxicity between normal and malignant cells, MTT assays reveal a similar pattern to what were seen in our previous work (Tan *et al.*, 2019). That is to say, all Schiff bases possess selective cytotoxicity on cancer cells over normal cells. But they have relevant inhibitory concentrations. The higher the IC_{50} value for selected malignant cells, the higher the value for responding normal cells. Among them, **BDHFI**, **BDHAI**, **BMHFI** and **BMHAI** displayed high potency and selectivity in all cell lines.

These experimental studies clearly predict cytotoxic activities of indole-containing Schiff bases. Such encouraging preliminary results confirm the feasibility and reliability of this excellent framework in the discovery of potent antitumour agents.

3.3. Reverse docking studies for target fishing

In order to find a few most possible molecular targets for these Schiff bases, Swiss Target Prediction web server (http://www.swisstargetprediction.ch/) (Daina *et al.*, 2019; Gfeller *et al.*, 2013) was used for the initial selection of potential targets. For each of these eight Schiff bases, 100 most potential targets were selected for further evaluation. Then cross screenings were carried out among these eight sets of potential targets based on the following method. Firstly, eight sets of targets were divided into two groups according to the antiproliferative activities of the Schiff bases. Four sets of potential targets related to **BDHFI**, **BDHAI**, **BMHFI** and **BMHAI** belong to group 1, and another four sets of potential targets related to **BDHMFI**, **BDHFN**, **BMHMFI** and **BMHFN** are group 2. Considering that all the Schiff bases in group 1 have a similar skeleton and have much higher activities than those in group 2, the targets in group 1 are probably the same, while the ligands in group 2 should not hit these targets. Technically, the most probable targets should be hit four times in group 1 and should not be hit in group 2. In our work, the targets that were hit four or three times in group 1 were selected (total of 32 targets) on account of random error in the prediction model. But if one target was also hit more than twice (including twice) in group 2, it should be removed (14 targets were removed). In the end, 18 targets remained for further screening through the reverse docking method.

As mentioned above, the initially assessed Rounds comprised a total of 18 targets. Only two of these targets do not have detailed 3D structural information, *i.e.* Neurokinin 2 receptor and Serotonin 6 (5-HT6) receptor. Thus, homology models built using the SWISS-MODEL server (https://swiss-model.expasy.org/) (Waterhouse *et al.*, 2018; Bienert *et al.*, 2017) and optimized by *SYBYL-X* (Tripos, 2012) were used. The structure of Neurokinin 2 receptor was modelled on the bovine rhodopsin crystal structure (PDB ID: 1f88) as a template (Chandrashekaran *et al.*, 2009), while the structure of the 5-HT6 receptor was modelled using the β2 adrenergic receptor template (PDB ID: 4lde) (Łażewska *et al.*, 2017) (Figs. S17 and S18 in the supporting information). Though the obtained models exhibit only limited accuracy, it has been demonstrated that the modelled receptor pocket conformations can be validated or improved *via* docking of known ligands. For the Neurokinin 2 receptor, ligand 6-methylbenzo-[*b*]thiophene-2-carboxylic acid (1-{(*S*)-1-benzyl-4-[4-(tetrahydropyran-4-ylmethyl)piperazin-1-yl]butylcarbamoyl}cyclopentyl)amide (abbreviated as 10i in the original article) was used as the well-known antagonist with high affinity (Fattori *et al.*, 2010). As for the 5-HT6 receptor, AVN-492, a new promising ligand (now tested in phase I trials) was selected (Ivachtchenko *et al.*, 2017; Łażewska *et al.*, 2019).

Eventually, all eight Schiff bases were docked into these 18 possible targets with the program *SYBYL-X* (Tripos, 2012) by calculating the Total Score of Surflex-dock (Table 3) (Rarey *et al.*, 1996). The docking results were then compared with MTT results to gain insight into the most possible molecular targets. Spearman's rank correlation coefficient ρ (Fieller *et al.*, 1957) was introduced to assess the strength of each target's monotonic relationship (Table 3). The closer ρ is to 1, the stronger the monotonic relationship. As we can see, ρ values of three targets [*i.e.* human ether-á-go-go-related (hERG) potassium channel, inhibitor of apoptosis protein 3 and serine/threonine-

Table 3
Total scores and Spearman's rank correlation coefficients (ρ in the last two rows) of 18 possible targets (PDB IDs are in brackets; two targets in the last two columns were docked using homology modules for the absence of detailed 3D information).

$$\rho_{A549} = 1 - \frac{6\Sigma\left(\mathrm{Rank}_i - \mathrm{Rank}_{A549}\right)^2}{n(n^2-1)} \quad (1)$$

$$\rho_{4T_1} = 1 - \frac{6\Sigma\left(\mathrm{Rank}_i - \mathrm{Rank}_{4T_1}\right)^2}{n(n^2-1)} \quad (2)$$

	c-Jun N-terminal kinase 3 (2r9s)	CaM kinase II (2vz6)	Delta opioid receptor (4n6h)	Gonadotropin-releasing hormone receptor (6nbf)	hERG (3o0u)	Inhibitor of apoptosis protein 3 (5c3h)	Kinesin-like protein 1 (3zcw)	Mu opioid receptor (4dkl)	Probable G-protein coupled receptor 88 (5xf1)
Ligand[i]	12.24	9.27	9.37	7.76	9.87	7.33	19.68	10.53	6.67
BDHFI	8.08	8.43	7.56	6.19	6.90	6.23	10.44	8.57	6.85
BDHAI	8.16	8.82	7.44	6.36	8.02	6.14	6.99	9.46	6.15
BDHMFI	5.96	6.92	6.53	6.77	4.54	5.07	8.61	8.23	5.28
BDHFN	5.94	7.59	7.05	5.00	6.25	5.33	9.04	7.45	5.84
BMHFI	6.64	7.32	7.44	5.29	5.97	5.83	9.44	7.31	4.39
BMHAI	5.60	6.80	6.32	5.88	6.41	4.77	8.27	6.15	4.52
BMHMFI	6.39	5.98	6.65	4.19	4.91	4.42	7.76	6.36	4.58
BMHFN	5.59	6.03	6.45	4.67	4.20	4.30	6.16	6.47	4.37
ρA549[ii]	0.67	0.74	0.57	0.71	**0.86**	**0.83**	0.48	0.52	0.62
$\rho4T_1$[iii]	0.69	0.76	0.55	0.74	**0.88**	**0.81**	0.33	0.55	0.60

	Protein kinase C alpha (4ra4)	Serine/threonine-protein kinase AKT2 (3d0e)	Serine/threonine-protein kinase PIM1 (1yxt)	Serine/threonine-protein kinase PIM2 (4x7q)	Serine/threonine-protein kinase PIM3 (5dwr)	Sigma opioid receptor (6dk0)	Tryptase beta-1 (4mpu)	Neurokinin 2 receptor (by homology)	5-HT6 receptor (by homology)
Ligand[i]	7.34	16.79	32.82	15.18	10.64	10.81	23.41	10.04	9.00
BDHFI	6.35	8.22	9.73	6.70	8.00	8.34	7.39	9.28	7.95
BDHAI	6.79	6.40	9.60	8.19	9.92	7.17	8.12	8.80	4.56
BDHMFI	5.27	5.65	6.64	5.56	4.45	1.87	6.02	8.17	6.40
BDHFN	5.47	5.51	7.59	5.63	5.51	5.23	7.99	8.73	7.07
BMHFI	4.43	7.06	7.95	7.87	6.39	6.41	5.44	6.71	5.05
BMHAI	4.87	6.67	7.01	7.68	7.49	8.27	5.51	5.68	5.50
BMHMFI	5.06	6.77	5.52	5.92	6.42	7.00	5.05	6.00	4.43
BMHFN	4.30	7.46	5.80	5.92	6.06	6.23	5.22	6.44	6.18
ρA549[ii]	0.60	0.12	**0.86**	0.62	0.69	0.69	0.62	0.52	0.17
$\rho4T_1$[iii]	0.62	0.00	**0.83**	0.69	0.71	0.64	0.67	0.50	0.02

Notes: (i) for all proteins with crystal structures, the 'ligand' means the natural ligand included in the protein structure; for the last two proteins built by homology modelling, the 'ligand' means the known ligand reported before, *i.e.* 10i and AVN-492 (see text). (ii) see equation (1) above; (iii) see equation (2) above, $n = 8$. Rank_i is the rank value of each Schiff base in the virtual screening, which is determined according to its sequence listed in descending order of total score value (see Table S22 in the supporting information). $\mathrm{Rank}_{A549}/\mathrm{Rank}_{4T1}$ is the rank value of each Schiff base in the A549/$4T_1$ cell growth MTT assays, which is determined according to its sequence listed in ascending order of IC_{50} value (see Table 2 and Table S23 in the supporting information).

protein kinase PIM1] are above 0.80, their correlations can be described as 'very strong' (bold in Table 3). Thus, they can be regarded as the most possible targets.

3.4. Comparison of binding modes between active and less active ligands

Among the three most possible targets, hERG (PDB ID 3o0u) has the highest Spearman's rank correlation coefficient values and is ranked as the best, so the comparison of binding modes is performed based on the docking results of eight Schiff bases with hERG, in order to gain insight into the nature of the structure–activity relationships.

According to our docking simulation, shown in Fig. 9, the active and less active ligands have different binding modes. In both **BDHFI** and **BDHAI**, two hydrogen bonds were formed, one is between the indole N—H group and GLN19/GLU59, and the other is between an imine N atom and HOH267/GLY66. But in both **BDHMFI** and **BDHFN**, no hydrogen bond was formed and aromatic hydrophobic interactions dominate the affinity between the protein and the ligand. This phenomenon can be confirmed by the Polar values, which are 2.60 and 2.18 for **BDHFI** and **BDHAI**, respectively, but zero for **BDHMFI** and **BDHFN**.

As for the **BMH** series of four mono-Schiff bases, all of them exhibit one to five hydrogen bonds within the active site (Fig. 10). Indole N—H groups and imine N atoms form one or two hydrogen bonds in both **BMHFI** and **BMHAI**. A carboxyl O atom forms an extra hydrogen bond in **BMHAI**, which is

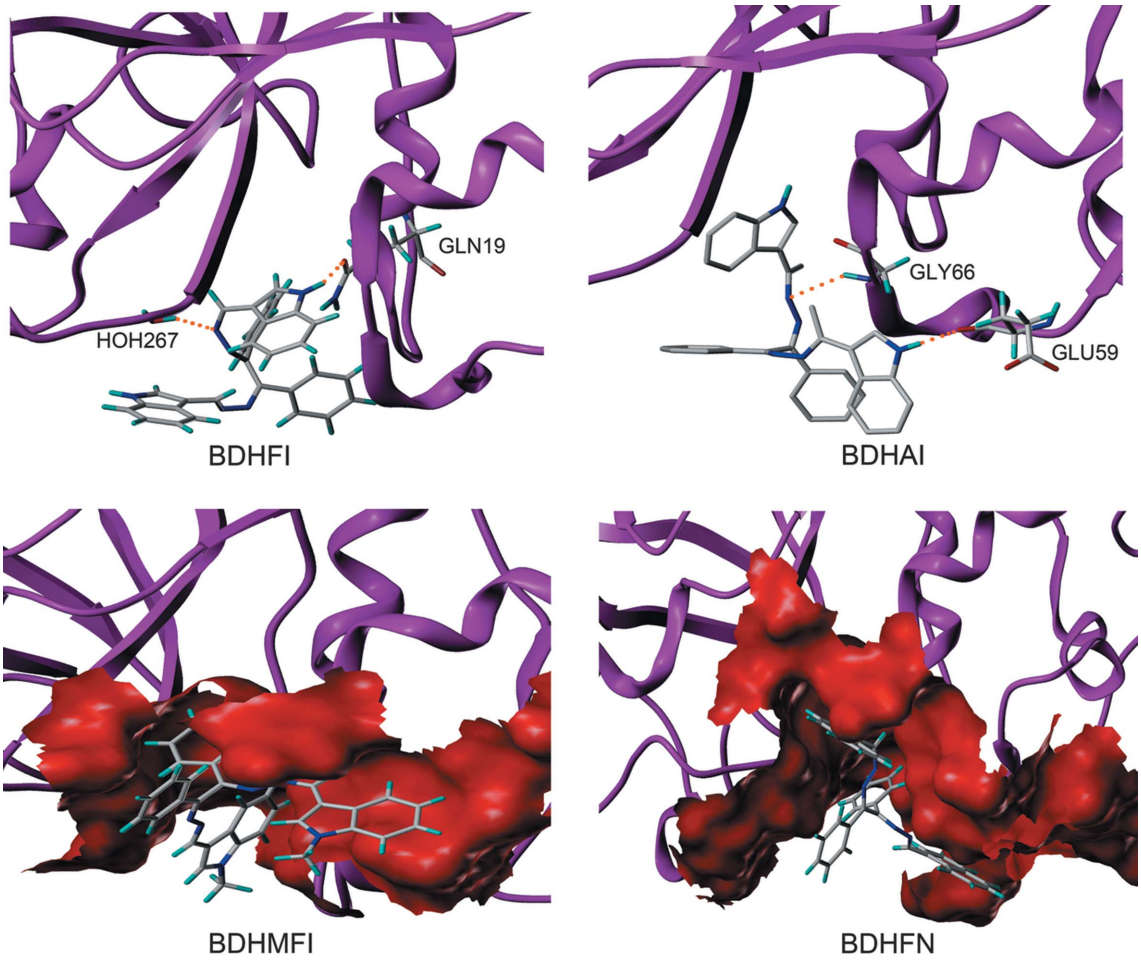

	Total_Score	Crash	Polar	Similarity	D_score	PMF_score	G_score	ChemScore
BDHFI	6.8994	-2.3222	2.5972	0.248	-130.2239	-5.6982	-207.9752	-27.1866
BDHAI	8.0205	-1.8365	2.1828	0.369	-184.6051	-6.2585	-278.7422	-36.6271
BDHMFI	4.5397	-2.5519	0.0001	0.402	-200.1143	-1.778	-296.3246	-35.8267
BDHFN	6.2457	-1.0928	0	0.407	-150.1006	68.1354	-225.1856	-32.8227

Figure 9
The calculated binding modes of **BDHFI**, **BDHAI**, **BDHMFI** and **BDHFN** with hERG (PDB ID: 3o0u). Hydrogen bonds are shown with orange dotted lines. If no hydrogen bond is formed, surfaces that contain the active sites are displayed (red surface). Total score values and seven additional contributing parts or scores are listed underneath for comparison.

the reason why it has a higher Total Score (also Polar value) than **BMHFI. BMHMFI** and **BMHFN** can form only one hydrogen bond with protein through a carboxyl O or imine N atom, so their docking Total Scores (also Polar values) are lower than those of **BMHFI** and **BMHAI**. Put simply, the more hydrogen bonds formed, the higher the Total Score values in the docking simulations, and the better the anti-proliferative activities of the ligands.

There is one phenomenon that seems confusing, *i.e.* **BDHFN** has a higher Total Score than **BMHFI** (6.25 *versus* 5.97), but the former has a lower cytotoxic activity than the latter. Apparently, the deviation between docking predictions and experimental activities may partly explain this result. Here, we consider another class of scoring function based on a potential of mean force, so-called PMF-based scores, which is a knowledge-based scoring approach based on the work of Muegge and Martin (Muegge & Martin, 1999; Muegge, 2006). The PMF-based scoring functions are statistical, because it is calculated as the sum of the overall atom-pair interaction Helmholtz free energies between the protein and ligand, neglecting other characteristics of the environment and mutual orientation of the atom (Lizunov *et al.*, 2015). As we know, the higher the PMF value, the poorer the protein–ligand binding affinity (Sharma & Ghoshal, 2006). From the seventh columns in Figs. 9 and 10, we can see that **BDHFN** has the highest PMF score (68.14) and is ranked as the worst with

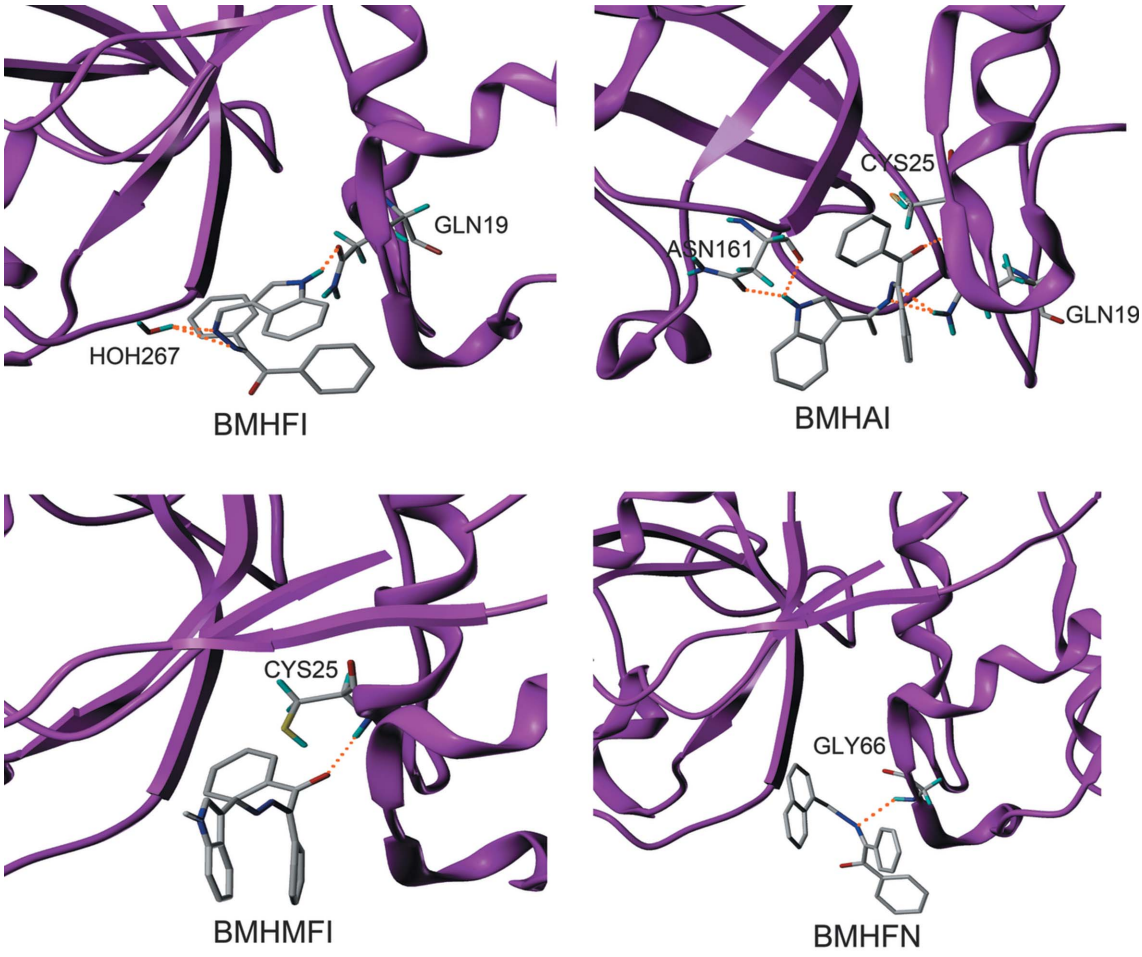

	Total_Score	Crash	Polar	Similarity	D_score	PMF_score	G_score	ChemScore
BMHFI	5.9744	-2.0025	2.5268	0.222	-108.1605	-12.0139	-166.6515	-26.6604
BMHAI	6.408	-1.027	4.2604	0.329	-110.4748	6.0784	-166.7928	-31.1578
BMHMFI	4.9056	-1.5938	1.0908	0.438	-143.612	10.3378	-217.7523	-30.984
BMHFN	4.2017	-1.0311	0.1059	0.361	-111.2041	28.928	-189.9784	-27.0685

Figure 10
The calculated binding modes of **BMHFI**, **BMHAI**, **BMHMFI** and **BMHFN** with hERG (PDB ID: 3o0u). Hydrogen bonds are shown with orange dotted lines. Total score values and seven additional contributing parts or scores are listed underneath for comparison.

respect to the means of the distance-dependent Helmholtz free energies. That is to say, a long distance between the protein and ligand has a detrimental contribution to the affinity, which has not been reflected apparently in the Total Score. On the other hand, this phenomenon confirms the conclusion that PMF has essential differences with all of the other scoring functions. Its unique knowledge-based algorithm parameterized using crystal complexes is distinctive (Liu *et al.*, 2012).

The above explanation is also suitable to **BMHAI** *versus* **BDHFI/BDHAI**. The former exhibit five hydrogen bonds within the active site, but it has a lower Total Score and weaker cytotoxic activity than the latter two. The PMF score of **BMHAI** is 6.08, revealing poorer binding affinities compared with the meager binding scores of **BDHFI** and **BDHAI** (−5.70 and −6.26, respectively).

In brief, all of the docking results were in good agreement with the experimental results, indicating the most probable target and reasonable structure–activity relationships.

4. Conclusion

Schiff bases have been used widely in the pharmaceutical industry because of their antimicrobial, anti-inflammatory and anticancer properties. We have described the synthesis and structural characterization of eight novel Schiff bases derived from **BDH/BMH**. These synthesized Schiff base compounds have similar molecular structures despite having different terminal fused two-ring aromatics and different substituents. MTT assays proved that the **BDH** series of compounds show higher inhibitory activity compared with the **BMH** series. The biological screening results favour the activities of indole-

containing Schiff bases instead of naphthalene-containing ones. The cytotoxic activity is also affected by the nature of the substituents at the indole N atom; the replacement of hydrogen by methyl will decrease the cytotoxic activities greatly, while the same replacement on the imine C—H group has little effect. Generally, our *in vitro* findings show that four of these compounds have high antiproliferative activity against human lung cancer cell line A549 and mouse breast cancer cell line $4T_1$; two show obvious and comparable activities with cisplatin. All compounds exhibited weaker cytotoxicity against normal cells than cancer cells.

Swiss Target Prediction online servers were used to screen compounds against large numbers of molecular targets. After careful examination, 18 possible targets were generated for further screening through the reverse docking approach. Afterwards, the three most possible targets were chosen on account of their correlation with experimental data. Bearing the highest consistency, the docking results of hERG (PDB ID: 3o0u) with eight Schiff bases can easily explain the structure–activity relationships obtained experimentally.

In conclusion, the present work indicates that introduction of an indole ring on the terminal of this kind of X-shaped Schiff base leads to the generation of potent anticancer agents.

Funding information

Funding for this research was provided by: Key Laboratory of Pulp and Paper Science and Technology of Ministry of Education/Shandong Province of China (award Nos. KF201712 and KF201821); State Key Laboratory of Biobased Material and Green Papermaking, Qilu University of Technology, Shandong Academy of Sciences (grant No. ZZ20190115).

References

Akula, M., Yogeeswari, P., Sriram, D., Jha, M. & Bhattacharya, A. (2016). *RSC Adv.* **6**, 46073–46080.
Ali Khan, M. S., Misbah Ahmed, N., Arifuddin, M., Rehman, A. & Ling, M. P. (2018). *Food Chem. Toxicol.* **118**, 953–962.
Anush, S. M., Vishalakshi, B., Kalluraya, B. & Manju, N. (2018). *Int. J. Biol. Macromol.* **119**, 446–452.
Ariyaeifar, M., Amiri Rudbari, H., Sahihi, M., Kazemi, Z., Kajani, A. A., Zali-Boeini, H., Kordestani, N., Bruno, G. & Gharaghani, S. (2018). *J. Mol. Struct.* **1161**, 497–511.
Atienza, B. J. P., Jensen, L. D., Noton, S. L., Ansalem, A. K. V., Hobman, T., Fearns, R., Marchant, D. J. & West, F. G. (2018). *J. Org. Chem.* **83**, 6829–6842.
Bach, R. D., Woodard, R. A., Anderson, T. J. & Glick, M. D. (1982). *J. Org. Chem.* **47**, 3707–3712.
Bai, J., Zhang, P., Bao, G., Gu, J.-G., Han, L., Zhang, L.-W. & Xu, Y. (2018). *Appl. Microbiol. Biotechnol.* **102**, 8493–8500.
Bai, Y., Gao, H., Qi, Z. Y. & Dang, D. B. (2012). *Synth. React. Inorg. Met.-Org. Nano-Met. Chem.* **42**, 53–58.
Bano, B., Khan, K. M., Jabeen, A., Hameed, A., Faheem, A., Taha, M., Perveen, S. & Iqbal, S. (2017). *ChemistrySelect*, **2**, 10050–10054.
Bao, B., Zhang, P., Lee, Y., Hong, J., Lee, C. O. & Jung, J. H. (2007). *Mar. Drugs* **5**, 31–39.
Becke, A. D. (1993). *J. Chem. Phys.* **98**, 5648–5652.
Bertamino, A., Iraci, N., Ostacolo, C., Ambrosino, P., Musella, S., Di Sarno, V., Ciaglia, T., Pepe, G., Sala, M., Soldovieri, M. V., Mosca, I., Gonzalez-Rodriguez, S., Fernandez-Carvajal, A., Ferrer-Montiel, A., Novellino, E., Taglialatela, M., Campiglia, P. & Gomez-Monterrey, I. (2018). *J. Med. Chem.* **61**, 6140–6152.
Bharathi Dileepan, A. G., Daniel Prakash, T., Ganesh Kumar, A., Shameela Rajam, P., Violet Dhayabaran, V. & Rajaram, R. (2018). *J. Photochem. Photobiol. B*, **183**, 191–200.
Bienert, S., Waterhouse, A., de Beer, T. A. P., Tauriello, G., Studer, G., Bordoli, L. & Schwede, T. (2017). *Nucleic Acids Res.* **45**, D313–D319.
Blunt, J. W., Copp, B. R., Munro, M. H., Northcote, P. T. & Prinsep, M. R. (2011). *Nat. Prod. Rep.* **28**, 196–268.
Boys, S. B. & Bernardi, F. (1970). *Mol. Phys.* **19**, 553–566.
Brandenburg, K. & Putz, H. (1999). *DIAMOND*. Crystal Impact GbR, Bonn, Germany.
Brigg, S., Pribut, N., Basson, A. E., Avgenikos, M., Venter, R., Blackie, A., van Otterlo, W. A. L. & Pelly, S. C. (2016). *Bioorg. Med. Chem. Lett.* **26**, 1580–1584.
Bruker (2000). *SMART*, *SAINT*, *SADABS*, *XPREP* and *SHELXTL*. Bruker AXS Inc., Madison, Wisconsin, USA.
Bu, F.-Z., Tan, X.-J., Xing, D.-X. & Wang, C. (2017). *Acta Cryst.* C**73**, 546–555.
Carreño, A., Zúñiga, C., Páez-Hernández, D., Gacitúa, M., Polanco, R., Otero, C., Arratia-Pérez, R. & Fuentes, J. A. (2018). *New J. Chem.* **42**, 8851–8863.
Chandra, S., Verma, S. & Gautam, A. (2007). *J. Saudi Chem. Soc.* **11**, 483–488.
Chandrashekaran, I. R., Rao, G. S. & Cowsik, S. M. (2009). *J. Chem. Inf. Model.* **49**, 1734–1740.
Chauhan, S., Swami, M., Malik, S. & Singh, R. V. (2008). *Main Group Met. Chem.* **31**, 263–272.
Cheng, S.-S., Shi, Y., Ma, X.-N., Xing, D.-X., Liu, L.-D., Liu, Y., Zhao, Y.-X., Sui, Q.-C. & Tan, X.-J. (2016). *J. Mol. Struct.* **1115**, 228–240.
Cihan-Üstündağ, G., Gürsoy, E., Naesens, L., Ulusoy-Güzeldemirci, N. & Çapan, G. (2016). *Bioorg. Med. Chem.* **24**, 240–246.
Dai, W., Jiang, X. L., Tao, J. Y. & Shi, F. (2016). *J. Org. Chem.* **81**, 185–192.
Daina, A., Michielin, O. & Zoete, V. (2019). *Nucleic Acids Res.* **47**, W357–W364.
De, S., Chowdhury, S., Tocher, D. A. & Datta, D. (2006). *CrystEngComm*, **8**, 670–673.
Drew, M. G. B., Parui, D., De, S., Chowdhury, S. & Datta, D. (2007). *New J. Chem.* **31**, 1763–1768.
El-Sawy, E. R., Bassyouni, F. A., Abu-Bakr, S. H., Rady, H. M. & Abdlla, M. M. (2010). *Acta Pharm.* **60**, 55–71.
El-Sawy, E. R., Mandour, A. H., El-Hallouty, S. M., Shaker, K. H. & Abo-Salem, H. M. (2013). *Arabian J. Chem.* **6**, 67–78.
El-Sawy, E. R., Mandour, A. H., Mahmoud, K., Islam, I. E. & Abo-Salem, H. M. (2012). *Acta Pharm.* **62**, 157–179.
Ensch, M., Maldonado, V. Y., Swain, G. M., Rechenberg, R., Becker, M. F., Schuelke, T. & Rusinek, C. A. (2018). *Anal. Chem.* **90**, 1951–1958.
Erxleben, A. (2018). *Inorg. Chim. Acta*, **472**, 40–57.
Estevão, M. S., Carvalho, L. C., Ribeiro, D., Couto, D., Freitas, M., Gomes, A., Ferreira, L. M., Fernandes, E. & Marques, M. M. B. (2010). *Eur. J. Med. Chem.* **45**, 4869–4878.
Evans, B. E., Rittle, K. E., Bock, M. G., DiPardo, R. M., Freidinger, R. M., Whitter, W. L., Lundell, G. F., Veber, D. F., Anderson, P. S., Chang, R. S., Lotti, V. J., Cerino, D. J., Chen, T. B., Kling, P. J., Kunkel, K. A., Springer, J. P. & Hirshfield, J. (1988). *J. Med. Chem.* **31**, 2235–2246.
Fantinati, A., Bianco, S., Guerrini, R., Salvadori, S., Pacifico, S., Cerlesi, M. C., Calo, G. & Trapella, C. (2017). *Sci. Rep. UK*, **7**, 1–7.
Farag, A. K., Elkamhawy, A., Londhe, A. M., Lee, K.-T., Pae, A. N. & Roh, E. J. (2017). *Eur. J. Med. Chem.* **141**, 657–675.
Farrugia, L. J. (2012). *J. Appl. Cryst.* **45**, 849–854.
Fattori, D., Porcelloni, M., D'Andrea, P., Catalioto, R.-M., Ettorre, A., Giuliani, S., Marastoni, E., Mauro, S., Meini, S., Rossi, C., Altamura, M. & Maggi, C. A. (2010). *J. Med. Chem.* **53**, 4148–4165.

Fieller, E. C., Hartley, H. O. & Pearson, E. S. (1957). *Biometrika*, **44**, 470–481.
Fisher, H. M. & Stoufer, R. C. (1966). *Inorg. Chem.* **5**, 1172–1177.
Fortes, M. P., da Silva, P. N. B., da Silva, T. G., Kaufman, T. S., Militão, G. C. G. & Silveira, C. C. (2016). *Eur. J. Med. Chem.* **118**, 21–26.
Frisch, M. J., Pople, J. A. & Binkley, J. S. (1984). *J. Chem. Phys.* **80**, 3265–3269.
Frisch, M. J., *et al.* (2004). *GAUSSIAN03*. Revision C.02. Gaussian Inc., Wallingford, CT, USA. http://www.gaussian.com.
Ganguly, A., Chakraborty, P., Banerjee, K. & Choudhuri, S. K. (2014). *Eur. J. Pharm. Sci.* **51**, 96–109.
George, S., Parameswaran, M. K., Chakraborty, A. & Ravi, T. K. (2008). *Acta Pharm.* **58**, 119–129.
Gfeller, D., Michielin, O. & Zoete, V. (2013). *Bioinformatics*, **29**, 3073–3079.
Gul, W. & Hamann, M. T. (2005). *Life Sci.* **78**, 442–453.
Gurer-Orhan, H., Karaaslan, C., Ozcan, S., Firuzi, O., Tavakkoli, M., Saso, L. & Suzen, S. (2016). *Bioorg. Med. Chem.* **24**, 1658–1664.
Hassam, M., Basson, A. E., Liotta, D. C., Morris, L., van Otterlo, W. A. L. & Pelly, S. C. (2012). *ACS Med. Chem. Lett.* **3**, 470–475.
Hirshfeld, F. L. (1977). *Theor. Chim. Acta*, **44**, 129–138.
Hong, W. D., Gibbons, P. D., Leung, S. C., Amewu, R., Stocks, P. A., Stachulski, A., Horta, P., Cristiano, M. L. S., Shone, A. E., Moss, D., Ardrey, A., Sharma, R., Warman, A. J., Bedingfield, P. T. P., Fisher, N. E., Aljayyoussi, G., Mead, S., Caws, M., Berry, N. G., Ward, S. A., Biagini, G. A., O'Neill, P. M. & Nixon, G. L. (2017). *J. Med. Chem.* **60**, 3703–3726.
Ivachtchenko, A. V., Okun, I., Aladinskiy, V., Ivanenkov, Y., Koryakova, A., Karapetyan, R., Mitkin, O., Salimov, R. & Ivashchenko, A. (2017). *J. Alzheimers Dis.* **58**, 1043–1063.
Johansson, H., Jørgensen, B. T., Gloriam, E. D., Bräuner-Osborne, H. & Pedersen, S. D. (2013). *RSC Adv.* **3**, 945–960.
Kalaiarasi, G., Rex Jeya Rajkumar, S., Aswini, G., Dharani, S., Fronczek, F. R. & Prabhakaran, R. (2018). *Spectrochim. Acta A Mol. Biomol. Spectrosc.* **200**, 246–262.
Kamath, P. R., Sunil, D., Ajees, A. A., Pai, K. S. R. & Biswas, S. (2016). *Eur. J. Med. Chem.* **120**, 134–147.
Ke, S., Wei, Y., Shi, L., Yang, Q. & Yang, Z. (2013). *Anticancer Agents Med. Chem.* **13**, 1291–1298.
Khayyat, S., Amr, A. E. E., Salam, O. I. A. E., Al-Omar, M. A. & Abdalla, M. M. (2015). *Int. J. Pharmacol.* **11**, 423–431.
Kim, S. & Yoon, J.-Y. (2004). *Sci. Synth.* **27**, 671–722.
Krishnan, R., Binkley, J. S., Seeger, R. & Pople, J. A. (1980). *J. Chem. Phys.* **72**, 650–654.
Kumar, D., Kumar, M. N., Akamatsu, K., Kusaka, E., Harada, H. & Ito, T. (2016). *Bioorg. Med. Chem. Let.* **20**, 3916–3919.
Lamie, P. F., Ali, W. A. M., Bazgier, V. & Rárová, L. (2016). *Eur. J. Med. Chem.* **123**, 803–813.
Łażewska, D., Kurczab, R., Więcek, M., Kamińska, K., Satała, G., Jastrzębska-Więsek, M., Partyka, A., Bojarski, A. J., Wesołowska, A., Kieć-Kononowicz, K. & Handzlik, J. (2017). *Eur. J. Med. Chem.* **135**, 117–124.
Łażewska, D., Kurczab, R., Więcek, M., Satała, G., Kieć-Kononowicz, K. & Handzlik, J. (2019). *Bioorg. Chem.* **84**, 319–325.
Lee, C., Yang, W. & Parr, R. G. (1988). *Phys. Rev. B*, **37**, 785–789.
Liu, S., Fu, R., Zhou, L.-H. & Chen, S.-P. (2012). *PLoS One*, **7**, e38086.
Lizunov, A. Y., Gonchar, A. L., Zaitseva, N. I. & Zosimov, V. V. (2015). *J. Chem. Inf. Model.* **55**, 2121–2137.
Ma, J.-Y., Quan, Y.-C., Jin, H.-G., Zhen, X.-H., Zhang, X.-W. & Guan, L.-P. (2016). *Chem. Biol. Drug Des.* **87**, 342–351.
Malik, M. A., Dar, O. A., Gull, P., Wani, M. Y. & Hashmi, A. A. (2018). *MedChemComm*, **9**, 409–436.
Mandour, A. H., El-Sawy, E. R., Shaker, K. H. & Mustafa, M. A. (2010). *Acta Pharm.* **60**, 73–88.
Mayans, J., Font-Bardia, M., Di Bari, L., Arrico, L., Zinna, F., Pescitelli, G. & Escuer, A. (2018). *Chem. Eur. J.* **24**, 7653–7663.
McLean, A. D. & Chandler, G. S. (1980). *J. Chem. Phys.* **72**, 5639–5648.
Mishra, S., Kaur, M., Chander, S., Murugesan, S., Nim, L., Arora, D. S. & Singh, P. (2018). *Eur. J. Med. Chem.* **155**, 658–669.
Møller, C. & Plesset, M. S. (1934). *Phys. Rev.* **46**, 618–622.
Mor, M., Silva, C., Vacondio, F., Plazzi, P. V., Bertoni, S., Spadoni, G., Diamantini, G., Bedini, A., Tarzia, G., Zusso, M., Franceschini, D. & Giusti, P. (2004). *J. Pineal Res.* **36**, 95–102.
Muegge, I. (2006). *J. Med. Chem.* **49**, 5895–5902.
Muegge, I. & Martin, Y. C. (1999). *J. Med. Chem.* **42**, 791–804.
Mukherjee, A., Dutta, A., JANA, A. D. & Patra, G. K. (2013). *Inorg. Chim. Acta*, **404**, 131–143.
Naidu, K. M., Srinivasarao, S., Agnieszka, N., Ewa, A. K., Kumar, M. M. K. & Chandra Sekhar, K. V. G. (2016). *Bioorg. Med. Chem. Lett.* **26**, 2245–2250.
Naim, M. J., Alam, O., Alam, Md. J., Bano, F., Alam, P. & Shrivastava, N. (2016). *Int. J. Pharm. Sci. Res.* **7**, 51–62.
Ndagijimana, A., Wang, X., Pan, G., Zhang, F., Feng, H. & Olaleye, O. (2013). *Fitoterapia*, **86**, 35–47.
Pedada, R. S., Yarla, S. N., Tambade, J. P., Dhananjaya, L. B., Bishayee, A., Arunasree, M. K., Philip, H. G., Dharmapuri, G., Aliev, G., Putta, S. & Rangaiah, G. (2016). *Eur. J. Med. Chem.* **112**, 289–297.
Pojarová, M., Kaufmann, D., Gastpar, R., Nishino, T., Reszka, P., Bednarski, P. J. & von Angerer, E. (2007). *Bioorg. Med. Chem.* **15**, 7368–7379.
Pramanik, K., Malpaharia, P., Colacio, E., Das, B. & Chandra, S. K. (2018). *New J. Chem.* **42**, 6332–6342.
Pu, C., Luo, R.-H., Zhang, M., Hou, X., Yan, G., Luo, J., Zheng, Y.-T. & Li, R. (2017). *Bioorg. Med. Chem. Lett.* **27**, 4150–4155.
Rarey, M., Kramer, B., Lengauer, T. & Klebe, G. (1996). *J. Mol. Biol.* **261**, 470–489.
Rassolov, V. A., Ratner, M. A., Pople, J. A., Redfern, P. C. & Curtiss, L. A. (2001). *J. Comput. Chem.* **22**, 976–984.
Sá Alves, F. R. de, Barreiro, E. J. & Fraga, C. A. (2009). *Mini Rev. Med. Chem.* **9**, 782–793.
Saini, T., Kumar, S. & Narasimhan, B. (2016). *Cent. Nerv. Syst. Agents Med. Chem.* **16**, 19–28.
Salavati-Niasari, M. & Hassani-Kabutarkhani, M. (2005). *Synth. React. Inorg. Met.-Org. Nano-Met. Chem.* **35**, 469–475.
Santhosh Kumar, G., Poornachandra, Y., Kumar Gunda, S., Ratnakar Reddy, K., Mohmed, J., Shaik, K., Ganesh Kumar, C. & Narsaiah, B. (2018). *Bioorg. Med. Chem. Lett.* **28**, 2328–2337.
Sellitto, G., Faruolo, A., de Caprariis, P., Altamura, S., Paonessa, G. & Ciliberto, G. (2010). *Bioorg. Med. Chem.* **18**, 6143–6148.
Shaaban, M. & Abdel-Aziz, M. S. (2007). *Nat. Prod. Res.* **21**, 1205–1211.
Shaaban, M., Maskey, R. P., Wagner-Döbler, I. & Laatsch, H. (2002). *J. Nat. Prod.* **65**, 1660–1663.
Sharma, P. & Ghoshal, N. (2006). *J. Chem. Inf. Model.* **46**, 1763–1774.
Sheldrick, G. M. (2015*a*). *Acta Cryst.* A**71**, 3–8.
Sheldrick, G. M. (2015*b*). *Acta Cryst.* C**71**, 3–8.
Singh, G., Kalra, P., Arora, A., Singh, A., Sharma, G., Sanchita, Maurya, I. K., Dutta, S., Munshi, P. & Verma, V. (2018). *ChemistrySelect*, **3**, 2366–2375.
Singh, R. V., Fahmi, N., Swami, M. & Chauhan, S. (2008). *J Macromol. Sci. A*, **45**, 159–163.
Spek, A. L. (2009). *Acta Cryst.* D**65**, 148–155.
Sugiyama, Y., Ito, Y., Suzuki, M. & Hirota, A. (2009). *J. Nat. Prod.* **72**, 2069–2071.
Suzen, S. & Buyukbingol, E. (2000). *Farmaco*, **55**, 246–248.
Tan, X.-J., Hao, X.-Q., Zhao, Q.-Z., Cheng, S.-S., Xie, W.-L., Xing, D.-X., Liu, Y. & Song, L.-Z. (2015). *J. Mol. Struct.* **1099**, 373–387.
Tan, X.-J., Zhang, L.-Y., Sun, Y.-K. & Zhou, X.-M. (2019). *Acta Cryst.* C**75**, 97–106.
Tripos (2012). *SYBYL-X*. Version 2.0. Tripos International, St Louis, MO, USA. http://www.tripos.com.
Turner, M. J., McKinnon, J. J., Wolff, S. K., Grimwood, D. J., Spackman, P. R., Jayatilaka, D. & Spackman, M. A. (2017).

CrystalExplorer17. University of Western Australia. http://crystalexplorer.scb.uwa.edu.au/.
Tzvetkov, N. T., Hinz, S., Küppers, P., Gastreich, M. & Müller, C. E. (2014). *J. Med. Chem.* **57**, 6679–6703.
Unver, Y. & Bektas, E. (2018). *Lett. Drug. Des. & Discov*. **15**, 706–712.
Vardhan, H., Mehta, A., Nath, I. & Verpoort, F. (2015). *RSC Adv.* **5**, 67011–67030.
Venkatesan, V., Kumar, S. K. A., Bothra, S. & Sahoo, S. K. (2018). *New J. Chem.* **42**, 6175–6182.
Wang, Q., Qu, Y., Xia, Q., Song, H.-J., Song, H.-B., Liu, Y. & Wang, Q. (2018). *Chem. Eur. J.* **24**, 11283–11287.
Waterhouse, A., Bertoni, M., Bienert, S., Studer, G., Tauriello, G., Gumienny, R., Heer, F. T., de Beer, T. A. P., Rempfer, C., Bordoli, L., Lepore, R. & Schwede, T. (2018). *Nucleic Acids Res.* **46**, W296–W303.
Wu, Y. S., Coumar, M. S., Chang, J. Y., Sun, H. Y., Kuo, F. M., Kuo, C. C., Chen, Y. J., Chang, C. Y., Hsiao, C. L., Liou, J. P., Chen, C. P., Yao, H. T., Chiang, Y. K., Tan, U. K., Chen, C. T., Chu, C. Y., Wu, S. Y., Yeh, T. K., Lin, C. Y. & Hsieh, H. P. (2009). *J. Med. Chem.* **52**, 4941–4945.
Yu, H.-F., Qin, X.-J., Ding, C.-F., Wei, X., Yang, J., Luo, J.-R., Liu, L., Khan, A., Zhang, L.-C., Xia, C.-F. & Luo, X.-D. (2018). *Org. Lett.* **20**, 4116–4120.
Zhao, C., Zhao, Y., Chai, H. & Gong, P. (2006). *Bioorg. Med. Chem.* **14**, 2552–2558.
Zhao, S.-Q., Xu, Y., Guan, J., Zhao, S., Zhang, G.-D. & Xu, Z. (2018). *J. Heterocycl. Chem.* **55**, 2172–2177.

supporting information

Acta Cryst. (2020). C**76**, 44-63 [https://doi.org/10.1107/S2053229619015687]

Synthesis, crystal structures, antiproliferative activities and reverse docking studies of eight novel Schiff bases derived from benzil

Xue-Jie Tan, Di Wang, Xiao-Ming Hei, Feng-Cun Yang, Ya-Ling Zhu, Dian-Xiang Xing and Jian-Ping Ma

Computing details

For all structures, data collection: *SMART* (Bruker, 2000); cell refinement: *SMART* (Bruker, 2000); data reduction: *SAINT* (Bruker, 2000); program(s) used to solve structure: *SHELXS2016* (Sheldrick, 2015a); program(s) used to refine structure: *SHELXL2016* (Sheldrick, 2015b); molecular graphics: *SHELXTL* (Bruker, 2000), *PLATON* (Spek, 2009) and *DIAMOND* (Brandenburg & Putz, 1999); software used to prepare material for publication: *SHELXL2016* (Sheldrick, 2015b) and *WinGX* (Farrugia, 2012).

(1*Z*,2*Z*)-1,2-Bis{(*E*)-[(1*H*-indol-3-yl)methylidene]hydrazinylidene}-1,2-diphenylethane (1-BDHFI)

Crystal data

$C_{32}H_{24}N_6$
M_r = 492.57
Monoclinic, $P2_1/c$
a = 13.023 (4) Å
b = 7.340 (2) Å
c = 27.762 (9) Å
β = 97.693 (5)°
V = 2630.0 (14) Å^3
Z = 4
$F(000)$ = 1032
D_x = 1.244 Mg m^{-3}
Mo $K\alpha$ radiation, λ = 0.71073 Å
Cell parameters from 380 reflections
θ = 2.5–26.0°
μ = 0.08 mm^{-1}
T = 293 K
Block, yellow
0.30 × 0.18 × 0.15 mm

Data collection

Bruker SMART CCD area detector diffractometer
Radiation source: fine-focus sealed tube
Detector resolution: 10.13 pixels mm^{-1}
phi and ω scans
Absorption correction: multi-scan (SADABS; Bruker, 2000)
T_{min} = 0.903, T_{max} = 0.939
13632 measured reflections
5145 independent reflections
2852 reflections with $I > 2\sigma(I)$
R_{int} = 0.046
θ_{max} = 26.0°, θ_{min} = 1.5°
h = −16→13
k = −8→9
l = −33→34

Refinement

Refinement on F^2
Least-squares matrix: full
$R[F^2 > 2\sigma(F^2)]$ = 0.049
$wR(F^2)$ = 0.103
S = 0.88
5145 reflections
367 parameters
0 restraints
Hydrogen site location: inferred from neighbouring sites
Only H-atom displacement parameters refined

$w = 1/[\sigma^2(F_o^2) + (0.0408P)^2]$
where $P = (F_o^2 + 2F_c^2)/3$
$(\Delta/\sigma)_{max} < 0.001$

$\Delta\rho_{max} = 0.15$ e Å^{-3}
$\Delta\rho_{min} = -0.22$ e Å^{-3}

Special details

Geometry. All esds (except the esd in the dihedral angle between two l.s. planes) are estimated using the full covariance matrix. The cell esds are taken into account individually in the estimation of esds in distances, angles and torsion angles; correlations between esds in cell parameters are only used when they are defined by crystal symmetry. An approximate (isotropic) treatment of cell esds is used for estimating esds involving l.s. planes.

Refinement. Refinement of F^2 against ALL reflections. The weighted R-factor wR and goodness of fit S are based on F^2, conventional R-factors R are based on F, with F set to zero for negative F^2. The threshold expression of $F^2 > 2\text{sigma}(F^2)$ is used only for calculating R-factors(gt) etc. and is not relevant to the choice of reflections for refinement. R-factors based on F^2 are statistically about twice as large as those based on F, and R- factors based on ALL data will be even larger.

Fractional atomic coordinates and isotropic or equivalent isotropic displacement parameters (Å²)

	x	*y*	*z*	U_{iso}*/U_{eq}
C1	0.83514 (13)	0.3197 (2)	0.09431 (6)	0.0363 (4)
C2	0.92588 (13)	0.2300 (2)	0.07841 (6)	0.0378 (5)
C3	0.94898 (15)	0.0495 (3)	0.08906 (7)	0.0474 (5)
H3	0.904843	−0.018427	0.105749	0.060 (6)*
C4	1.03531 (16)	−0.0314 (3)	0.07558 (8)	0.0600 (6)
H4	1.049033	−0.153332	0.082980	0.069 (7)*
C5	1.10143 (19)	0.0661 (3)	0.05130 (8)	0.0713 (7)
H5	1.160256	0.011204	0.042183	0.084 (8)*
C6	1.08036 (19)	0.2454 (4)	0.04047 (9)	0.0768 (7)
H6	1.125208	0.312545	0.023980	0.089 (8)*
C7	0.99353 (16)	0.3268 (3)	0.05380 (7)	0.0592 (6)
H7	0.980068	0.448615	0.046176	0.051 (6)*
C8	0.82392 (13)	0.5230 (2)	0.08899 (6)	0.0377 (4)
C9	0.74742 (14)	0.5987 (3)	0.05028 (7)	0.0437 (5)
C10	0.70293 (18)	0.4886 (4)	0.01317 (8)	0.0734 (7)
H10	0.720298	0.365746	0.013003	0.079 (8)*
C11	0.6329 (2)	0.5586 (5)	−0.02378 (10)	0.1124 (11)
H11	0.603863	0.483089	−0.048881	0.153 (13)*
C12	0.6059 (2)	0.7378 (5)	−0.02370 (11)	0.1102 (11)
H12	0.558179	0.784282	−0.048581	0.119 (10)*
C13	0.64870 (18)	0.8485 (4)	0.01274 (10)	0.0823 (8)
H13	0.630452	0.970999	0.012709	0.077 (8)*
C14	0.71892 (15)	0.7801 (3)	0.04968 (8)	0.0580 (6)
H14	0.747607	0.856790	0.074567	0.066 (7)*
C15	0.99888 (13)	0.6384 (3)	0.18379 (7)	0.0411 (5)
H15	0.984927	0.762714	0.183158	0.046 (5)*
C16	1.07404 (13)	0.5654 (2)	0.22132 (6)	0.0385 (5)
C17	1.12335 (12)	0.3906 (3)	0.22344 (6)	0.0369 (4)
C18	1.12274 (14)	0.2432 (3)	0.19159 (7)	0.0439 (5)
H18	1.084885	0.248467	0.160739	0.042 (5)*
C19	1.17878 (15)	0.0908 (3)	0.20652 (8)	0.0539 (6)
H19	1.177756	−0.008483	0.185639	0.058 (6)*

C20	1.23696 (15)	0.0810 (3)	0.25202 (8)	0.0580 (6)
H20	1.274298	−0.024387	0.261014	0.061 (6)*
C21	1.24053 (15)	0.2222 (3)	0.28373 (8)	0.0544 (6)
H21	1.280095	0.215710	0.314160	0.055 (6)*
C22	1.18325 (13)	0.3765 (3)	0.26927 (7)	0.0416 (5)
C23	1.10613 (14)	0.6476 (3)	0.26490 (7)	0.0486 (5)
H23	1.086467	0.763553	0.273594	0.043 (5)*
C24	0.62285 (14)	0.2475 (3)	0.14849 (7)	0.0484 (5)
H24	0.634232	0.123968	0.154452	0.048 (6)*
C25	0.53425 (14)	0.3321 (3)	0.16411 (7)	0.0505 (5)
C26	0.49308 (14)	0.5105 (3)	0.15329 (7)	0.0505 (5)
C27	0.52005 (16)	0.6557 (3)	0.12573 (8)	0.0562 (6)
H27	0.579267	0.650487	0.110411	0.052 (6)*
C28	0.45807 (19)	0.8070 (3)	0.12143 (10)	0.0786 (7)
H28	0.476153	0.905300	0.103174	0.076 (8)*
C29	0.3689 (2)	0.8173 (4)	0.14363 (12)	0.1049 (10)
H29	0.328037	0.921466	0.139702	0.122 (10)*
C30	0.3405 (2)	0.6771 (4)	0.17108 (12)	0.1036 (10)
H30	0.281159	0.683543	0.186279	0.101 (9)*
C31	0.40318 (18)	0.5254 (4)	0.17543 (10)	0.0733 (7)
C32	0.46970 (18)	0.2500 (4)	0.19247 (9)	0.0773 (7)
H32	0.477661	0.132346	0.204873	0.071 (7)*
N1	0.76775 (11)	0.2260 (2)	0.11353 (5)	0.0405 (4)
N2	0.68695 (11)	0.3368 (2)	0.12654 (5)	0.0433 (4)
N3	0.88012 (11)	0.6319 (2)	0.11766 (5)	0.0419 (4)
N4	0.95074 (11)	0.5349 (2)	0.15116 (5)	0.0432 (4)
N5	1.17037 (12)	0.5365 (2)	0.29348 (6)	0.0519 (5)
H35	1.198934	0.561788	0.322448	0.065 (7)*
N6	0.39279 (16)	0.3652 (3)	0.19973 (9)	0.0954 (8)
H36	0.344338	0.341855	0.217039	0.103 (9)*

Atomic displacement parameters (Å²)

	U^{11}	U^{22}	U^{33}	U^{12}	U^{13}	U^{23}
C1	0.0382 (11)	0.0372 (11)	0.0317 (10)	−0.0033 (9)	−0.0014 (9)	0.0022 (9)
C2	0.0403 (11)	0.0408 (12)	0.0317 (10)	−0.0045 (9)	0.0029 (9)	0.0017 (9)
C3	0.0471 (12)	0.0435 (13)	0.0517 (12)	−0.0016 (10)	0.0076 (10)	−0.0016 (11)
C4	0.0624 (15)	0.0486 (15)	0.0702 (16)	0.0082 (12)	0.0130 (12)	−0.0046 (12)
C5	0.0667 (17)	0.0754 (18)	0.0768 (17)	0.0164 (15)	0.0276 (14)	−0.0022 (15)
C6	0.0735 (17)	0.0847 (19)	0.0810 (18)	0.0034 (15)	0.0430 (15)	0.0145 (16)
C7	0.0676 (15)	0.0539 (15)	0.0602 (14)	0.0078 (12)	0.0244 (12)	0.0141 (12)
C8	0.0348 (10)	0.0393 (12)	0.0395 (11)	−0.0019 (9)	0.0063 (9)	0.0061 (9)
C9	0.0402 (11)	0.0441 (12)	0.0460 (12)	−0.0054 (10)	0.0029 (9)	0.0133 (10)
C10	0.0896 (19)	0.0590 (17)	0.0626 (15)	−0.0068 (14)	−0.0226 (14)	0.0078 (13)
C11	0.139 (3)	0.095 (2)	0.084 (2)	−0.016 (2)	−0.059 (2)	0.0148 (19)
C12	0.100 (2)	0.109 (3)	0.104 (2)	−0.008 (2)	−0.0505 (19)	0.045 (2)
C13	0.0655 (16)	0.0687 (19)	0.107 (2)	0.0087 (15)	−0.0107 (15)	0.0384 (17)
C14	0.0476 (13)	0.0526 (14)	0.0711 (15)	−0.0012 (11)	−0.0019 (12)	0.0162 (13)

C15	0.0357 (11)	0.0341 (12)	0.0541 (13)	0.0003 (9)	0.0086 (10)	−0.0037 (10)
C16	0.0303 (10)	0.0425 (12)	0.0421 (11)	−0.0002 (9)	0.0028 (9)	−0.0082 (10)
C17	0.0279 (10)	0.0447 (12)	0.0384 (11)	−0.0037 (9)	0.0052 (8)	−0.0024 (9)
C18	0.0381 (11)	0.0480 (13)	0.0445 (12)	0.0010 (10)	0.0016 (9)	−0.0051 (10)
C19	0.0461 (13)	0.0457 (13)	0.0700 (15)	0.0040 (11)	0.0084 (11)	−0.0045 (13)
C20	0.0451 (13)	0.0558 (15)	0.0730 (16)	0.0089 (12)	0.0069 (12)	0.0171 (13)
C21	0.0378 (12)	0.0779 (17)	0.0457 (13)	0.0011 (12)	−0.0010 (10)	0.0176 (13)
C22	0.0323 (10)	0.0540 (13)	0.0388 (11)	−0.0034 (10)	0.0059 (9)	0.0001 (10)
C23	0.0365 (11)	0.0500 (14)	0.0592 (13)	−0.0020 (10)	0.0054 (10)	−0.0159 (11)
C24	0.0394 (12)	0.0478 (14)	0.0568 (13)	−0.0046 (10)	0.0017 (10)	0.0080 (11)
C25	0.0363 (12)	0.0561 (14)	0.0599 (14)	−0.0085 (11)	0.0097 (10)	0.0034 (11)
C26	0.0360 (12)	0.0565 (14)	0.0593 (14)	−0.0070 (10)	0.0076 (10)	−0.0086 (12)
C27	0.0464 (13)	0.0570 (15)	0.0650 (15)	−0.0012 (12)	0.0071 (11)	−0.0049 (12)
C28	0.0728 (18)	0.0533 (16)	0.112 (2)	0.0033 (14)	0.0201 (16)	−0.0005 (16)
C29	0.078 (2)	0.070 (2)	0.173 (3)	0.0164 (18)	0.040 (2)	−0.009 (2)
C30	0.0711 (19)	0.083 (2)	0.169 (3)	0.0079 (17)	0.061 (2)	−0.018 (2)
C31	0.0542 (15)	0.0665 (17)	0.105 (2)	−0.0063 (14)	0.0320 (14)	−0.0091 (16)
C32	0.0602 (16)	0.0682 (18)	0.109 (2)	−0.0021 (14)	0.0310 (15)	0.0156 (16)
N1	0.0377 (9)	0.0403 (9)	0.0432 (9)	0.0002 (8)	0.0047 (8)	0.0053 (8)
N2	0.0371 (9)	0.0443 (10)	0.0486 (10)	−0.0012 (8)	0.0064 (8)	0.0054 (8)
N3	0.0391 (9)	0.0377 (10)	0.0472 (9)	0.0001 (8)	−0.0012 (8)	0.0063 (8)
N4	0.0424 (9)	0.0375 (9)	0.0471 (10)	0.0013 (8)	−0.0034 (8)	0.0011 (8)
N5	0.0405 (10)	0.0736 (13)	0.0397 (10)	−0.0041 (9)	−0.0013 (8)	−0.0112 (10)
N6	0.0672 (14)	0.0917 (18)	0.141 (2)	−0.0066 (13)	0.0629 (15)	0.0055 (16)

Geometric parameters (Å, º)

C1—N1	1.286 (2)	C18—C19	1.370 (2)
C1—C2	1.471 (2)	C18—H18	0.9300
C1—C8	1.505 (2)	C19—C20	1.385 (3)
C2—C7	1.382 (2)	C19—H19	0.9300
C2—C3	1.382 (2)	C20—C21	1.357 (3)
C3—C4	1.367 (3)	C20—H20	0.9300
C3—H3	0.9300	C21—C22	1.386 (3)
C4—C5	1.365 (3)	C21—H21	0.9300
C4—H4	0.9300	C22—N5	1.374 (2)
C5—C6	1.370 (3)	C23—N5	1.348 (2)
C5—H5	0.9300	C23—H23	0.9300
C6—C7	1.373 (3)	C24—N2	1.278 (2)
C6—H6	0.9300	C24—C25	1.428 (3)
C7—H7	0.9300	C24—H24	0.9300
C8—N3	1.286 (2)	C25—C32	1.367 (3)
C8—C9	1.473 (2)	C25—C26	1.431 (3)
C9—C10	1.375 (3)	C26—C27	1.384 (3)
C9—C14	1.382 (3)	C26—C31	1.398 (3)
C10—C11	1.378 (3)	C27—C28	1.369 (3)
C10—H10	0.9300	C27—H27	0.9300
C11—C12	1.361 (4)	C28—C29	1.387 (3)

C11—H11	0.9300	C28—H28	0.9300
C12—C13	1.358 (3)	C29—C30	1.361 (4)
C12—H12	0.9300	C29—H29	0.9300
C13—C14	1.374 (3)	C30—C31	1.376 (3)
C13—H13	0.9300	C30—H30	0.9300
C14—H14	0.9300	C31—N6	1.371 (3)
C15—N4	1.280 (2)	C32—N6	1.347 (3)
C15—C16	1.435 (2)	C32—H32	0.9300
C15—H15	0.9300	N1—N2	1.4146 (19)
C16—C23	1.367 (2)	N3—N4	1.4104 (18)
C16—C17	1.432 (2)	N5—H35	0.8600
C17—C18	1.397 (2)	N6—H36	0.8600
C17—C22	1.404 (2)		

N1—C1—C2	120.37 (17)	C17—C18—H18	120.5
N1—C1—C8	120.56 (16)	C18—C19—C20	121.5 (2)
C2—C1—C8	119.05 (16)	C18—C19—H19	119.2
C7—C2—C3	117.65 (19)	C20—C19—H19	119.2
C7—C2—C1	120.61 (18)	C21—C20—C19	121.3 (2)
C3—C2—C1	121.69 (17)	C21—C20—H20	119.4
C4—C3—C2	121.4 (2)	C19—C20—H20	119.4
C4—C3—H3	119.3	C20—C21—C22	117.78 (19)
C2—C3—H3	119.3	C20—C21—H21	121.1
C5—C4—C3	120.2 (2)	C22—C21—H21	121.1
C5—C4—H4	119.9	N5—C22—C21	130.74 (18)
C3—C4—H4	119.9	N5—C22—C17	106.91 (17)
C4—C5—C6	119.4 (2)	C21—C22—C17	122.34 (19)
C4—C5—H5	120.3	N5—C23—C16	110.24 (18)
C6—C5—H5	120.3	N5—C23—H23	124.9
C5—C6—C7	120.5 (2)	C16—C23—H23	124.9
C5—C6—H6	119.8	N2—C24—C25	121.8 (2)
C7—C6—H6	119.8	N2—C24—H24	119.1
C6—C7—C2	120.8 (2)	C25—C24—H24	119.1
C6—C7—H7	119.6	C32—C25—C24	124.6 (2)
C2—C7—H7	119.6	C32—C25—C26	106.42 (19)
N3—C8—C9	119.37 (17)	C24—C25—C26	129.00 (19)
N3—C8—C1	121.09 (16)	C27—C26—C31	118.2 (2)
C9—C8—C1	119.54 (16)	C27—C26—C25	134.79 (19)
C10—C9—C14	118.1 (2)	C31—C26—C25	107.0 (2)
C10—C9—C8	120.07 (19)	C28—C27—C26	118.9 (2)
C14—C9—C8	121.78 (19)	C28—C27—H27	120.6
C9—C10—C11	120.6 (3)	C26—C27—H27	120.6
C9—C10—H10	119.7	C27—C28—C29	121.6 (3)
C11—C10—H10	119.7	C27—C28—H28	119.2
C12—C11—C10	120.3 (3)	C29—C28—H28	119.2
C12—C11—H11	119.9	C30—C29—C28	120.9 (3)
C10—C11—H11	119.9	C30—C29—H29	119.5
C13—C12—C11	119.9 (3)	C28—C29—H29	119.5

C13—C12—H12	120.0	C29—C30—C31	117.3 (3)
C11—C12—H12	120.0	C29—C30—H30	121.4
C12—C13—C14	120.2 (3)	C31—C30—H30	121.4
C12—C13—H13	119.9	N6—C31—C30	129.8 (2)
C14—C13—H13	119.9	N6—C31—C26	107.0 (2)
C13—C14—C9	120.8 (2)	C30—C31—C26	123.2 (3)
C13—C14—H14	119.6	N6—C32—C25	109.6 (2)
C9—C14—H14	119.6	N6—C32—H32	125.2
N4—C15—C16	120.91 (17)	C25—C32—H32	125.2
N4—C15—H15	119.5	C1—N1—N2	111.77 (15)
C16—C15—H15	119.5	C24—N2—N1	112.49 (16)
C23—C16—C17	106.07 (16)	C8—N3—N4	111.16 (15)
C23—C16—C15	125.16 (17)	C15—N4—N3	112.39 (15)
C17—C16—C15	128.56 (16)	C23—N5—C22	109.62 (16)
C18—C17—C22	118.16 (17)	C23—N5—H35	125.2
C18—C17—C16	134.69 (17)	C22—N5—H35	125.2
C22—C17—C16	107.15 (16)	C32—N6—C31	109.9 (2)
C19—C18—C17	118.92 (18)	C32—N6—H36	125.0
C19—C18—H18	120.5	C31—N6—H36	125.0

Hydrogen-bond geometry (Å, º)

D—H···*A*	*D*—H	H···*A*	*D*···*A*	*D*—H···*A*
N5—H35···N1^{i}	0.86	2.14	2.948 (2)	156
C3—H3···N3^{ii}	0.93	2.61	3.320 (3)	133

Symmetry codes: (i) −*x*+2, *y*+1/2, −*z*+1/2; (ii) *x*, *y*−1, *z*.

(1*Z*,2*Z*)-1,2-Bis{(*E*)-[1-(1*H*-indol-3-yl)ethylidene]hydrazinylidene}-1,2-diphenylethane (2-BDHAI)

Crystal data

$C_{34}H_{28}N_6$
M_r = 520.62
Triclinic, $P\overline{1}$
a = 10.2585 (4) Å
b = 11.9610 (5) Å
c = 12.8232 (6) Å
α = 64.941 (4)°
β = 79.573 (3)°
γ = 76.829 (4)°
V = 1381.45 (11) Å^3

Z = 2
F(000) = 548
D_x = 1.252 Mg m^{-3}
Mo *Kα* radiation, *λ* = 0.71073 Å
Cell parameters from 380 reflections
θ = 2.5–26.0°
μ = 0.08 mm^{-1}
T = 293 K
Bar, yellow
0.35 × 0.15 × 0.12 mm

Data collection

Bruker SMART CCD area detector diffractometer
Radiation source: fine-focus sealed tube
Detector resolution: 10.13 pixels mm^{-1}
phi and *ω* scans
Absorption correction: multi-scan (SADABS; Bruker, 2000)
T_{min} = 0.903, T_{max} = 0.939

15195 measured reflections
5328 independent reflections
4490 reflections with $I > 2\sigma(I)$
R_{int} = 0.026
θ_{max} = 26.0°, θ_{min} = 1.8°
h = −12→12
k = −14→14
l = −13→15

Refinement

Refinement on F^2
Least-squares matrix: full
$R[F^2 > 2\sigma(F^2)] = 0.044$
$wR(F^2) = 0.129$
$S = 1.05$
5328 reflections
392 parameters
0 restraints
Hydrogen site location: inferred from neighbouring sites
Only H-atom displacement parameters refined
$w = 1/[\sigma^2(F_o^2) + (0.0694P)^2 + 0.1725P]$ where $P = (F_o^2 + 2F_c^2)/3$
$(\Delta/\sigma)_{max} < 0.001$
$\Delta\rho_{max} = 0.19$ e Å^{-3}
$\Delta\rho_{min} = -0.18$ e Å^{-3}
Extinction correction: SHELXL2016 (Sheldrick, 2015b), $Fc^*=kFc[1+0.001xFc^2\lambda^3/\sin(2\theta)]^{-1/4}$
Extinction coefficient: 0.083 (4)

Special details

Geometry. All esds (except the esd in the dihedral angle between two l.s. planes) are estimated using the full covariance matrix. The cell esds are taken into account individually in the estimation of esds in distances, angles and torsion angles; correlations between esds in cell parameters are only used when they are defined by crystal symmetry. An approximate (isotropic) treatment of cell esds is used for estimating esds involving l.s. planes.

Refinement. Refinement of F^2 against ALL reflections. The weighted R-factor wR and goodness of fit S are based on F^2, conventional R-factors R are based on F, with F set to zero for negative F^2. The threshold expression of $F^2 > 2$sigma(F^2) is used only for calculating R-factors(gt) etc. and is not relevant to the choice of reflections for refinement. R-factors based on F^2 are statistically about twice as large as those based on F, and R- factors based on ALL data will be even larger.

Fractional atomic coordinates and isotropic or equivalent isotropic displacement parameters (Å²)

	x	*y*	*z*	U_{iso}*/U_{eq}
C1	0.21600 (13)	0.84926 (13)	0.45306 (11)	0.0462 (3)
C2	0.24638 (13)	0.97764 (13)	0.38744 (12)	0.0491 (3)
C3	0.15001 (16)	1.07464 (15)	0.32585 (16)	0.0648 (4)
H2	0.067148	1.057647	0.322519	0.081 (6)*
C4	0.17520 (19)	1.19565 (16)	0.26959 (17)	0.0746 (5)
H3	0.109933	1.259075	0.227799	0.097 (7)*
C5	0.2954 (2)	1.22291 (17)	0.27488 (16)	0.0739 (5)
H4	0.311226	1.304989	0.238380	0.085 (6)*
C6	0.3928 (2)	1.12876 (18)	0.33426 (16)	0.0747 (5)
H5	0.474994	1.147161	0.337453	0.092 (6)*
C7	0.36938 (16)	1.00565 (16)	0.38983 (14)	0.0618 (4)
H6	0.436524	0.942110	0.428646	0.072 (5)*
C8	0.32668 (13)	0.74348 (13)	0.50875 (12)	0.0483 (3)
C9	0.34159 (15)	0.70585 (14)	0.63212 (12)	0.0551 (4)
C10	0.26077 (17)	0.77226 (18)	0.69346 (14)	0.0658 (4)
H7	0.196310	0.840386	0.656770	0.065 (5)*
C11	0.2755 (2)	0.7377 (2)	0.80900 (17)	0.0877 (6)
H10	0.221187	0.782867	0.849312	0.088 (6)*
C12	0.3700 (3)	0.6372 (3)	0.86403 (18)	0.1028 (8)
H12	0.379338	0.613722	0.941672	0.113 (8)*
C13	0.4506 (3)	0.5713 (2)	0.80406 (19)	0.0961 (7)
H13	0.514323	0.502950	0.841665	0.118 (8)*
C14	0.4385 (2)	0.60529 (17)	0.68842 (16)	0.0721 (5)
H11	0.495074	0.560945	0.648337	0.099 (7)*
C15	0.49611 (13)	0.72877 (13)	0.26579 (13)	0.0491 (3)

C16	0.48156 (13)	0.78461 (14)	0.14310 (13)	0.0501 (3)
C17	0.36770 (13)	0.86989 (13)	0.08418 (12)	0.0484 (3)
C18	0.24161 (14)	0.92420 (14)	0.11937 (14)	0.0546 (4)
H18	0.214228	0.904063	0.197491	0.058 (4)*
C19	0.15878 (17)	1.00782 (16)	0.03671 (16)	0.0668 (4)
H19	0.074912	1.044421	0.059733	0.071 (5)*
C20	0.19753 (19)	1.03927 (18)	−0.08130 (17)	0.0753 (5)
H20	0.138681	1.095426	−0.135092	0.091 (6)*
C21	0.32077 (19)	0.98860 (17)	−0.11877 (16)	0.0722 (5)
H21	0.347018	1.009515	−0.197140	0.085 (6)*
C22	0.40519 (15)	0.90475 (15)	−0.03532 (14)	0.0580 (4)
C23	0.57959 (16)	0.77510 (17)	0.05713 (15)	0.0646 (4)
H23	0.665006	0.727371	0.069683	0.077 (5)*
C24	−0.03270 (14)	0.68082 (14)	0.52381 (12)	0.0518 (3)
C25	−0.07215 (13)	0.56489 (14)	0.61098 (13)	0.0506 (3)
C26	−0.03001 (13)	0.49580 (13)	0.72570 (12)	0.0466 (3)
C27	0.05813 (13)	0.51142 (13)	0.78861 (13)	0.0493 (3)
H27	0.108227	0.575950	0.754067	0.056 (4)*
C28	0.06910 (15)	0.42989 (14)	0.90189 (14)	0.0572 (4)
H28	0.126490	0.440283	0.944331	0.063 (4)*
C29	−0.00429 (17)	0.33154 (16)	0.95472 (15)	0.0654 (4)
H29	0.005442	0.277666	1.031582	0.076 (5)*
C30	−0.09047 (17)	0.31280 (15)	0.89550 (14)	0.0638 (4)
H30	−0.139175	0.247275	0.930808	0.067 (5)*
C31	−0.10219 (14)	0.39519 (14)	0.78113 (13)	0.0523 (3)
C32	−0.16427 (15)	0.50232 (15)	0.60219 (14)	0.0587 (4)
H32	−0.208006	0.525861	0.536678	0.069 (5)*
C33	0.63359 (15)	0.6710 (2)	0.30611 (17)	0.0733 (5)
H33A	0.627256	0.598418	0.377122	0.100 (7)*
H33B	0.670603	0.730677	0.318564	0.135 (10)*
H33C	0.690878	0.646881	0.248427	0.141 (10)*
C34	−0.1161 (2)	0.7575 (2)	0.42427 (18)	0.0840 (6)
H34A	−0.209716	0.760959	0.451964	0.145 (10)*
H34B	−0.096409	0.719957	0.369015	0.187 (15)*
H34C	−0.095464	0.840849	0.388088	0.162 (12)*
N1	0.09402 (11)	0.83288 (11)	0.46297 (10)	0.0520 (3)
N2	0.07283 (11)	0.71200 (11)	0.53875 (10)	0.0511 (3)
N3	0.41191 (12)	0.68906 (12)	0.45120 (11)	0.0548 (3)
N4	0.38813 (11)	0.73680 (11)	0.33433 (10)	0.0519 (3)
N5	0.53458 (14)	0.84467 (15)	−0.04798 (13)	0.0703 (4)
H35	0.579886	0.850515	−0.112912	0.078 (6)*
N6	−0.18231 (13)	0.40170 (13)	0.70225 (12)	0.0616 (3)
H36	−0.235238	0.350076	0.714696	0.067 (5)*

Atomic displacement parameters (Å²)

	U^{11}	U^{22}	U^{33}	U^{12}	U^{13}	U^{23}
C1	0.0423 (7)	0.0552 (8)	0.0428 (7)	−0.0102 (6)	−0.0023 (5)	−0.0209 (6)

C2	0.0477 (7)	0.0542 (8)	0.0474 (7)	−0.0112 (6)	0.0035 (6)	−0.0240 (6)
C3	0.0527 (9)	0.0554 (9)	0.0832 (12)	−0.0035 (7)	−0.0033 (8)	−0.0290 (8)
C4	0.0773 (12)	0.0530 (9)	0.0828 (12)	0.0011 (8)	−0.0006 (9)	−0.0258 (9)
C5	0.0939 (13)	0.0564 (10)	0.0705 (11)	−0.0265 (9)	0.0144 (10)	−0.0263 (9)
C6	0.0774 (12)	0.0841 (12)	0.0683 (11)	−0.0422 (10)	0.0061 (9)	−0.0267 (10)
C7	0.0584 (9)	0.0682 (10)	0.0558 (9)	−0.0233 (8)	−0.0028 (7)	−0.0168 (8)
C8	0.0423 (7)	0.0525 (7)	0.0497 (7)	−0.0145 (6)	−0.0069 (5)	−0.0159 (6)
C9	0.0551 (8)	0.0637 (9)	0.0482 (8)	−0.0273 (7)	−0.0065 (6)	−0.0146 (7)
C10	0.0615 (9)	0.0890 (12)	0.0559 (9)	−0.0315 (9)	0.0007 (7)	−0.0307 (9)
C11	0.0973 (15)	0.1285 (18)	0.0574 (11)	−0.0604 (14)	0.0098 (10)	−0.0423 (12)
C12	0.135 (2)	0.129 (2)	0.0500 (11)	−0.0707 (17)	−0.0199 (12)	−0.0125 (12)
C13	0.1239 (19)	0.0874 (14)	0.0670 (13)	−0.0360 (13)	−0.0424 (13)	0.0009 (11)
C14	0.0827 (12)	0.0656 (10)	0.0621 (10)	−0.0199 (9)	−0.0247 (9)	−0.0091 (8)
C15	0.0371 (7)	0.0541 (8)	0.0646 (9)	−0.0047 (5)	−0.0092 (6)	−0.0316 (7)
C16	0.0397 (7)	0.0592 (8)	0.0596 (8)	−0.0084 (6)	−0.0049 (6)	−0.0314 (7)
C17	0.0443 (7)	0.0536 (8)	0.0555 (8)	−0.0133 (6)	−0.0074 (6)	−0.0260 (6)
C18	0.0440 (7)	0.0601 (9)	0.0617 (9)	−0.0089 (6)	−0.0080 (6)	−0.0249 (7)
C19	0.0504 (8)	0.0666 (10)	0.0792 (11)	−0.0039 (7)	−0.0157 (8)	−0.0245 (9)
C20	0.0709 (11)	0.0730 (11)	0.0739 (12)	−0.0109 (9)	−0.0270 (9)	−0.0144 (9)
C21	0.0812 (12)	0.0785 (12)	0.0560 (10)	−0.0214 (9)	−0.0127 (8)	−0.0197 (9)
C22	0.0572 (9)	0.0658 (9)	0.0582 (9)	−0.0174 (7)	−0.0040 (7)	−0.0287 (8)
C23	0.0454 (8)	0.0799 (11)	0.0728 (11)	−0.0033 (7)	−0.0008 (7)	−0.0403 (9)
C24	0.0452 (7)	0.0626 (8)	0.0514 (8)	−0.0116 (6)	−0.0077 (6)	−0.0238 (7)
C25	0.0412 (7)	0.0605 (8)	0.0553 (8)	−0.0120 (6)	−0.0053 (6)	−0.0261 (7)
C26	0.0370 (6)	0.0511 (7)	0.0550 (8)	−0.0065 (5)	−0.0015 (5)	−0.0259 (6)
C27	0.0393 (7)	0.0533 (8)	0.0597 (8)	−0.0076 (6)	−0.0050 (6)	−0.0268 (7)
C28	0.0507 (8)	0.0632 (9)	0.0612 (9)	−0.0041 (7)	−0.0113 (7)	−0.0285 (8)
C29	0.0717 (10)	0.0629 (9)	0.0559 (9)	−0.0118 (8)	−0.0085 (7)	−0.0173 (8)
C30	0.0667 (10)	0.0600 (9)	0.0637 (10)	−0.0212 (8)	−0.0015 (7)	−0.0205 (8)
C31	0.0451 (7)	0.0556 (8)	0.0615 (9)	−0.0124 (6)	−0.0015 (6)	−0.0279 (7)
C32	0.0517 (8)	0.0719 (10)	0.0592 (9)	−0.0199 (7)	−0.0093 (7)	−0.0264 (8)
C33	0.0415 (8)	0.1008 (14)	0.0788 (12)	0.0007 (8)	−0.0161 (8)	−0.0393 (12)
C34	0.0788 (13)	0.0926 (14)	0.0750 (12)	−0.0343 (10)	−0.0343 (10)	−0.0076 (11)
N1	0.0446 (6)	0.0569 (7)	0.0529 (7)	−0.0122 (5)	−0.0037 (5)	−0.0189 (6)
N2	0.0433 (6)	0.0556 (7)	0.0527 (7)	−0.0142 (5)	−0.0052 (5)	−0.0170 (5)
N3	0.0479 (6)	0.0619 (7)	0.0532 (7)	−0.0043 (5)	−0.0122 (5)	−0.0211 (6)
N4	0.0417 (6)	0.0623 (7)	0.0527 (7)	−0.0022 (5)	−0.0094 (5)	−0.0253 (6)
N5	0.0636 (8)	0.0916 (10)	0.0592 (8)	−0.0122 (7)	0.0065 (7)	−0.0386 (8)
N6	0.0556 (7)	0.0690 (8)	0.0689 (8)	−0.0282 (6)	−0.0055 (6)	−0.0271 (7)

Geometric parameters (Å, º)

C1—N1	1.2858 (17)	C19—H19	0.9300
C1—C2	1.4805 (19)	C20—C21	1.369 (3)
C1—C8	1.5078 (19)	C20—H20	0.9300
C2—C7	1.386 (2)	C21—C22	1.390 (2)
C2—C3	1.390 (2)	C21—H21	0.9300
C3—C4	1.379 (2)	C22—N5	1.375 (2)

C3—H2	0.9300	C23—N5	1.350 (2)
C4—C5	1.365 (3)	C23—H23	0.9300
C4—H3	0.9300	C24—N2	1.2913 (17)
C5—C6	1.372 (3)	C24—C25	1.454 (2)
C5—H4	0.9300	C24—C34	1.499 (2)
C6—C7	1.394 (2)	C25—C32	1.3777 (19)
C6—H5	0.9300	C25—C26	1.439 (2)
C7—H6	0.9300	C26—C27	1.4042 (19)
C8—N3	1.2832 (18)	C26—C31	1.4116 (19)
C8—C9	1.4771 (19)	C27—C28	1.372 (2)
C9—C10	1.389 (2)	C27—H27	0.9300
C9—C14	1.391 (2)	C28—C29	1.398 (2)
C10—C11	1.387 (2)	C28—H28	0.9300
C10—H7	0.9300	C29—C30	1.373 (2)
C11—C12	1.371 (3)	C29—H29	0.9300
C11—H10	0.9300	C30—C31	1.386 (2)
C12—C13	1.372 (4)	C30—H30	0.9300
C12—H12	0.9300	C31—N6	1.3819 (19)
C13—C14	1.383 (3)	C32—N6	1.355 (2)
C13—H13	0.9300	C32—H32	0.9300
C14—H11	0.9300	C33—H33A	0.9600
C15—N4	1.2959 (17)	C33—H33B	0.9600
C15—C16	1.447 (2)	C33—H33C	0.9600
C15—C33	1.5004 (19)	C34—H34A	0.9600
C16—C23	1.376 (2)	C34—H34B	0.9600
C16—C17	1.4489 (19)	C34—H34C	0.9600
C17—C18	1.397 (2)	N1—N2	1.3995 (16)
C17—C22	1.410 (2)	N3—N4	1.4055 (16)
C18—C19	1.374 (2)	N5—H35	0.8600
C18—H18	0.9300	N6—H36	0.8600
C19—C20	1.399 (3)		

N1—C1—C2	118.19 (12)	C19—C20—H20	119.5
N1—C1—C8	122.27 (12)	C20—C21—C22	117.52 (17)
C2—C1—C8	119.51 (11)	C20—C21—H21	121.2
C7—C2—C3	118.12 (14)	C22—C21—H21	121.2
C7—C2—C1	121.02 (13)	N5—C22—C21	129.92 (16)
C3—C2—C1	120.80 (13)	N5—C22—C17	107.44 (14)
C4—C3—C2	121.09 (16)	C21—C22—C17	122.61 (15)
C4—C3—H2	119.5	N5—C23—C16	110.58 (14)
C2—C3—H2	119.5	N5—C23—H23	124.7
C5—C4—C3	120.37 (17)	C16—C23—H23	124.7
C5—C4—H3	119.8	N2—C24—C25	116.86 (13)
C3—C4—H3	119.8	N2—C24—C34	123.95 (14)
C4—C5—C6	119.76 (16)	C25—C24—C34	119.18 (13)
C4—C5—H4	120.1	C32—C25—C26	105.77 (13)
C6—C5—H4	120.1	C32—C25—C24	126.47 (14)
C5—C6—C7	120.38 (16)	C26—C25—C24	127.68 (12)

C5—C6—H5	119.8	C27—C26—C31	118.54 (13)
C7—C6—H5	119.8	C27—C26—C25	134.21 (13)
C2—C7—C6	120.25 (16)	C31—C26—C25	107.20 (12)
C2—C7—H6	119.9	C28—C27—C26	118.90 (13)
C6—C7—H6	119.9	C28—C27—H27	120.5
N3—C8—C9	118.99 (13)	C26—C27—H27	120.5
N3—C8—C1	122.12 (12)	C27—C28—C29	121.28 (15)
C9—C8—C1	118.80 (12)	C27—C28—H28	119.4
C10—C9—C14	118.74 (16)	C29—C28—H28	119.4
C10—C9—C8	120.44 (14)	C30—C29—C28	121.37 (15)
C14—C9—C8	120.81 (15)	C30—C29—H29	119.3
C11—C10—C9	120.5 (2)	C28—C29—H29	119.3
C11—C10—H7	119.8	C29—C30—C31	117.54 (15)
C9—C10—H7	119.8	C29—C30—H30	121.2
C12—C11—C10	120.2 (2)	C31—C30—H30	121.2
C12—C11—H10	119.9	N6—C31—C30	130.41 (14)
C10—C11—H10	119.9	N6—C31—C26	107.20 (13)
C11—C12—C13	119.71 (19)	C30—C31—C26	122.35 (14)
C11—C12—H12	120.1	N6—C32—C25	110.60 (13)
C13—C12—H12	120.1	N6—C32—H32	124.7
C12—C13—C14	120.9 (2)	C25—C32—H32	124.7
C12—C13—H13	119.6	C15—C33—H33A	109.5
C14—C13—H13	119.6	C15—C33—H33B	109.5
C13—C14—C9	119.9 (2)	H33A—C33—H33B	109.5
C13—C14—H11	120.0	C15—C33—H33C	109.5
C9—C14—H11	120.0	H33A—C33—H33C	109.5
N4—C15—C16	116.92 (12)	H33B—C33—H33C	109.5
N4—C15—C33	123.90 (14)	C24—C34—H34A	109.5
C16—C15—C33	119.11 (13)	C24—C34—H34B	109.5
C23—C16—C15	126.10 (13)	H34A—C34—H34B	109.5
C23—C16—C17	105.66 (13)	C24—C34—H34C	109.5
C15—C16—C17	128.03 (12)	H34A—C34—H34C	109.5
C18—C17—C22	118.36 (14)	H34B—C34—H34C	109.5
C18—C17—C16	134.83 (13)	C1—N1—N2	113.49 (11)
C22—C17—C16	106.73 (12)	C24—N2—N1	114.33 (12)
C19—C18—C17	118.92 (15)	C8—N3—N4	112.87 (11)
C19—C18—H18	120.5	C15—N4—N3	113.57 (11)
C17—C18—H18	120.5	C23—N5—C22	109.58 (13)
C18—C19—C20	121.59 (16)	C23—N5—H35	125.2
C18—C19—H19	119.2	C22—N5—H35	125.2
C20—C19—H19	119.2	C32—N6—C31	109.22 (12)
C21—C20—C19	120.99 (16)	C32—N6—H36	125.4
C21—C20—H20	119.5	C31—N6—H36	125.4

Hydrogen-bond geometry (Å, º)

D—H···*A*	*D*—H	H···*A*	*D*···*A*	*D*—H···*A*
N6—H36···N4^{i}	0.86	2.36	3.1675 (17)	156

C14—H11···N3	0.93	2.52	2.815 (2)	99
C18—H18···N4	0.93	2.61	3.1003 (19)	114
C27—H27···N2	0.93	2.59	3.0859 (19)	114
C34—H34*C*···N1	0.96	2.29	2.712 (2)	106

Symmetry code: (i) −*x*, −*y*+1, −*z*+1.

(1*Z*,2*Z*)-1,2-Bis{(*E*)-[(1-methyl-1*H*-indol-3-yl)\ methylidene]hydrazinylidene}-1,2-diphenylethane acetonitrile hemisolvate (3-BDHMFI)

Crystal data

$2C_{34}H_{28}N_6{\cdot}C_2H_3N$
M_r = 1082.30
Triclinic, $P\overline{1}$
a = 11.2710 (6) Å
b = 11.6944 (7) Å
c = 12.5164 (6) Å
α = 79.875 (4)°
β = 87.701 (4)°
γ = 64.941 (6)°
V = 1470.10 (15) Å^3
Z = 1
$F(000)$ = 570
D_x = 1.222 Mg m^{-3}
Mo $K\alpha$ radiation, λ = 0.71073 Å
Cell parameters from 380 reflections
θ = 2.5–26.0°
μ = 0.08 mm^{-1}
T = 293 K
Block, yellow
0.35 × 0.20 × 0.15 mm

Data collection

Bruker SMART CCD area detector diffractometer
Radiation source: fine-focus sealed tube
Detector resolution: 10.13 pixels mm^{-1}
phi and ω scans
Absorption correction: multi-scan (SADABS; Bruker, 2000)
T_{min} = 0.905, T_{max} = 0.943
13418 measured reflections
5640 independent reflections
4445 reflections with $I > 2\sigma(I)$
R_{int} = 0.029
θ_{max} = 26.0°, θ_{min} = 2.1°
h = −13→13
k = −14→14
l = −15→10

Refinement

Refinement on F^2
Least-squares matrix: full
$R[F^2 > 2\sigma(F^2)]$ = 0.049
$wR(F^2)$ = 0.151
S = 1.04
5640 reflections
424 parameters
2 restraints
Hydrogen site location: mixed
Only H-atom displacement parameters refined
$w = 1/[\sigma^2(F_o^2) + (0.0801P)^2 + 0.1656P]$ where $P = (F_o^2 + 2F_c^2)/3$
$(\Delta/\sigma)_{max}$ < 0.001
$\Delta\rho_{max}$ = 0.22 e Å^{-3}
$\Delta\rho_{min}$ = −0.17 e Å^{-3}
Extinction correction: SHELXL2016 (Sheldrick, 2015b), $Fc^*=kFc[1+0.001xFc^2\lambda^3/\sin(2\theta)]^{-1/4}$
Extinction coefficient: 0.017 (2)

Special details

Geometry. All esds (except the esd in the dihedral angle between two l.s. planes) are estimated using the full covariance matrix. The cell esds are taken into account individually in the estimation of esds in distances, angles and torsion angles; correlations between esds in cell parameters are only used when they are defined by crystal symmetry. An approximate (isotropic) treatment of cell esds is used for estimating esds involving l.s. planes.

Refinement. Refinement of F^2 against ALL reflections. The weighted R-factor wR and goodness of fit S are based on F^2, conventional R-factors R are based on F, with F set to zero for negative F^2. The threshold expression of $F^2 > 2\text{sigma}(F^2)$ is used only for calculating R-factors(gt) etc. and is not relevant to the choice of reflections for refinement. R-factors based on F^2 are statistically about twice as large as those based on F, and R- factors based on ALL data will be even larger.

Fractional atomic coordinates and isotropic or equivalent isotropic displacement parameters (Å²)

	x	*y*	*z*	U_{iso}*/U_{eq}	Occ. (<1)
C1	1.02888 (14)	0.32026 (15)	0.22614 (13)	0.0468 (4)	
C2	0.90615 (15)	0.33587 (15)	0.17364 (13)	0.0501 (4)	
C3	0.84410 (18)	0.4332 (2)	0.08691 (16)	0.0645 (5)	
H3	0.880544	0.489721	0.058970	0.072 (6)*	
C4	0.7277 (2)	0.4466 (2)	0.04165 (18)	0.0781 (6)	
H4	0.687632	0.511274	−0.017495	0.099 (8)*	
C5	0.6708 (2)	0.3663 (3)	0.0825 (2)	0.0849 (7)	
H5	0.592178	0.376884	0.051894	0.107 (9)*	
C6	0.7306 (2)	0.2703 (3)	0.1687 (2)	0.0930 (8)	
H6	0.692732	0.215144	0.196816	0.116 (10)*	
C7	0.8474 (2)	0.2552 (2)	0.21409 (19)	0.0738 (6)	
H7	0.887172	0.189680	0.272778	0.076 (6)*	
C8	1.09142 (14)	0.20654 (15)	0.31530 (13)	0.0461 (3)	
C9	1.04864 (15)	0.22239 (16)	0.42683 (13)	0.0511 (4)	
C10	0.98055 (18)	0.34437 (19)	0.45203 (16)	0.0630 (5)	
H10	0.966044	0.416152	0.399284	0.081 (7)*	
C11	0.9343 (2)	0.3596 (2)	0.55484 (18)	0.0753 (6)	
H11	0.889723	0.441633	0.570951	0.110 (9)*	
C12	0.9535 (2)	0.2554 (3)	0.63306 (18)	0.0829 (7)	
H12	0.921076	0.266331	0.701841	0.095 (8)*	
C13	1.0203 (3)	0.1356 (3)	0.60969 (18)	0.0939 (8)	
H13	1.034229	0.064590	0.663129	0.118 (10)*	
C14	1.0679 (2)	0.1181 (2)	0.50706 (17)	0.0777 (6)	
H14	1.113059	0.035600	0.492203	0.091 (7)*	
C15	1.28895 (16)	−0.00541 (16)	0.16524 (14)	0.0531 (4)	
H15	1.328560	−0.073073	0.222419	0.064 (5)*	
C16	1.33243 (15)	−0.02026 (16)	0.05718 (14)	0.0518 (4)	
C17	1.28980 (15)	0.07087 (16)	−0.04259 (14)	0.0515 (4)	
C18	1.19676 (17)	0.19828 (18)	−0.07107 (16)	0.0614 (5)	
H18	1.143422	0.241346	−0.019130	0.052 (5)*	
C19	1.1861 (2)	0.2582 (2)	−0.17750 (19)	0.0774 (6)	
H19	1.125306	0.343031	−0.196933	0.097 (8)*	
C20	1.2642 (2)	0.1949 (2)	−0.25722 (19)	0.0811 (6)	
H20	1.254078	0.238143	−0.328465	0.086 (7)*	
C21	1.3557 (2)	0.0698 (2)	−0.23207 (17)	0.0701 (5)	
H21	1.407365	0.027264	−0.284991	0.078 (6)*	
C22	1.36791 (16)	0.00935 (17)	−0.12438 (14)	0.0542 (4)	
C23	1.43327 (17)	−0.12886 (17)	0.03118 (15)	0.0577 (4)	
H23	1.480119	−0.202937	0.080814	0.062 (5)*	
C24	1.22609 (15)	0.46706 (16)	0.23777 (13)	0.0498 (4)	
H24	1.177296	0.540514	0.188221	0.052 (5)*	
C25	1.34296 (15)	0.45677 (15)	0.28885 (13)	0.0493 (4)	
C26	1.43056 (16)	0.35601 (16)	0.37025 (13)	0.0516 (4)	
C27	1.4353 (2)	0.23960 (18)	0.42710 (16)	0.0646 (5)	
H27	1.369824	0.213841	0.416084	0.060 (5)*	

C28	1.5388 (2)	0.1642 (2)	0.49961 (18)	0.0786 (6)	
H28	1.543129	0.086425	0.537232	0.087 (7)*	
C29	1.6376 (2)	0.2015 (2)	0.51809 (18)	0.0779 (6)	
H29	1.706043	0.148178	0.567771	0.094 (7)*	
C30	1.63570 (19)	0.3150 (2)	0.46446 (16)	0.0698 (5)	
H30	1.701242	0.340156	0.476842	0.068 (6)*	
C31	1.53133 (16)	0.39131 (17)	0.39055 (14)	0.0555 (4)	
C32	1.39468 (16)	0.54558 (17)	0.26514 (15)	0.0552 (4)	
H32	1.357655	0.621279	0.214953	0.068 (6)*	
C33	1.55867 (19)	−0.2047 (2)	−0.13077 (19)	0.0711 (6)	
H33A	1.632691	−0.254020	−0.081217	0.161 (14)*	
H33B	1.584307	−0.159587	−0.192192	0.148 (12)*	
H33C	1.527555	−0.261002	−0.154903	0.097 (8)*	
C34	1.5904 (2)	0.5748 (2)	0.3191 (2)	0.0755 (6)	
H34A	1.608336	0.583200	0.390918	0.137 (12)*	
H34B	1.547020	0.658432	0.275475	0.135 (12)*	
H34C	1.671310	0.527112	0.286992	0.125 (10)*	
C35	1.000000	0.000000	0.000000	0.173 (3)	
C36	1.0793 (6)	−0.1065 (6)	0.0557 (5)	0.0879 (13)	0.5
N1	1.07253 (12)	0.40608 (13)	0.19845 (11)	0.0508 (3)	
N2	1.18768 (12)	0.37708 (13)	0.25908 (11)	0.0518 (3)	
N3	1.17284 (13)	0.09578 (13)	0.29627 (11)	0.0507 (3)	
N4	1.19636 (13)	0.09946 (13)	0.18477 (11)	0.0526 (3)	
N5	1.45459 (13)	−0.11286 (14)	−0.07613 (12)	0.0575 (4)	
N6	1.50671 (14)	0.50781 (15)	0.32476 (12)	0.0584 (4)	
N7	1.1399 (6)	−0.1952 (6)	0.1118 (5)	0.1225 (18)	0.5
H35A	0.948 (6)	0.003 (8)	0.059 (4)	0.25 (3)*	
H35B	1.025 (14)	0.055 (10)	0.029 (13)	0.26 (6)*	0.5

Atomic displacement parameters (Å²)

	U^{11}	U^{22}	U^{33}	U^{12}	U^{13}	U^{23}
C1	0.0396 (7)	0.0456 (8)	0.0531 (8)	−0.0121 (6)	0.0104 (6)	−0.0208 (7)
C2	0.0426 (8)	0.0491 (8)	0.0564 (9)	−0.0143 (7)	0.0062 (6)	−0.0179 (7)
C3	0.0576 (10)	0.0676 (11)	0.0639 (11)	−0.0239 (9)	0.0023 (8)	−0.0074 (9)
C4	0.0607 (11)	0.0894 (15)	0.0692 (13)	−0.0193 (11)	−0.0102 (10)	−0.0063 (11)
C5	0.0580 (11)	0.1048 (18)	0.0918 (16)	−0.0351 (12)	−0.0151 (11)	−0.0115 (13)
C6	0.0724 (13)	0.1002 (18)	0.116 (2)	−0.0521 (14)	−0.0175 (13)	0.0022 (15)
C7	0.0634 (11)	0.0706 (12)	0.0878 (14)	−0.0331 (10)	−0.0137 (10)	0.0010 (11)
C8	0.0385 (7)	0.0481 (8)	0.0530 (9)	−0.0163 (6)	0.0068 (6)	−0.0180 (7)
C9	0.0420 (7)	0.0575 (9)	0.0539 (9)	−0.0176 (7)	0.0071 (6)	−0.0205 (7)
C10	0.0605 (10)	0.0645 (11)	0.0661 (11)	−0.0225 (9)	0.0168 (8)	−0.0298 (9)
C11	0.0735 (12)	0.0859 (15)	0.0723 (13)	−0.0295 (11)	0.0224 (10)	−0.0440 (12)
C12	0.0815 (14)	0.1096 (18)	0.0604 (12)	−0.0359 (13)	0.0220 (10)	−0.0384 (13)
C13	0.118 (2)	0.0915 (17)	0.0575 (12)	−0.0331 (15)	0.0197 (12)	−0.0110 (12)
C14	0.0913 (15)	0.0663 (12)	0.0632 (12)	−0.0206 (11)	0.0185 (10)	−0.0182 (10)
C15	0.0486 (8)	0.0464 (8)	0.0613 (10)	−0.0142 (7)	0.0069 (7)	−0.0183 (7)
C16	0.0443 (8)	0.0489 (8)	0.0631 (10)	−0.0157 (7)	0.0107 (7)	−0.0247 (7)

C17	0.0429 (7)	0.0534 (9)	0.0631 (10)	−0.0205 (7)	0.0080 (7)	−0.0240 (8)
C18	0.0509 (9)	0.0574 (10)	0.0722 (12)	−0.0157 (8)	0.0050 (8)	−0.0218 (9)
C19	0.0696 (12)	0.0657 (12)	0.0843 (14)	−0.0173 (10)	−0.0061 (10)	−0.0092 (10)
C20	0.0868 (15)	0.0903 (16)	0.0654 (13)	−0.0385 (13)	−0.0005 (11)	−0.0080 (11)
C21	0.0690 (12)	0.0851 (14)	0.0655 (12)	−0.0374 (11)	0.0152 (9)	−0.0272 (10)
C22	0.0470 (8)	0.0598 (10)	0.0638 (10)	−0.0251 (8)	0.0112 (7)	−0.0263 (8)
C23	0.0520 (9)	0.0495 (9)	0.0693 (11)	−0.0154 (7)	0.0108 (8)	−0.0226 (8)
C24	0.0450 (8)	0.0483 (8)	0.0551 (9)	−0.0155 (7)	0.0138 (7)	−0.0199 (7)
C25	0.0476 (8)	0.0492 (8)	0.0536 (9)	−0.0198 (7)	0.0135 (7)	−0.0201 (7)
C26	0.0507 (8)	0.0545 (9)	0.0518 (9)	−0.0207 (7)	0.0151 (7)	−0.0220 (7)
C27	0.0730 (12)	0.0600 (11)	0.0632 (11)	−0.0294 (9)	0.0133 (9)	−0.0160 (9)
C28	0.0930 (16)	0.0637 (12)	0.0678 (12)	−0.0256 (11)	0.0102 (11)	−0.0049 (10)
C29	0.0685 (12)	0.0789 (14)	0.0649 (12)	−0.0123 (11)	0.0008 (10)	−0.0080 (10)
C30	0.0538 (10)	0.0875 (14)	0.0651 (11)	−0.0245 (10)	0.0061 (8)	−0.0206 (10)
C31	0.0505 (9)	0.0621 (10)	0.0537 (9)	−0.0208 (8)	0.0134 (7)	−0.0206 (8)
C32	0.0526 (9)	0.0530 (9)	0.0608 (10)	−0.0214 (7)	0.0107 (7)	−0.0166 (8)
C33	0.0602 (11)	0.0689 (12)	0.0935 (14)	−0.0259 (10)	0.0314 (10)	−0.0473 (11)
C34	0.0682 (12)	0.0879 (15)	0.0898 (15)	−0.0486 (12)	0.0146 (11)	−0.0260 (12)
C35	0.101 (4)	0.159 (7)	0.271 (12)	−0.075 (5)	−0.041 (6)	−0.008 (7)
C36	0.073 (3)	0.098 (4)	0.101 (4)	−0.045 (3)	0.006 (3)	−0.015 (3)
N1	0.0423 (6)	0.0490 (7)	0.0604 (8)	−0.0161 (6)	0.0079 (6)	−0.0178 (6)
N2	0.0425 (7)	0.0513 (8)	0.0625 (8)	−0.0180 (6)	0.0083 (6)	−0.0185 (6)
N3	0.0487 (7)	0.0484 (7)	0.0506 (7)	−0.0139 (6)	0.0088 (6)	−0.0168 (6)
N4	0.0497 (7)	0.0493 (7)	0.0533 (8)	−0.0124 (6)	0.0103 (6)	−0.0195 (6)
N5	0.0499 (7)	0.0563 (8)	0.0704 (9)	−0.0196 (7)	0.0190 (6)	−0.0329 (7)
N6	0.0529 (8)	0.0640 (9)	0.0666 (9)	−0.0302 (7)	0.0104 (6)	−0.0195 (7)
N7	0.123 (4)	0.127 (4)	0.113 (4)	−0.058 (4)	0.005 (3)	0.003 (3)

Geometric parameters (Å, º)

C1—N1	1.285 (2)	C21—C22	1.390 (3)
C1—C2	1.482 (2)	C21—H21	0.9300
C1—C8	1.503 (2)	C22—N5	1.387 (2)
C2—C3	1.384 (3)	C23—N5	1.349 (2)
C2—C7	1.385 (3)	C23—H23	0.9300
C3—C4	1.386 (3)	C24—N2	1.282 (2)
C3—H3	0.9300	C24—C25	1.437 (2)
C4—C5	1.367 (3)	C24—H24	0.9300
C4—H4	0.9300	C25—C32	1.377 (2)
C5—C6	1.368 (3)	C25—C26	1.440 (2)
C5—H5	0.9300	C26—C27	1.401 (3)
C6—C7	1.383 (3)	C26—C31	1.408 (2)
C6—H6	0.9300	C27—C28	1.377 (3)
C7—H7	0.9300	C27—H27	0.9300
C8—N3	1.289 (2)	C28—C29	1.397 (3)
C8—C9	1.475 (2)	C28—H28	0.9300
C9—C14	1.380 (3)	C29—C30	1.371 (3)
C9—C10	1.391 (2)	C29—H29	0.9300

C10—C11	1.381 (3)	C30—C31	1.394 (3)
C10—H10	0.9300	C30—H30	0.9300
C11—C12	1.365 (3)	C31—N6	1.384 (2)
C11—H11	0.9300	C32—N6	1.354 (2)
C12—C13	1.359 (3)	C32—H32	0.9300
C12—H12	0.9300	C33—N5	1.457 (2)
C13—C14	1.387 (3)	C33—H33A	0.9600
C13—H13	0.9300	C33—H33B	0.9600
C14—H14	0.9300	C33—H33C	0.9600
C15—N4	1.286 (2)	C34—N6	1.453 (2)
C15—C16	1.434 (2)	C34—H34A	0.9600
C15—H15	0.9300	C34—H34B	0.9600
C16—C23	1.380 (2)	C34—H34C	0.9600
C16—C17	1.440 (3)	C35—C36^{i}	1.280 (7)
C17—C18	1.402 (2)	C35—C36	1.280 (7)
C17—C22	1.411 (2)	C35—H35A	0.92 (2)
C18—C19	1.376 (3)	C35—H35B	0.93 (2)
C18—H18	0.9300	C35—H35A^{i}	0.92 (2)
C19—C20	1.399 (3)	C35—H35B^{i}	0.93 (2)
C19—H19	0.9300	C36—N7	1.104 (7)
C20—C21	1.374 (3)	N1—N2	1.4110 (19)
C20—H20	0.9300	N3—N4	1.4067 (19)

N1—C1—C2	119.59 (15)	N5—C23—H23	124.6
N1—C1—C8	123.36 (14)	C16—C23—H23	124.6
C2—C1—C8	116.93 (14)	N2—C24—C25	121.38 (16)
C3—C2—C7	118.14 (16)	N2—C24—H24	119.3
C3—C2—C1	121.77 (16)	C25—C24—H24	119.3
C7—C2—C1	120.03 (16)	C32—C25—C24	124.65 (16)
C2—C3—C4	120.1 (2)	C32—C25—C26	106.03 (15)
C2—C3—H3	120.0	C24—C25—C26	129.31 (15)
C4—C3—H3	120.0	C27—C26—C31	118.55 (17)
C5—C4—C3	121.1 (2)	C27—C26—C25	134.91 (17)
C5—C4—H4	119.4	C31—C26—C25	106.54 (15)
C3—C4—H4	119.4	C28—C27—C26	118.6 (2)
C4—C5—C6	119.4 (2)	C28—C27—H27	120.7
C4—C5—H5	120.3	C26—C27—H27	120.7
C6—C5—H5	120.3	C27—C28—C29	121.7 (2)
C5—C6—C7	120.1 (2)	C27—C28—H28	119.2
C5—C6—H6	119.9	C29—C28—H28	119.2
C7—C6—H6	119.9	C30—C29—C28	121.3 (2)
C6—C7—C2	121.1 (2)	C30—C29—H29	119.3
C6—C7—H7	119.4	C28—C29—H29	119.3
C2—C7—H7	119.4	C29—C30—C31	117.2 (2)
N3—C8—C9	119.91 (15)	C29—C30—H30	121.4
N3—C8—C1	122.34 (14)	C31—C30—H30	121.4
C9—C8—C1	117.58 (13)	N6—C31—C30	129.16 (18)
C14—C9—C10	118.14 (17)	N6—C31—C26	108.11 (15)

C14—C9—C8	121.49 (16)	C30—C31—C26	122.72 (18)
C10—C9—C8	120.27 (17)	N6—C32—C25	110.85 (16)
C11—C10—C9	120.5 (2)	N6—C32—H32	124.6
C11—C10—H10	119.8	C25—C32—H32	124.6
C9—C10—H10	119.8	N5—C33—H33A	109.5
C12—C11—C10	120.6 (2)	N5—C33—H33B	109.5
C12—C11—H11	119.7	H33A—C33—H33B	109.5
C10—C11—H11	119.7	N5—C33—H33C	109.5
C13—C12—C11	119.5 (2)	H33A—C33—H33C	109.5
C13—C12—H12	120.2	H33B—C33—H33C	109.5
C11—C12—H12	120.2	N6—C34—H34A	109.5
C12—C13—C14	120.8 (2)	N6—C34—H34B	109.5
C12—C13—H13	119.6	H34A—C34—H34B	109.5
C14—C13—H13	119.6	N6—C34—H34C	109.5
C9—C14—C13	120.5 (2)	H34A—C34—H34C	109.5
C9—C14—H14	119.8	H34B—C34—H34C	109.5
C13—C14—H14	119.8	C36^{i}—C35—C36	180.0
N4—C15—C16	121.41 (16)	C36^{i}—C35—H35A	96 (4)
N4—C15—H15	119.3	C36—C35—H35A	84 (4)
C16—C15—H15	119.3	C36^{i}—C35—H35B	81 (8)
C23—C16—C15	124.28 (17)	C36—C35—H35B	99 (8)
C23—C16—C17	106.21 (15)	H35A—C35—H35B	86 (8)
C15—C16—C17	129.43 (14)	C36^{i}—C35—H35A^{i}	84 (4)
C18—C17—C22	118.62 (17)	C36—C35—H35A^{i}	96 (4)
C18—C17—C16	134.93 (16)	H35A—C35—H35A^{i}	180.0
C22—C17—C16	106.42 (14)	H35B—C35—H35A^{i}	94 (8)
C19—C18—C17	118.58 (18)	C36^{i}—C35—H35B^{i}	99 (8)
C19—C18—H18	120.7	C36—C35—H35B^{i}	81 (8)
C17—C18—H18	120.7	H35A—C35—H35B^{i}	94 (8)
C18—C19—C20	121.7 (2)	H35B—C35—H35B^{i}	180 (6)
C18—C19—H19	119.2	H35A^{i}—C35—H35B^{i}	86 (8)
C20—C19—H19	119.2	N7—C36—C35	173.2 (7)
C21—C20—C19	121.1 (2)	C1—N1—N2	111.60 (14)
C21—C20—H20	119.4	C24—N2—N1	111.89 (14)
C19—C20—H20	119.4	C8—N3—N4	111.13 (13)
C20—C21—C22	117.36 (19)	C15—N4—N3	112.23 (14)
C20—C21—H21	121.3	C23—N5—C22	108.75 (13)
C22—C21—H21	121.3	C23—N5—C33	125.59 (17)
N5—C22—C21	129.47 (16)	C22—N5—C33	125.48 (17)
N5—C22—C17	107.90 (16)	C32—N6—C31	108.47 (15)
C21—C22—C17	122.60 (17)	C32—N6—C34	126.40 (17)
N5—C23—C16	110.71 (17)	C31—N6—C34	125.10 (17)

Symmetry code: (i) −*x*+2, −*y*, −*z*.

Hydrogen-bond geometry (Å, º)

D—H···*A*	*D*—H	H···*A*	*D*···*A*	*D*—H···*A*

C12—H12···N7^{ii}	0.93	2.51	3.372 (6)	155

Symmetry code: (ii) −*x*+2, −*y*, −*z*+1.

(1*Z*,2*Z*)-1,2-Bis{(*E*)-[(naphthalen-1-yl)methylidene]hydrazinylidene}-1,2-diphenylethane (4-BDHFN)

Crystal data

$C_{36}H_{26}N_4$
M_r = 514.61
Monoclinic, *C*2/*c*
a = 26.195 (8) Å
b = 9.809 (3) Å
c = 11.806 (4) Å
β = 115.230 (5)°
V = 2744.2 (15) Å^3
Z = 4

F(000) = 1080
D_x = 1.246 Mg m^{-3}
Mo *Kα* radiation, *λ* = 0.71073 Å
Cell parameters from 380 reflections
θ = 2.5–26.0°
μ = 0.07 mm^{-1}
T = 298 K
Block, yellow
0.30 × 0.16 × 0.10 mm

Data collection

Bruker SMART CCD area detector diffractometer
Radiation source: fine-focus sealed tube
Detector resolution: 10.22 pixels mm^{-1}
phi and *ω* scans
Absorption correction: multi-scan (SADABS; Bruker, 2000)
T_{min} = 0.986, T_{max} = 0.993

6631 measured reflections
2413 independent reflections
1197 reflections with $I > 2\sigma(I)$
R_{int} = 0.058
θ_{max} = 25.0°, θ_{min} = 1.7°
h = −31→29
k = −11→11
l = −14→12

Refinement

Refinement on F^2
Least-squares matrix: full
$R[F^2 > 2\sigma(F^2)]$ = 0.062
$wR(F^2)$ = 0.130
S = 0.95
2413 reflections
194 parameters
0 restraints

Hydrogen site location: inferred from neighbouring sites
Only H-atom displacement parameters refined
$w = 1/[\sigma^2(F_o^2) + (0.0447P)^2]$ where $P = (F_o^2 + 2F_c^2)/3$
$(\Delta/\sigma)_{max} < 0.001$
$\Delta\rho_{max}$ = 0.11 e Å^{-3}
$\Delta\rho_{min}$ = −0.10 e Å^{-3}

Special details

Geometry. All esds (except the esd in the dihedral angle between two l.s. planes) are estimated using the full covariance matrix. The cell esds are taken into account individually in the estimation of esds in distances, angles and torsion angles; correlations between esds in cell parameters are only used when they are defined by crystal symmetry. An approximate (isotropic) treatment of cell esds is used for estimating esds involving l.s. planes.

Refinement. Refinement of F^2 against ALL reflections. The weighted R-factor wR and goodness of fit S are based on F^2, conventional R-factors R are based on F, with F set to zero for negative F^2. The threshold expression of $F^2 > 2\text{sigma}(F^2)$ is used only for calculating R-factors(gt) etc. and is not relevant to the choice of reflections for refinement. R-factors based on F^2 are statistically about twice as large as those based on F, and R- factors based on ALL data will be even larger.

Fractional atomic coordinates and isotropic or equivalent isotropic displacement parameters (Å^2)

	x	*y*	*z*	U_{iso}*/U_{eq}
C1	0.47469 (10)	0.0592 (3)	0.1862 (2)	0.0498 (7)
C2	0.42618 (10)	−0.0283 (3)	0.1669 (2)	0.0492 (7)
C3	0.38212 (11)	−0.0443 (3)	0.0497 (3)	0.0657 (8)

H3	0.382634	0.002388	−0.018428	0.065 (8)*
C4	0.33781 (13)	−0.1281 (3)	0.0331 (3)	0.0816 (10)
H4	0.308409	−0.137174	−0.046358	0.075 (9)*
C5	0.33585 (14)	−0.1977 (3)	0.1294 (3)	0.0845 (10)
H5	0.305668	−0.255394	0.116304	0.074 (9)*
C6	0.37835 (14)	−0.1830 (3)	0.2459 (4)	0.0864 (10)
H6	0.377201	−0.229986	0.313221	0.097 (11)*
C7	0.42297 (12)	−0.0986 (3)	0.2640 (3)	0.0715 (9)
H7	0.451750	−0.088900	0.344135	0.052 (7)*
C8	0.52380 (14)	0.2815 (3)	0.0423 (3)	0.0670 (8)
H8	0.489868	0.285791	−0.029219	0.085 (11)*
C9	0.56973 (13)	0.3652 (3)	0.0431 (3)	0.0660 (8)
C10	0.55680 (17)	0.4528 (3)	−0.0558 (3)	0.0855 (10)
H10	0.520013	0.454005	−0.118007	0.117 (14)*
C11	0.59585 (18)	0.5391 (4)	−0.0671 (4)	0.1027 (12)
H11	0.585478	0.598432	−0.134758	0.100 (11)*
C12	0.65000 (19)	0.5357 (4)	0.0229 (4)	0.1035 (12)
H12	0.676527	0.593874	0.015764	0.123 (13)*
C13	0.66715 (15)	0.4466 (3)	0.1267 (3)	0.0799 (9)
C14	0.62661 (13)	0.3581 (3)	0.1381 (3)	0.0635 (8)
C15	0.64564 (14)	0.2666 (3)	0.2393 (3)	0.0694 (8)
H15	0.619942	0.207560	0.248826	0.077 (9)*
C16	0.70059 (14)	0.2621 (4)	0.3236 (3)	0.0824 (10)
H16	0.712101	0.200221	0.389491	0.097 (12)*
C17	0.73971 (18)	0.3498 (4)	0.3116 (4)	0.1014 (12)
H17	0.777285	0.346277	0.369719	0.112 (13)*
C18	0.72364 (17)	0.4395 (4)	0.2167 (4)	0.1034 (12)
H18	0.750268	0.497894	0.210383	0.086 (10)*
N1	0.47400 (9)	0.1318 (2)	0.0954 (2)	0.0609 (6)
N2	0.52522 (9)	0.2036 (2)	0.1286 (2)	0.0634 (7)

Atomic displacement parameters (Å²)

	U^{11}	U^{22}	U^{33}	U^{12}	U^{13}	U^{23}
C1	0.0526 (17)	0.0542 (16)	0.0440 (15)	0.0071 (13)	0.0219 (13)	−0.0013 (13)
C2	0.0451 (16)	0.0574 (17)	0.0440 (16)	0.0016 (13)	0.0179 (15)	−0.0031 (14)
C3	0.0600 (19)	0.084 (2)	0.0522 (19)	−0.0039 (17)	0.0225 (18)	−0.0002 (17)
C4	0.054 (2)	0.111 (3)	0.070 (2)	−0.0156 (19)	0.017 (2)	−0.017 (2)
C5	0.065 (2)	0.100 (3)	0.095 (3)	−0.030 (2)	0.040 (2)	−0.019 (2)
C6	0.085 (3)	0.096 (3)	0.082 (3)	−0.025 (2)	0.039 (2)	0.006 (2)
C7	0.062 (2)	0.087 (2)	0.056 (2)	−0.0173 (17)	0.0163 (19)	0.0009 (17)
C8	0.072 (2)	0.064 (2)	0.065 (2)	0.0010 (16)	0.029 (2)	0.0022 (16)
C9	0.074 (2)	0.0621 (19)	0.068 (2)	−0.0001 (17)	0.036 (2)	0.0008 (17)
C10	0.100 (3)	0.081 (3)	0.087 (3)	0.000 (2)	0.051 (3)	0.022 (2)
C11	0.123 (3)	0.091 (3)	0.108 (3)	0.014 (3)	0.063 (3)	0.036 (3)
C12	0.128 (3)	0.084 (3)	0.131 (4)	−0.009 (3)	0.086 (3)	0.019 (3)
C13	0.087 (3)	0.074 (2)	0.094 (3)	−0.012 (2)	0.053 (2)	−0.005 (2)
C14	0.078 (2)	0.0603 (19)	0.064 (2)	−0.0020 (17)	0.0415 (19)	−0.0036 (16)

C15	0.065 (2)	0.080 (2)	0.067 (2)	−0.0083 (19)	0.031 (2)	−0.0062 (17)
C16	0.071 (2)	0.096 (3)	0.078 (2)	−0.005 (2)	0.029 (2)	−0.004 (2)
C17	0.076 (3)	0.120 (4)	0.110 (3)	−0.017 (2)	0.040 (3)	−0.002 (3)
C18	0.091 (3)	0.103 (3)	0.128 (4)	−0.028 (3)	0.057 (3)	−0.004 (3)
N1	0.0583 (15)	0.0688 (16)	0.0549 (15)	−0.0016 (13)	0.0235 (13)	0.0049 (12)
N2	0.0633 (16)	0.0688 (16)	0.0597 (16)	−0.0061 (13)	0.0278 (14)	0.0139 (13)

Geometric parameters (Å, º)

C1—N1	1.280 (3)	C9—C14	1.434 (3)
C1—C2	1.469 (3)	C10—C11	1.378 (4)
C1—C1^{i}	1.525 (4)	C10—H10	0.9300
C2—C7	1.371 (3)	C11—C12	1.363 (4)
C2—C3	1.382 (3)	C11—H11	0.9300
C3—C4	1.367 (4)	C12—C13	1.414 (4)
C3—H3	0.9300	C12—H12	0.9300
C4—C5	1.346 (4)	C13—C18	1.409 (4)
C4—H4	0.9300	C13—C14	1.422 (4)
C5—C6	1.359 (4)	C14—C15	1.406 (4)
C5—H5	0.9300	C15—C16	1.357 (4)
C6—C7	1.373 (4)	C15—H15	0.9300
C6—H6	0.9300	C16—C17	1.390 (4)
C7—H7	0.9300	C16—H16	0.9300
C8—N2	1.261 (3)	C17—C18	1.343 (4)
C8—C9	1.453 (4)	C17—H17	0.9300
C8—H8	0.9300	C18—H18	0.9300
C9—C10	1.371 (4)	N1—N2	1.415 (3)
N1—C1—C2	119.5 (2)	C9—C10—H10	118.5
N1—C1—C1^{i}	121.5 (2)	C11—C10—H10	118.5
C2—C1—C1^{i}	118.9 (2)	C12—C11—C10	118.6 (4)
C7—C2—C3	117.3 (3)	C12—C11—H11	120.7
C7—C2—C1	121.5 (2)	C10—C11—H11	120.7
C3—C2—C1	121.3 (3)	C11—C12—C13	122.1 (4)
C4—C3—C2	120.5 (3)	C11—C12—H12	118.9
C4—C3—H3	119.8	C13—C12—H12	118.9
C2—C3—H3	119.8	C18—C13—C12	121.9 (4)
C5—C4—C3	121.3 (3)	C18—C13—C14	119.0 (3)
C5—C4—H4	119.3	C12—C13—C14	119.0 (3)
C3—C4—H4	119.3	C15—C14—C13	117.5 (3)
C4—C5—C6	119.4 (3)	C15—C14—C9	124.7 (3)
C4—C5—H5	120.3	C13—C14—C9	117.7 (3)
C6—C5—H5	120.3	C16—C15—C14	121.6 (3)
C5—C6—C7	119.8 (3)	C16—C15—H15	119.2
C5—C6—H6	120.1	C14—C15—H15	119.2
C7—C6—H6	120.1	C15—C16—C17	120.2 (4)
C2—C7—C6	121.7 (3)	C15—C16—H16	119.9
C2—C7—H7	119.2	C17—C16—H16	119.9

C6—C7—H7	119.2	C18—C17—C16	120.5 (4)
N2—C8—C9	126.7 (3)	C18—C17—H17	119.8
N2—C8—H8	116.7	C16—C17—H17	119.8
C9—C8—H8	116.7	C17—C18—C13	121.1 (4)
C10—C9—C14	119.5 (3)	C17—C18—H18	119.4
C10—C9—C8	116.4 (3)	C13—C18—H18	119.4
C14—C9—C8	124.0 (3)	C1—N1—N2	111.8 (2)
C9—C10—C11	123.0 (4)	C8—N2—N1	112.3 (2)

Symmetry code: (i) −*x*+1, *y*, −*z*+1/2.

Hydrogen-bond geometry (Å, º)

D—H···*A*	*D*—H	H···*A*	*D*···*A*	*D*—H···*A*
C15—H15···N2	0.93	2.27	2.920 (4)	126

(*Z*)-2-{(*E*)-[(1*H*-Indol-3-yl)methylidene]hydrazinylidene}-\ 1,2-diphenylethanone (5-BMHFI)

Crystal data

$C_{23}H_{17}N_3O$
M_r = 351.39
Orthorhombic, $P2_12_12_1$
a = 6.8767 (1) Å
b = 8.3698 (2) Å
c = 32.6317 (6) Å
V = 1878.17 (6) Å^3
Z = 4
F(000) = 736
D_x = 1.243 Mg m^{-3}
Melting point: 470.4 K
Mo *Kα* radiation, *λ* = 0.71073 Å
Cell parameters from 380 reflections
θ = 2.5–26.0°
μ = 0.08 mm^{-1}
T = 293 K
Needle, yellow
0.35 × 0.1 × 0.09 mm

Data collection

Bruker SMART CCD area detector diffractometer
Radiation source: fine-focus sealed tube
Detector resolution: 10.11 pixels mm^{-1}
phi and *ω* scans
Absorption correction: multi-scan (SADABS; Bruker, 2000)
T_{min} = 0.903, T_{max} = 0.939
10418 measured reflections
3641 independent reflections
3444 reflections with $I > 2\sigma(I)$
R_{int} = 0.023
θ_{max} = 26.1°, θ_{min} = 2.5°
h = −7→8
k = −10→10
l = −39→40

Refinement

Refinement on F^2
Least-squares matrix: full
$R[F^2 > 2\sigma(F^2)]$ = 0.035
$wR(F^2)$ = 0.096
S = 1.02
3641 reflections
262 parameters
0 restraints
Hydrogen site location: inferred from neighbouring sites
Only H-atom displacement parameters refined
$w = 1/[\sigma^2(F_o^2) + (0.0555P)^2 + 0.1425P]$ where $P = (F_o^2 + 2F_c^2)/3$
$(\Delta/\sigma)_{max}$ = 0.001
$\Delta\rho_{max}$ = 0.15 e Å^{-3}
$\Delta\rho_{min}$ = −0.13 e Å^{-3}
Extinction correction: SHELXL2016 (Sheldrick, 2015b), $Fc^*=kFc[1+0.001xFc^2\lambda^3/\sin(2\theta)]^{-1/4}$
Extinction coefficient: 0.014 (2)
Absolute structure: Flack *x* determined using 1312 quotients [(I+)-(I-)]/[(I+)+(I-)] (Parsons *et al.*, 2013)
The diffraction data did not permit a clear determination of the absolute structure.
Absolute structure parameter: −1.4 (6)

Special details

Geometry. All esds (except the esd in the dihedral angle between two l.s. planes) are estimated using the full covariance matrix. The cell esds are taken into account individually in the estimation of esds in distances, angles and torsion angles; correlations between esds in cell parameters are only used when they are defined by crystal symmetry. An approximate (isotropic) treatment of cell esds is used for estimating esds involving l.s. planes.

Refinement. Refinement of F^2 against ALL reflections. The weighted R-factor wR and goodness of fit S are based on F^2, conventional R-factors R are based on F, with F set to zero for negative F^2. The threshold expression of $F^2 > 2\text{sigma}(F^2)$ is used only for calculating R-factors(gt) etc. and is not relevant to the choice of reflections for refinement. R-factors based on F^2 are statistically about twice as large as those based on F, and R- factors based on ALL data will be even larger.

Fractional atomic coordinates and isotropic or equivalent isotropic displacement parameters (Å²)

	x	*y*	*z*	U_{iso}*/U_{eq}
C1	0.7517 (3)	0.2656 (2)	0.85621 (6)	0.0427 (4)
C2	0.8141 (3)	0.1859 (2)	0.81814 (6)	0.0470 (4)
C3	1.0008 (4)	0.1258 (3)	0.81425 (7)	0.0669 (6)
H3	1.089269	0.138070	0.835570	0.076 (8)*
C4	1.0561 (5)	0.0477 (4)	0.77895 (9)	0.0874 (9)
H4	1.181704	0.007482	0.776671	0.106 (11)*
C5	0.9281 (5)	0.0289 (4)	0.74721 (9)	0.0923 (10)
H5	0.966311	−0.024678	0.723578	0.102 (10)*
C6	0.7443 (5)	0.0890 (4)	0.75035 (8)	0.0843 (9)
H6	0.657486	0.076835	0.728722	0.100 (10)*
C7	0.6864 (4)	0.1677 (3)	0.78550 (7)	0.0636 (6)
H7	0.561082	0.208836	0.787316	0.062 (7)*
C8	0.5398 (3)	0.3144 (2)	0.86038 (5)	0.0423 (4)
C9	0.4897 (3)	0.4854 (3)	0.85595 (6)	0.0494 (5)
C10	0.2996 (4)	0.5330 (4)	0.86342 (7)	0.0711 (7)
H10	0.205386	0.458336	0.870592	0.079 (9)*
C11	0.2525 (7)	0.6924 (5)	0.86005 (11)	0.1074 (13)
H11	0.125781	0.725582	0.865180	0.136 (15)*
C12	0.3901 (8)	0.8024 (4)	0.84926 (12)	0.1188 (16)
H12	0.356149	0.909601	0.847176	0.119 (12)*
C13	0.5766 (7)	0.7565 (4)	0.84152 (11)	0.1043 (12)
H13	0.669543	0.831779	0.834033	0.160 (18)*
C14	0.6268 (4)	0.5965 (3)	0.84490 (8)	0.0704 (7)
H14	0.753805	0.564317	0.839654	0.079 (9)*
C15	0.8754 (3)	0.3567 (2)	0.95253 (6)	0.0472 (4)
H15	1.003366	0.321156	0.951208	0.050 (6)*
C16	0.7994 (3)	0.4113 (2)	0.99091 (6)	0.0457 (4)
C17	0.6165 (3)	0.4884 (2)	1.00009 (6)	0.0438 (4)
C18	0.4611 (3)	0.5458 (2)	0.97686 (7)	0.0521 (5)
H18	0.462304	0.536961	0.948449	0.058 (6)*
C19	0.3066 (4)	0.6156 (3)	0.99655 (8)	0.0646 (6)
H19	0.203049	0.654739	0.981207	0.073 (7)*
C20	0.3018 (4)	0.6290 (3)	1.03919 (8)	0.0685 (6)
H20	0.195263	0.676936	1.051704	0.074 (8)*
C21	0.4506 (4)	0.5730 (3)	1.06286 (7)	0.0614 (6)

H21	0.446523	0.580472	1.091284	0.068 (7)*
C22	0.6087 (3)	0.5045 (2)	1.04290 (6)	0.0490 (5)
C23	0.8892 (3)	0.3850 (3)	1.02803 (6)	0.0558 (5)
H23	1.009720	0.336291	1.031394	0.063 (7)*
N1	0.8691 (2)	0.2859 (2)	0.88638 (5)	0.0493 (4)
N2	0.7709 (2)	0.3555 (2)	0.91982 (5)	0.0481 (4)
N3	0.7772 (3)	0.4399 (2)	1.05867 (5)	0.0580 (5)
H24	0.806292	0.435508	1.084278	0.087 (9)*
O1	0.4184 (2)	0.21208 (19)	0.86624 (5)	0.0593 (4)

Atomic displacement parameters (Å²)

	U^{11}	U^{22}	U^{33}	U^{12}	U^{13}	U^{23}
C1	0.0455 (9)	0.0417 (9)	0.0410 (9)	0.0001 (8)	0.0002 (8)	0.0052 (7)
C2	0.0552 (11)	0.0454 (10)	0.0403 (9)	0.0018 (9)	0.0022 (8)	0.0040 (8)
C3	0.0636 (13)	0.0814 (16)	0.0558 (12)	0.0192 (13)	0.0002 (11)	−0.0060 (12)
C4	0.0847 (19)	0.106 (2)	0.0712 (16)	0.0347 (18)	0.0091 (14)	−0.0160 (15)
C5	0.115 (2)	0.105 (2)	0.0569 (14)	0.026 (2)	0.0091 (16)	−0.0225 (14)
C6	0.095 (2)	0.111 (2)	0.0468 (12)	0.0072 (19)	−0.0077 (13)	−0.0148 (13)
C7	0.0627 (14)	0.0796 (16)	0.0486 (11)	0.0074 (12)	−0.0031 (10)	−0.0037 (11)
C8	0.0438 (9)	0.0491 (10)	0.0342 (8)	−0.0034 (8)	0.0009 (7)	0.0032 (7)
C9	0.0552 (10)	0.0531 (11)	0.0400 (9)	0.0087 (9)	−0.0072 (8)	−0.0021 (8)
C10	0.0679 (14)	0.0868 (18)	0.0585 (13)	0.0256 (15)	−0.0039 (11)	−0.0098 (12)
C11	0.117 (3)	0.108 (3)	0.097 (2)	0.069 (2)	−0.023 (2)	−0.030 (2)
C12	0.181 (4)	0.0616 (18)	0.114 (3)	0.048 (3)	−0.063 (3)	−0.0235 (19)
C13	0.150 (3)	0.0520 (15)	0.111 (3)	−0.002 (2)	−0.043 (3)	0.0109 (15)
C14	0.0793 (17)	0.0521 (12)	0.0798 (16)	−0.0026 (12)	−0.0157 (14)	0.0109 (11)
C15	0.0434 (9)	0.0473 (10)	0.0509 (10)	0.0047 (9)	−0.0062 (8)	−0.0019 (8)
C16	0.0475 (10)	0.0425 (9)	0.0469 (9)	0.0014 (8)	−0.0118 (8)	−0.0030 (8)
C17	0.0496 (10)	0.0350 (8)	0.0467 (9)	−0.0023 (8)	−0.0065 (8)	−0.0021 (7)
C18	0.0551 (11)	0.0477 (10)	0.0535 (11)	0.0026 (9)	−0.0131 (9)	0.0002 (9)
C19	0.0568 (13)	0.0599 (13)	0.0770 (15)	0.0121 (11)	−0.0091 (12)	−0.0001 (11)
C20	0.0628 (14)	0.0628 (14)	0.0798 (16)	0.0096 (12)	0.0087 (13)	−0.0073 (12)
C21	0.0763 (15)	0.0548 (12)	0.0531 (12)	0.0016 (12)	0.0053 (11)	−0.0072 (10)
C22	0.0602 (12)	0.0402 (10)	0.0466 (10)	0.0005 (9)	−0.0058 (9)	−0.0012 (8)
C23	0.0575 (12)	0.0551 (11)	0.0548 (11)	0.0090 (10)	−0.0158 (10)	−0.0058 (9)
N1	0.0456 (9)	0.0585 (10)	0.0437 (8)	0.0059 (8)	−0.0012 (7)	−0.0030 (7)
N2	0.0450 (8)	0.0569 (9)	0.0424 (8)	0.0056 (8)	−0.0019 (7)	−0.0038 (7)
N3	0.0738 (12)	0.0595 (10)	0.0407 (9)	0.0084 (10)	−0.0158 (8)	−0.0051 (7)
O1	0.0542 (8)	0.0652 (9)	0.0586 (9)	−0.0152 (8)	0.0019 (7)	0.0079 (7)

Geometric parameters (Å, º)

C1—N1	1.284 (3)	C13—C14	1.387 (4)
C1—C2	1.474 (3)	C13—H13	0.9300
C1—C8	1.520 (3)	C14—H14	0.9300
C2—C3	1.385 (3)	C15—N2	1.287 (2)
C2—C7	1.389 (3)	C15—C16	1.432 (3)

C3—C4	1.378 (4)	C15—H15	0.9300
C3—H3	0.9300	C16—C23	1.377 (3)
C4—C5	1.368 (4)	C16—C17	1.445 (3)
C4—H4	0.9300	C17—C18	1.395 (3)
C5—C6	1.364 (4)	C17—C22	1.404 (3)
C5—H5	0.9300	C18—C19	1.372 (3)
C6—C7	1.381 (3)	C18—H18	0.9300
C6—H6	0.9300	C19—C20	1.396 (4)
C7—H7	0.9300	C19—H19	0.9300
C8—O1	1.211 (2)	C20—C21	1.365 (3)
C8—C9	1.479 (3)	C20—H20	0.9300
C9—C14	1.372 (3)	C21—C22	1.391 (3)
C9—C10	1.388 (3)	C21—H21	0.9300
C10—C11	1.378 (5)	C22—N3	1.378 (3)
C10—H10	0.9300	C23—N3	1.343 (3)
C11—C12	1.366 (6)	C23—H23	0.9300
C11—H11	0.9300	N1—N2	1.410 (2)
C12—C13	1.362 (6)	N3—H24	0.8600
C12—H12	0.9300		

N1—C1—C2	121.53 (18)	C12—C13—H13	120.3
N1—C1—C8	119.90 (17)	C14—C13—H13	120.3
C2—C1—C8	118.45 (16)	C9—C14—C13	120.3 (3)
C3—C2—C7	118.4 (2)	C9—C14—H14	119.9
C3—C2—C1	120.79 (19)	C13—C14—H14	119.9
C7—C2—C1	120.79 (19)	N2—C15—C16	121.61 (18)
C4—C3—C2	120.3 (2)	N2—C15—H15	119.2
C4—C3—H3	119.8	C16—C15—H15	119.2
C2—C3—H3	119.8	C23—C16—C15	123.68 (18)
C5—C4—C3	120.7 (3)	C23—C16—C17	106.22 (17)
C5—C4—H4	119.7	C15—C16—C17	129.90 (17)
C3—C4—H4	119.7	C18—C17—C22	118.56 (18)
C6—C5—C4	119.8 (3)	C18—C17—C16	135.04 (18)
C6—C5—H5	120.1	C22—C17—C16	106.40 (17)
C4—C5—H5	120.1	C19—C18—C17	119.0 (2)
C5—C6—C7	120.3 (3)	C19—C18—H18	120.5
C5—C6—H6	119.8	C17—C18—H18	120.5
C7—C6—H6	119.8	C18—C19—C20	121.3 (2)
C6—C7—C2	120.5 (2)	C18—C19—H19	119.4
C6—C7—H7	119.8	C20—C19—H19	119.4
C2—C7—H7	119.8	C21—C20—C19	121.3 (2)
O1—C8—C9	122.64 (19)	C21—C20—H20	119.4
O1—C8—C1	119.01 (18)	C19—C20—H20	119.4
C9—C8—C1	118.33 (17)	C20—C21—C22	117.5 (2)
C14—C9—C10	119.9 (2)	C20—C21—H21	121.2
C14—C9—C8	121.4 (2)	C22—C21—H21	121.2
C10—C9—C8	118.7 (2)	N3—C22—C21	130.1 (2)
C11—C10—C9	119.0 (3)	N3—C22—C17	107.56 (18)

C11—C10—H10	120.5	C21—C22—C17	122.37 (19)
C9—C10—H10	120.5	N3—C23—C16	110.04 (18)
C12—C11—C10	120.7 (4)	N3—C23—H23	125.0
C12—C11—H11	119.7	C16—C23—H23	125.0
C10—C11—H11	119.7	C1—N1—N2	110.30 (16)
C13—C12—C11	120.7 (3)	C15—N2—N1	112.19 (16)
C13—C12—H12	119.7	C23—N3—C22	109.78 (17)
C11—C12—H12	119.7	C23—N3—H24	125.1
C12—C13—C14	119.4 (4)	C22—N3—H24	125.1

Hydrogen-bond geometry (Å, º)

D—H···*A*	*D*—H	H···*A*	*D*···*A*	*D*—H···*A*
C3—H3···O1^{i}	0.93	2.55	3.413 (3)	154
N3—H24···O1^{ii}	0.86	2.17	2.927 (2)	146

Symmetry codes: (i) *x*+1, *y*, *z*; (ii) *x*+1/2, −*y*+1/2, −*z*+2.

(*Z*)-2-{(*E*)-[1-(1*H*-Indol-3-yl)ethylidene]hydrazinylidene}-\ 1,2-diphenylethanone (6-BMHAI)

Crystal data

$C_{24}H_{19}N_3O$
M_r = 365.42
Tetragonal, $P4_32_12$
a = 8.3580 (1) Å
c = 54.6705 (7) Å
V = 3819.07 (10) Å^3
Z = 8
$F(000)$ = 1536
D_x = 1.271 Mg m^{-3}
Mo $K\alpha$ radiation, λ = 0.71073 Å
Cell parameters from 380 reflections
θ = 2.5–26.0°
μ = 0.08 mm^{-1}
T = 293 K
Needle, yellow
0.3 × 0.1 × 0.1 mm

Data collection

Bruker SMART CCD area detector diffractometer
Radiation source: fine-focus sealed tube
Detector resolution: 10.32 pixels mm^{-1}
phi and ω scans
Absorption correction: multi-scan (SADABS; Bruker, 2000)
T_{min} = 0.983, T_{max} = 0.998
21746 measured reflections
3759 independent reflections
3565 reflections with $I > 2\sigma(I)$
R_{int} = 0.030
θ_{max} = 26.0°, θ_{min} = 1.5°
h = −6→10
k = −9→9
l = −66→66

Refinement

Refinement on F^2
Least-squares matrix: full
$R[F^2 > 2\sigma(F^2)]$ = 0.041
$wR(F^2)$ = 0.113
S = 1.06
3759 reflections
274 parameters
0 restraints
Hydrogen site location: inferred from neighbouring sites
Only H-atom displacement parameters refined
$w = 1/[\sigma^2(F_o^2) + (0.0638P)^2 + 0.5669P]$ where $P = (F_o^2 + 2F_c^2)/3$
$(\Delta/\sigma)_{max} < 0.001$
$\Delta\rho_{max}$ = 0.16 e Å^{-3}
$\Delta\rho_{min}$ = −0.12 e Å^{-3}
Extinction correction: SHELXL2016 (Sheldrick, 2015b), $Fc^*=kFc[1+0.001xFc^2\lambda^3/\sin(2\theta)]^{-1/4}$
Extinction coefficient: 0.0060 (10)
Absolute structure: Flack x determined using 1258 quotients [(I+)-(I-)]/[(I+)+(I-)] (Parsons *et al.*, 2013)
The diffraction data did not permit a clear determination of the absolute structure.
Absolute structure parameter: −1.5 (6)

Special details

Geometry. All esds (except the esd in the dihedral angle between two l.s. planes) are estimated using the full covariance matrix. The cell esds are taken into account individually in the estimation of esds in distances, angles and torsion angles; correlations between esds in cell parameters are only used when they are defined by crystal symmetry. An approximate (isotropic) treatment of cell esds is used for estimating esds involving l.s. planes.

Refinement. Refinement of F^2 against ALL reflections. The weighted R-factor wR and goodness of fit S are based on F^2, conventional R-factors R are based on F, with F set to zero for negative F^2. The threshold expression of $F^2 > 2\text{sigma}(F^2)$ is used only for calculating R-factors(gt) etc. and is not relevant to the choice of reflections for refinement. R-factors based on F^2 are statistically about twice as large as those based on F, and R- factors based on ALL data will be even larger.

Fractional atomic coordinates and isotropic or equivalent isotropic displacement parameters (Å²)

	x	*y*	*z*	U_{iso}*/U_{eq}
C1	1.1474 (3)	0.3991 (2)	0.03774 (4)	0.0375 (4)
C2	1.0797 (3)	0.4604 (2)	0.01468 (4)	0.0399 (5)
C3	1.1757 (3)	0.5262 (3)	−0.00339 (4)	0.0536 (6)
H3	1.285832	0.530978	−0.001107	0.093 (11)*
C4	1.1095 (4)	0.5845 (4)	−0.02472 (4)	0.0638 (7)
H4	1.175243	0.629370	−0.036611	0.085 (10)*
C5	0.9483 (4)	0.5770 (4)	−0.02850 (5)	0.0702 (8)
H5	0.904020	0.618015	−0.042792	0.112 (13)*
C6	0.8528 (4)	0.5092 (5)	−0.01127 (6)	0.0887 (12)
H6	0.743289	0.501715	−0.014035	0.134 (16)*
C7	0.9165 (3)	0.4509 (4)	0.01037 (5)	0.0688 (8)
H7	0.849569	0.405348	0.022041	0.080 (10)*
C8	1.0347 (3)	0.3189 (2)	0.05573 (3)	0.0357 (4)
C9	1.0165 (3)	0.1422 (3)	0.05565 (4)	0.0385 (5)
C10	0.9186 (3)	0.0725 (3)	0.07313 (4)	0.0485 (6)
H10	0.865994	0.135854	0.084567	0.064 (9)*
C11	0.8998 (4)	−0.0923 (3)	0.07344 (5)	0.0639 (7)
H11	0.834722	−0.139926	0.085166	0.107 (13)*
C12	0.9768 (4)	−0.1849 (3)	0.05651 (6)	0.0740 (9)
H12	0.963375	−0.295330	0.056759	0.110 (13)*
C13	1.0735 (4)	−0.1166 (3)	0.03917 (7)	0.0765 (9)
H13	1.125833	−0.180829	0.027809	0.097 (12)*
C14	1.0937 (3)	0.0485 (3)	0.03852 (5)	0.0565 (6)
H14	1.158469	0.095295	0.026686	0.061 (8)*
C15	1.4732 (2)	0.3899 (3)	0.07414 (4)	0.0394 (5)
C16	1.5313 (2)	0.2955 (3)	0.09468 (4)	0.0396 (5)
C17	1.4917 (2)	0.1302 (3)	0.09979 (4)	0.0383 (5)
C18	1.3983 (3)	0.0148 (3)	0.08826 (4)	0.0462 (5)
H18	1.342170	0.039309	0.074057	0.064 (8)*
C19	1.3903 (4)	−0.1359 (3)	0.09820 (5)	0.0614 (7)
H19	1.327760	−0.213486	0.090633	0.071 (9)*
C20	1.4748 (5)	−0.1750 (4)	0.11958 (5)	0.0710 (9)
H20	1.467785	−0.278356	0.125807	0.094 (11)*
C21	1.5667 (4)	−0.0651 (4)	0.13138 (5)	0.0661 (8)
H21	1.622214	−0.091123	0.145572	0.097 (12)*

C22	1.5744 (3)	0.0886 (3)	0.12134 (4)	0.0487 (6)
C23	1.6341 (3)	0.3418 (3)	0.11298 (5)	0.0534 (6)
H23	1.679950	0.442841	0.114289	0.073 (9)*
C24	1.5707 (3)	0.5277 (3)	0.06510 (5)	0.0569 (7)
H24A	1.667158	0.535719	0.074549	0.156 (19)*
H24B	1.510208	0.624774	0.066728	0.18 (2)*
H24C	1.597308	0.511150	0.048203	0.121 (15)*
N1	1.2956 (2)	0.4223 (2)	0.04307 (3)	0.0462 (5)
N2	1.3383 (2)	0.3443 (2)	0.06501 (3)	0.0455 (5)
N3	1.6592 (3)	0.2208 (3)	0.12874 (4)	0.0609 (6)
H25	1.719109	0.225541	0.141506	0.074 (10)*
O1	0.9581 (2)	0.4039 (2)	0.06942 (3)	0.0527 (4)

Atomic displacement parameters (Å²)

	U^{11}	U^{22}	U^{33}	U^{12}	U^{13}	U^{23}
C1	0.0424 (11)	0.0314 (10)	0.0386 (10)	0.0004 (8)	−0.0045 (9)	0.0036 (8)
C2	0.0495 (12)	0.0335 (10)	0.0367 (10)	0.0004 (9)	−0.0053 (9)	0.0043 (8)
C3	0.0571 (15)	0.0570 (15)	0.0468 (12)	−0.0025 (11)	0.0007 (11)	0.0080 (11)
C4	0.085 (2)	0.0643 (17)	0.0427 (12)	−0.0019 (15)	0.0041 (13)	0.0151 (12)
C5	0.085 (2)	0.079 (2)	0.0462 (13)	0.0060 (17)	−0.0175 (14)	0.0186 (13)
C6	0.0621 (19)	0.136 (4)	0.0682 (18)	0.003 (2)	−0.0228 (16)	0.035 (2)
C7	0.0510 (15)	0.101 (2)	0.0540 (14)	−0.0045 (15)	−0.0100 (12)	0.0274 (15)
C8	0.0386 (10)	0.0359 (10)	0.0326 (8)	0.0017 (8)	−0.0067 (8)	0.0027 (8)
C9	0.0420 (11)	0.0354 (10)	0.0380 (9)	−0.0012 (8)	−0.0074 (9)	0.0031 (8)
C10	0.0533 (13)	0.0490 (13)	0.0433 (11)	−0.0057 (10)	−0.0038 (10)	0.0080 (10)
C11	0.0720 (18)	0.0547 (15)	0.0649 (15)	−0.0184 (14)	−0.0094 (14)	0.0209 (13)
C12	0.087 (2)	0.0362 (14)	0.098 (2)	−0.0104 (14)	−0.0130 (19)	0.0024 (15)
C13	0.090 (2)	0.0446 (15)	0.095 (2)	−0.0013 (15)	0.0128 (19)	−0.0203 (15)
C14	0.0642 (16)	0.0440 (13)	0.0614 (14)	−0.0059 (12)	0.0087 (13)	−0.0086 (11)
C15	0.0322 (10)	0.0393 (11)	0.0467 (10)	0.0002 (8)	−0.0004 (9)	0.0020 (9)
C16	0.0311 (10)	0.0456 (12)	0.0420 (10)	0.0012 (9)	−0.0029 (9)	0.0015 (9)
C17	0.0336 (10)	0.0460 (12)	0.0354 (9)	0.0072 (8)	0.0017 (8)	0.0040 (8)
C18	0.0480 (12)	0.0470 (12)	0.0437 (11)	−0.0002 (10)	0.0013 (9)	0.0032 (9)
C19	0.0777 (19)	0.0472 (14)	0.0593 (14)	−0.0006 (13)	0.0133 (14)	0.0079 (12)
C20	0.104 (3)	0.0494 (15)	0.0602 (15)	0.0214 (16)	0.0204 (17)	0.0186 (13)
C21	0.083 (2)	0.0711 (19)	0.0446 (13)	0.0318 (16)	0.0022 (13)	0.0160 (13)
C22	0.0447 (13)	0.0619 (15)	0.0395 (11)	0.0159 (11)	−0.0005 (9)	0.0034 (10)
C23	0.0412 (13)	0.0594 (15)	0.0597 (13)	−0.0011 (11)	−0.0118 (11)	−0.0079 (12)
C24	0.0482 (14)	0.0501 (14)	0.0723 (17)	−0.0120 (12)	0.0006 (13)	0.0104 (13)
N1	0.0433 (10)	0.0463 (11)	0.0489 (10)	−0.0053 (8)	−0.0090 (8)	0.0139 (9)
N2	0.0409 (10)	0.0468 (11)	0.0489 (10)	−0.0065 (8)	−0.0108 (8)	0.0144 (8)
N3	0.0518 (12)	0.0784 (16)	0.0525 (11)	0.0118 (11)	−0.0218 (10)	−0.0041 (11)
O1	0.0628 (11)	0.0440 (9)	0.0512 (9)	0.0070 (8)	0.0083 (8)	−0.0033 (7)

Geometric parameters (Å, º)

C1—N1	1.287 (3)	C13—H13	0.9300
C1—C2	1.474 (3)	C14—H14	0.9300
C1—C8	1.518 (3)	C15—N2	1.290 (3)
C2—C3	1.386 (3)	C15—C16	1.456 (3)
C2—C7	1.386 (4)	C15—C24	1.495 (3)
C3—C4	1.380 (3)	C16—C23	1.375 (3)
C3—H3	0.9300	C16—C17	1.448 (3)
C4—C5	1.365 (4)	C17—C18	1.392 (3)
C4—H4	0.9300	C17—C22	1.409 (3)
C5—C6	1.358 (4)	C18—C19	1.373 (3)
C5—H5	0.9300	C18—H18	0.9300
C6—C7	1.386 (4)	C19—C20	1.404 (4)
C6—H6	0.9300	C19—H19	0.9300
C7—H7	0.9300	C20—C21	1.360 (5)
C8—O1	1.214 (3)	C20—H20	0.9300
C8—C9	1.485 (3)	C21—C22	1.399 (4)
C9—C14	1.381 (3)	C21—H21	0.9300
C9—C10	1.386 (3)	C22—N3	1.373 (4)
C10—C11	1.387 (4)	C23—N3	1.345 (4)
C10—H10	0.9300	C23—H23	0.9300
C11—C12	1.367 (5)	C24—H24A	0.9600
C11—H11	0.9300	C24—H24B	0.9600
C12—C13	1.370 (5)	C24—H24C	0.9600
C12—H12	0.9300	N1—N2	1.411 (2)
C13—C14	1.391 (4)	N3—H25	0.8600
N1—C1—C2	120.7 (2)	C9—C14—H14	120.4
N1—C1—C8	121.11 (18)	C13—C14—H14	120.4
C2—C1—C8	118.00 (18)	N2—C15—C16	115.46 (19)
C3—C2—C7	118.1 (2)	N2—C15—C24	125.1 (2)
C3—C2—C1	121.7 (2)	C16—C15—C24	119.4 (2)
C7—C2—C1	120.2 (2)	C23—C16—C17	105.7 (2)
C4—C3—C2	120.7 (3)	C23—C16—C15	128.1 (2)
C4—C3—H3	119.7	C17—C16—C15	126.14 (19)
C2—C3—H3	119.7	C18—C17—C22	118.9 (2)
C5—C4—C3	120.5 (3)	C18—C17—C16	134.59 (19)
C5—C4—H4	119.8	C22—C17—C16	106.5 (2)
C3—C4—H4	119.8	C19—C18—C17	118.9 (2)
C6—C5—C4	119.6 (2)	C19—C18—H18	120.5
C6—C5—H5	120.2	C17—C18—H18	120.5
C4—C5—H5	120.2	C18—C19—C20	121.2 (3)
C5—C6—C7	120.9 (3)	C18—C19—H19	119.4
C5—C6—H6	119.6	C20—C19—H19	119.4
C7—C6—H6	119.6	C21—C20—C19	121.4 (3)
C6—C7—C2	120.2 (3)	C21—C20—H20	119.3
C6—C7—H7	119.9	C19—C20—H20	119.3

C2—C7—H7	119.9	C20—C21—C22	117.4 (2)
O1—C8—C9	122.0 (2)	C20—C21—H21	121.3
O1—C8—C1	117.96 (19)	C22—C21—H21	121.3
C9—C8—C1	120.03 (18)	N3—C22—C21	130.3 (2)
C14—C9—C10	120.3 (2)	N3—C22—C17	107.5 (2)
C14—C9—C8	121.2 (2)	C21—C22—C17	122.1 (3)
C10—C9—C8	118.4 (2)	N3—C23—C16	110.6 (2)
C9—C10—C11	119.5 (3)	N3—C23—H23	124.7
C9—C10—H10	120.2	C16—C23—H23	124.7
C11—C10—H10	120.2	C15—C24—H24A	109.5
C12—C11—C10	120.0 (3)	C15—C24—H24B	109.5
C12—C11—H11	120.0	H24A—C24—H24B	109.5
C10—C11—H11	120.0	C15—C24—H24C	109.5
C11—C12—C13	120.7 (2)	H24A—C24—H24C	109.5
C11—C12—H12	119.7	H24B—C24—H24C	109.5
C13—C12—H12	119.7	C1—N1—N2	111.51 (18)
C12—C13—C14	120.1 (3)	C15—N2—N1	114.44 (18)
C12—C13—H13	119.9	C23—N3—C22	109.6 (2)
C14—C13—H13	119.9	C23—N3—H25	125.2
C9—C14—C13	119.3 (3)	C22—N3—H25	125.2

Hydrogen-bond geometry (Å, º)

D—H···*A*	*D*—H	H···*A*	*D*···*A*	*D*—H···*A*
C18—H18···N2	0.93	2.60	3.074 (3)	112

\ (*Z*)-2-{(*E*)-[(1-Methyl-1*H*-indol-3-yl)\ methylidene]hydrazinylidene}-1,2-diphenylethanone (7-BMHMFI)

Crystal data

$C_{24}H_{19}N_3O$
$M_r = 365.42$
Monoclinic, $P2_1/c$
$a = 18.6779$ (6) Å
$b = 8.6694$ (3) Å
$c = 12.7956$ (4) Å
$\beta = 106.910$ (4)°
$V = 1982.36$ (12) Å^3
$Z = 4$
$F(000) = 768$
$D_x = 1.224$ Mg m^{-3}
Mo $K\alpha$ radiation, $\lambda = 0.71073$ Å
Cell parameters from 380 reflections
$\theta = 2.5$–26.0°
$\mu = 0.08$ mm^{-1}
$T = 293$ K
Block, yellow
0.33 × 0.28 × 0.25 mm

Data collection

Bruker SMART CCD area detector diffractometer
Radiation source: fine-focus sealed tube
Detector resolution: 10.11 pixels mm^{-1}
phi and ω scans
Absorption correction: multi-scan (SADABS; Bruker, 2000)
$T_{min} = 0.971$, $T_{max} = 0.987$
9410 measured reflections
3837 independent reflections
2964 reflections with $I > 2\sigma(I)$
$R_{int} = 0.021$
$\theta_{max} = 26.1°$, $\theta_{min} = 2.3°$
$h = -14 \rightarrow 22$
$k = -10 \rightarrow 10$
$l = -15 \rightarrow 15$

Refinement

Refinement on F^2
Least-squares matrix: full
$R[F^2 > 2\sigma(F^2)] = 0.045$
$wR(F^2) = 0.140$
$S = 1.03$
3837 reflections
274 parameters
0 restraints
Hydrogen site location: inferred from neighbouring sites
Only H-atom displacement parameters refined
$w = 1/[\sigma^2(F_o^2) + (0.0721P)^2 + 0.203P]$ where $P = (F_o^2 + 2F_c^2)/3$
$(\Delta/\sigma)_{max} < 0.001$
$\Delta\rho_{max} = 0.16$ e Å^{-3}
$\Delta\rho_{min} = -0.15$ e Å^{-3}
Extinction correction: SHELXL2016 (Sheldrick, 2015b), $Fc^*=kFc[1+0.001xFc^2\lambda^3/\sin(2\theta)]^{-1/4}$
Extinction coefficient: 0.0045 (13)

Special details

Geometry. All esds (except the esd in the dihedral angle between two l.s. planes) are estimated using the full covariance matrix. The cell esds are taken into account individually in the estimation of esds in distances, angles and torsion angles; correlations between esds in cell parameters are only used when they are defined by crystal symmetry. An approximate (isotropic) treatment of cell esds is used for estimating esds involving l.s. planes.

Refinement. Refinement of F^2 against ALL reflections. The weighted R-factor wR and goodness of fit S are based on F^2, conventional R-factors R are based on F, with F set to zero for negative F^2. The threshold expression of $F^2 > 2$sigma(F^2) is used only for calculating R-factors(gt) etc. and is not relevant to the choice of reflections for refinement. R-factors based on F^2 are statistically about twice as large as those based on F, and R- factors based on ALL data will be even larger.

Fractional atomic coordinates and isotropic or equivalent isotropic displacement parameters (Å²)

	x	*y*	*z*	U_{iso}*/U_{eq}
C1	0.80896 (9)	0.5549 (2)	0.27473 (14)	0.0584 (4)
C2	0.88286 (10)	0.6191 (2)	0.33323 (15)	0.0659 (4)
C3	0.89301 (12)	0.7045 (3)	0.42794 (18)	0.0837 (6)
H3	0.852945	0.720693	0.455994	0.075 (6)*
C4	0.96264 (15)	0.7658 (4)	0.4811 (2)	0.1081 (9)
H4	0.969070	0.823302	0.544526	0.120 (10)*
C5	1.02223 (14)	0.7419 (4)	0.4403 (3)	0.1200 (11)
H5	1.068774	0.784014	0.475643	0.125 (10)*
C6	1.01287 (14)	0.6567 (5)	0.3485 (3)	0.1234 (11)
H6	1.053354	0.639808	0.321499	0.134 (11)*
C7	0.94374 (11)	0.5945 (3)	0.2945 (2)	0.0953 (7)
H7	0.938221	0.535900	0.231818	0.099 (8)*
C8	0.79924 (9)	0.4658 (2)	0.16966 (14)	0.0603 (4)
C9	0.79785 (8)	0.2948 (2)	0.17403 (13)	0.0576 (4)
C10	0.77856 (11)	0.2110 (3)	0.07773 (17)	0.0757 (5)
H10	0.766790	0.261502	0.010761	0.083 (6)*
C11	0.77691 (13)	0.0510 (3)	0.0818 (2)	0.0955 (7)
H11	0.763005	−0.005355	0.017221	0.120 (9)*
C12	0.79548 (14)	−0.0243 (3)	0.1796 (3)	0.1008 (8)
H12	0.795084	−0.131493	0.181433	0.128 (10)*
C13	0.81477 (13)	0.0581 (3)	0.2755 (2)	0.0891 (6)
H13	0.827294	0.006791	0.342203	0.111 (9)*
C14	0.81552 (10)	0.2171 (2)	0.27258 (16)	0.0679 (5)
H14	0.828040	0.272649	0.337583	0.073 (6)*
C15	0.62962 (9)	0.54270 (18)	0.27528 (13)	0.0556 (4)

H15	0.635990	0.605392	0.336293	0.060 (5)*
C16	0.55620 (8)	0.48955 (17)	0.21907 (12)	0.0496 (3)
C17	0.53199 (9)	0.38820 (16)	0.12688 (12)	0.0487 (3)
C18	0.56873 (10)	0.29923 (18)	0.06710 (14)	0.0592 (4)
H18	0.620638	0.300348	0.083982	0.067 (5)*
C19	0.52650 (13)	0.2104 (2)	−0.01693 (15)	0.0733 (5)
H19	0.550354	0.149515	−0.056525	0.095 (7)*
C20	0.44874 (13)	0.2091 (2)	−0.04436 (15)	0.0771 (6)
H20	0.421868	0.148219	−0.102360	0.085 (6)*
C21	0.41058 (11)	0.2957 (2)	0.01205 (13)	0.0644 (4)
H21	0.358599	0.295302	−0.006658	0.068 (5)*
C22	0.45351 (9)	0.38363 (17)	0.09833 (12)	0.0522 (4)
C23	0.49247 (9)	0.53965 (19)	0.24184 (13)	0.0556 (4)
H23	0.491806	0.606454	0.298423	0.071 (5)*
C24	0.35385 (10)	0.5102 (3)	0.16663 (19)	0.0815 (6)
H24A	0.331755	0.419249	0.186891	0.139 (11)*
H24B	0.326182	0.540419	0.093916	0.117 (9)*
H24C	0.352681	0.592153	0.216577	0.136 (11)*
N1	0.75252 (8)	0.57812 (18)	0.31109 (12)	0.0640 (4)
N2	0.68730 (7)	0.50715 (17)	0.24473 (12)	0.0591 (3)
N3	0.43088 (7)	0.47817 (16)	0.17043 (11)	0.0557 (3)
O1	0.79386 (9)	0.53693 (19)	0.08597 (11)	0.0846 (4)

Atomic displacement parameters (Å²)

	U^{11}	U^{22}	U^{33}	U^{12}	U^{13}	U^{23}
C1	0.0518 (8)	0.0596 (9)	0.0633 (9)	0.0000 (7)	0.0160 (7)	0.0068 (7)
C2	0.0539 (9)	0.0692 (10)	0.0702 (10)	−0.0027 (8)	0.0113 (8)	0.0106 (9)
C3	0.0734 (12)	0.0917 (15)	0.0820 (13)	−0.0150 (11)	0.0162 (10)	−0.0051 (11)
C4	0.0916 (17)	0.123 (2)	0.0935 (17)	−0.0272 (16)	0.0017 (13)	−0.0131 (16)
C5	0.0637 (14)	0.161 (3)	0.119 (2)	−0.0317 (16)	0.0000 (14)	−0.005 (2)
C6	0.0605 (13)	0.184 (3)	0.125 (2)	−0.0248 (17)	0.0246 (14)	−0.014 (2)
C7	0.0583 (11)	0.132 (2)	0.0959 (16)	−0.0114 (12)	0.0230 (11)	−0.0120 (15)
C8	0.0471 (8)	0.0759 (11)	0.0583 (9)	0.0023 (7)	0.0157 (7)	0.0095 (8)
C9	0.0421 (7)	0.0717 (10)	0.0614 (9)	0.0081 (7)	0.0188 (7)	0.0002 (8)
C10	0.0638 (10)	0.0927 (14)	0.0693 (11)	0.0210 (10)	0.0173 (9)	−0.0073 (10)
C11	0.0848 (15)	0.0903 (16)	0.1062 (18)	0.0155 (12)	0.0196 (13)	−0.0320 (15)
C12	0.0933 (16)	0.0695 (14)	0.139 (2)	0.0118 (12)	0.0321 (16)	−0.0062 (15)
C13	0.0887 (15)	0.0769 (13)	0.1043 (17)	0.0142 (11)	0.0320 (13)	0.0206 (13)
C14	0.0649 (10)	0.0727 (11)	0.0673 (10)	0.0060 (8)	0.0213 (8)	0.0072 (9)
C15	0.0585 (9)	0.0524 (8)	0.0588 (9)	0.0006 (7)	0.0219 (7)	−0.0042 (7)
C16	0.0537 (8)	0.0460 (7)	0.0532 (8)	0.0023 (6)	0.0223 (6)	0.0026 (6)
C17	0.0581 (8)	0.0425 (7)	0.0503 (7)	0.0016 (6)	0.0236 (6)	0.0085 (6)
C18	0.0748 (11)	0.0516 (8)	0.0613 (9)	0.0005 (7)	0.0357 (8)	0.0007 (7)
C19	0.1042 (15)	0.0615 (10)	0.0650 (10)	−0.0013 (10)	0.0414 (11)	−0.0083 (8)
C20	0.1085 (16)	0.0655 (11)	0.0537 (9)	−0.0138 (10)	0.0180 (10)	−0.0076 (8)
C21	0.0688 (10)	0.0644 (10)	0.0560 (9)	−0.0103 (8)	0.0117 (8)	0.0086 (8)
C22	0.0611 (9)	0.0486 (8)	0.0486 (8)	0.0003 (6)	0.0187 (7)	0.0111 (6)

C23	0.0600 (9)	0.0555 (8)	0.0557 (8)	0.0047 (7)	0.0236 (7)	−0.0024 (7)
C24	0.0540 (10)	0.0998 (16)	0.0919 (14)	0.0166 (10)	0.0231 (10)	0.0061 (13)
N1	0.0530 (7)	0.0666 (9)	0.0714 (9)	−0.0037 (6)	0.0165 (6)	−0.0065 (7)
N2	0.0498 (7)	0.0627 (8)	0.0663 (8)	−0.0020 (6)	0.0191 (6)	−0.0072 (7)
N3	0.0515 (7)	0.0610 (8)	0.0575 (7)	0.0046 (6)	0.0206 (6)	0.0057 (6)
O1	0.0949 (10)	0.0924 (10)	0.0669 (8)	−0.0030 (8)	0.0239 (7)	0.0199 (7)

Geometric parameters (Å, º)

C1—N1	1.286 (2)	C13—H13	0.9300
C1—C2	1.474 (2)	C14—H14	0.9300
C1—C8	1.515 (2)	C15—N2	1.286 (2)
C2—C7	1.383 (3)	C15—C16	1.427 (2)
C2—C3	1.385 (3)	C15—H15	0.9300
C3—C4	1.386 (3)	C16—C23	1.376 (2)
C3—H3	0.9300	C16—C17	1.434 (2)
C4—C5	1.375 (4)	C17—C18	1.399 (2)
C4—H4	0.9300	C17—C22	1.404 (2)
C5—C6	1.355 (4)	C18—C19	1.371 (3)
C5—H5	0.9300	C18—H18	0.9300
C6—C7	1.384 (3)	C19—C20	1.392 (3)
C6—H6	0.9300	C19—H19	0.9300
C7—H7	0.9300	C20—C21	1.375 (3)
C8—O1	1.214 (2)	C20—H20	0.9300
C8—C9	1.483 (3)	C21—C22	1.389 (2)
C9—C14	1.382 (2)	C21—H21	0.9300
C9—C10	1.385 (3)	C22—N3	1.389 (2)
C10—C11	1.388 (3)	C23—N3	1.353 (2)
C10—H10	0.9300	C23—H23	0.9300
C11—C12	1.364 (4)	C24—N3	1.452 (2)
C11—H11	0.9300	C24—H24A	0.9600
C12—C13	1.374 (4)	C24—H24B	0.9600
C12—H12	0.9300	C24—H24C	0.9600
C13—C14	1.379 (3)	N1—N2	1.4077 (19)
N1—C1—C2	120.14 (17)	C13—C14—H14	119.7
N1—C1—C8	120.11 (15)	C9—C14—H14	119.7
C2—C1—C8	119.72 (15)	N2—C15—C16	122.45 (15)
C7—C2—C3	118.56 (19)	N2—C15—H15	118.8
C7—C2—C1	120.41 (19)	C16—C15—H15	118.8
C3—C2—C1	121.03 (18)	C23—C16—C15	123.72 (15)
C2—C3—C4	120.3 (2)	C23—C16—C17	106.40 (14)
C2—C3—H3	119.9	C15—C16—C17	129.73 (14)
C4—C3—H3	119.9	C18—C17—C22	118.90 (15)
C5—C4—C3	120.2 (3)	C18—C17—C16	134.43 (15)
C5—C4—H4	119.9	C22—C17—C16	106.66 (13)
C3—C4—H4	119.9	C19—C18—C17	118.49 (17)
C6—C5—C4	119.8 (2)	C19—C18—H18	120.8

C6—C5—H5	120.1	C17—C18—H18	120.8
C4—C5—H5	120.1	C18—C19—C20	121.50 (17)
C5—C6—C7	120.7 (3)	C18—C19—H19	119.2
C5—C6—H6	119.6	C20—C19—H19	119.2
C7—C6—H6	119.6	C21—C20—C19	121.71 (18)
C2—C7—C6	120.4 (3)	C21—C20—H20	119.1
C2—C7—H7	119.8	C19—C20—H20	119.1
C6—C7—H7	119.8	C20—C21—C22	116.71 (18)
O1—C8—C9	122.88 (17)	C20—C21—H21	121.6
O1—C8—C1	118.77 (18)	C22—C21—H21	121.6
C9—C8—C1	118.35 (14)	C21—C22—N3	129.45 (16)
C14—C9—C10	119.15 (19)	C21—C22—C17	122.67 (15)
C14—C9—C8	121.27 (16)	N3—C22—C17	107.87 (13)
C10—C9—C8	119.58 (17)	N3—C23—C16	110.52 (14)
C9—C10—C11	119.6 (2)	N3—C23—H23	124.7
C9—C10—H10	120.2	C16—C23—H23	124.7
C11—C10—H10	120.2	N3—C24—H24A	109.5
C12—C11—C10	120.7 (2)	N3—C24—H24B	109.5
C12—C11—H11	119.7	H24A—C24—H24B	109.5
C10—C11—H11	119.7	N3—C24—H24C	109.5
C11—C12—C13	120.1 (2)	H24A—C24—H24C	109.5
C11—C12—H12	120.0	H24B—C24—H24C	109.5
C13—C12—H12	120.0	C1—N1—N2	111.71 (15)
C12—C13—C14	119.8 (2)	C15—N2—N1	111.49 (14)
C12—C13—H13	120.1	C23—N3—C22	108.54 (13)
C14—C13—H13	120.1	C23—N3—C24	125.92 (16)
C13—C14—C9	120.7 (2)	C22—N3—C24	125.50 (16)

(*Z*)-2-{(*E*)-[(Naphthalen-1-yl)methylidene]hydrazinylidene}-1,2-diphenylethanone (8-BDHFN)

Crystal data

$C_{25}H_{18}N_2O$
M_r = 362.41
Monoclinic, $P2_1/c$
a = 17.2081 (13) Å
b = 9.4075 (8) Å
c = 11.9703 (9) Å
β = 94.814 (7)°
V = 1931.0 (3) Å^3
Z = 4
$F(000)$ = 760
D_x = 1.247 Mg m^{-3}
Mo $K\alpha$ radiation, λ = 0.71073 Å
Cell parameters from 380 reflections
θ = 2.5–26.0°
μ = 0.08 mm^{-1}
T = 293 K
Block, yellow
0.40 × 0.40 × 0.16 mm

Data collection

Bruker SMART CCD area detector diffractometer
Radiation source: fine-focus sealed tube
Detector resolution: 10.12 pixels mm^{-1}
phi and ω scans
Absorption correction: multi-scan (SADABS; Bruker, 2000)
T_{min} = 0.970, T_{max} = 0.989
10556 measured reflections
3396 independent reflections
1411 reflections with $I > 2\sigma(I)$
R_{int} = 0.078
θ_{max} = 25.0°, θ_{min} = 3.0°
h = −20→20
k = −11→10
l = −14→14

Refinement

Refinement on F^2
Least-squares matrix: full
$R[F^2 > 2\sigma(F^2)] = 0.052$
$wR(F^2) = 0.083$
$S = 0.87$
3396 reflections
272 parameters
0 restraints
Hydrogen site location: inferred from neighbouring sites
Only H-atom displacement parameters refined
$w = 1/[\sigma^2(F_o^2) + (0.0024P)^2]$ where $P = (F_o^2 + 2F_c^2)/3$
$(\Delta/\sigma)_{max} < 0.001$
$\Delta\rho_{max} = 0.14$ e Å^{-3}
$\Delta\rho_{min} = -0.14$ e Å^{-3}
Extinction correction: SHELXL2016 (Sheldrick, 2015b), $Fc^*=kFc[1+0.001xFc^2\lambda^3/\sin(2\theta)]^{-1/4}$
Extinction coefficient: 0.00135 (15)

Special details

Geometry. All esds (except the esd in the dihedral angle between two l.s. planes) are estimated using the full covariance matrix. The cell esds are taken into account individually in the estimation of esds in distances, angles and torsion angles; correlations between esds in cell parameters are only used when they are defined by crystal symmetry. An approximate (isotropic) treatment of cell esds is used for estimating esds involving l.s. planes.

Fractional atomic coordinates and isotropic or equivalent isotropic displacement parameters (Å^2)

	x	*y*	*z*	U_{iso}*/U_{eq}
C1	0.38170 (16)	0.3245 (3)	0.5324 (2)	0.0479 (7)
C2	0.45003 (16)	0.2405 (3)	0.5767 (2)	0.0492 (8)
C3	0.51422 (17)	0.2274 (3)	0.5158 (3)	0.0695 (10)
H3	0.515242	0.274493	0.447585	0.063 (9)*
C4	0.57683 (19)	0.1451 (4)	0.5553 (3)	0.0787 (11)
H4	0.619504	0.135979	0.513009	0.096 (12)*
C5	0.57676 (19)	0.0761 (4)	0.6569 (3)	0.0700 (10)
H5	0.619147	0.020890	0.683658	0.072 (10)*
C6	0.51344 (19)	0.0901 (3)	0.7175 (3)	0.0696 (10)
H6	0.512814	0.044390	0.786371	0.077 (10)*
C7	0.45071 (18)	0.1709 (3)	0.6779 (2)	0.0628 (9)
H7	0.407940	0.178794	0.720078	0.051 (8)*
C8	0.30593 (16)	0.3112 (3)	0.5892 (2)	0.0506 (8)
C9	0.24449 (15)	0.2118 (3)	0.5424 (2)	0.0471 (7)
C10	0.25215 (19)	0.1364 (3)	0.4446 (2)	0.0645 (9)
H10	0.296674	0.147167	0.406439	0.068 (10)*
C11	0.1942 (2)	0.0460 (4)	0.4042 (3)	0.0811 (11)
H11	0.199667	−0.004809	0.338738	0.075 (11)*
C12	0.1284 (2)	0.0298 (4)	0.4592 (4)	0.0904 (12)
H12	0.089288	−0.032034	0.431149	0.105 (14)*
C13	0.1199 (2)	0.1044 (4)	0.5554 (3)	0.0878 (12)
H13	0.074829	0.093934	0.592373	0.111 (13)*
C14	0.17771 (18)	0.1948 (4)	0.5978 (3)	0.0675 (10)
H14	0.171980	0.244559	0.663753	0.075 (11)*
C15	0.31775 (17)	0.5533 (3)	0.3302 (2)	0.0556 (8)
H15	0.366978	0.567807	0.305639	0.066 (9)*
C16	0.25293 (16)	0.6289 (3)	0.2709 (2)	0.0491 (8)
C17	0.27243 (19)	0.7208 (3)	0.1884 (2)	0.0634 (9)

H17	0.324544	0.731061	0.174771	0.042 (7)*
C18	0.2158 (2)	0.7989 (3)	0.1247 (3)	0.0724 (10)
H18	0.230588	0.860029	0.069249	0.075 (10)*
C19	0.1399 (2)	0.7866 (4)	0.1429 (3)	0.0739 (10)
H19	0.102806	0.839726	0.100082	0.099 (12)*
C20	0.11607 (19)	0.6942 (3)	0.2262 (2)	0.0578 (8)
C21	0.17273 (17)	0.6118 (3)	0.2911 (2)	0.0489 (8)
C22	0.14497 (17)	0.5146 (3)	0.3686 (2)	0.0534 (8)
H22	0.180386	0.457731	0.411164	0.053 (9)*
C23	0.06746 (18)	0.5025 (3)	0.3824 (2)	0.0632 (9)
H23	0.050872	0.437604	0.433924	0.039 (8)*
C24	0.0127 (2)	0.5861 (4)	0.3203 (3)	0.0771 (10)
H24	−0.039946	0.578124	0.331423	0.100 (12)*
C25	0.0365 (2)	0.6792 (4)	0.2435 (3)	0.0790 (11)
H25	−0.000333	0.733990	0.201654	0.074 (10)*
N1	0.38670 (13)	0.4055 (3)	0.44718 (19)	0.0589 (7)
N2	0.31309 (13)	0.4685 (3)	0.41351 (19)	0.0569 (7)
O1	0.29977 (11)	0.3808 (2)	0.67417 (16)	0.0753 (7)

Atomic displacement parameters (Å²)

	U^{11}	U^{22}	U^{33}	U^{12}	U^{13}	U^{23}
C1	0.0473 (18)	0.049 (2)	0.0467 (17)	0.0024 (16)	0.0003 (14)	−0.0007 (15)
C2	0.0482 (18)	0.055 (2)	0.0429 (18)	0.0022 (16)	−0.0030 (15)	0.0009 (15)
C3	0.061 (2)	0.090 (3)	0.059 (2)	0.013 (2)	0.0103 (18)	0.021 (2)
C4	0.051 (2)	0.104 (3)	0.081 (3)	0.019 (2)	0.012 (2)	0.013 (2)
C5	0.056 (2)	0.081 (3)	0.071 (2)	0.024 (2)	−0.0086 (18)	−0.002 (2)
C6	0.073 (2)	0.081 (3)	0.053 (2)	0.022 (2)	−0.0043 (18)	0.010 (2)
C7	0.062 (2)	0.074 (3)	0.0531 (19)	0.0133 (19)	0.0109 (18)	0.0073 (18)
C8	0.0479 (19)	0.056 (2)	0.0477 (17)	0.0112 (17)	0.0042 (15)	0.0088 (16)
C9	0.0436 (17)	0.046 (2)	0.0520 (18)	0.0033 (16)	0.0070 (14)	0.0075 (15)
C10	0.063 (2)	0.071 (3)	0.060 (2)	−0.009 (2)	0.0118 (19)	−0.0078 (18)
C11	0.084 (3)	0.078 (3)	0.079 (3)	−0.015 (2)	−0.003 (2)	−0.016 (2)
C12	0.074 (3)	0.093 (3)	0.101 (3)	−0.028 (3)	−0.010 (3)	0.020 (3)
C13	0.060 (3)	0.113 (4)	0.092 (3)	−0.011 (2)	0.013 (2)	0.020 (3)
C14	0.059 (2)	0.086 (3)	0.059 (2)	0.006 (2)	0.0130 (18)	0.007 (2)
C15	0.046 (2)	0.061 (2)	0.060 (2)	0.0003 (17)	0.0028 (16)	0.0022 (17)
C16	0.054 (2)	0.048 (2)	0.0447 (17)	0.0007 (17)	0.0011 (15)	−0.0002 (15)
C17	0.060 (2)	0.069 (3)	0.061 (2)	−0.0101 (19)	0.0059 (18)	0.0118 (18)
C18	0.094 (3)	0.059 (2)	0.062 (2)	−0.002 (2)	−0.008 (2)	0.0230 (19)
C19	0.077 (3)	0.068 (3)	0.074 (2)	0.007 (2)	−0.009 (2)	0.012 (2)
C20	0.066 (2)	0.049 (2)	0.057 (2)	0.0008 (19)	−0.0016 (17)	−0.0001 (17)
C21	0.059 (2)	0.045 (2)	0.0420 (17)	0.0005 (17)	−0.0022 (15)	0.0001 (15)
C22	0.054 (2)	0.057 (2)	0.0481 (18)	0.0011 (18)	−0.0054 (16)	0.0010 (17)
C23	0.062 (2)	0.064 (2)	0.064 (2)	−0.001 (2)	0.0039 (18)	0.0066 (19)
C24	0.055 (2)	0.082 (3)	0.094 (3)	0.006 (2)	0.003 (2)	0.006 (2)
C25	0.070 (3)	0.074 (3)	0.089 (3)	0.019 (2)	−0.011 (2)	0.020 (2)
N1	0.0497 (16)	0.0657 (19)	0.0605 (16)	0.0099 (14)	−0.0009 (13)	0.0128 (14)

N2	0.0538 (17)	0.0599 (19)	0.0564 (16)	0.0068 (14)	0.0019 (13)	0.0143 (13)
O1	0.0744 (16)	0.0946 (19)	0.0576 (13)	0.0072 (13)	0.0088 (11)	−0.0200 (13)

Geometric parameters (Å, º)

C1—N1	1.282 (3)	C13—H13	0.9300
C1—C2	1.478 (3)	C14—H14	0.9300
C1—C8	1.525 (3)	C15—N2	1.284 (3)
C2—C7	1.376 (3)	C15—C16	1.457 (3)
C2—C3	1.379 (3)	C15—H15	0.9300
C3—C4	1.378 (4)	C16—C17	1.374 (3)
C3—H3	0.9300	C16—C21	1.430 (3)
C4—C5	1.379 (4)	C17—C18	1.395 (4)
C4—H4	0.9300	C17—H17	0.9300
C5—C6	1.366 (4)	C18—C19	1.347 (4)
C5—H5	0.9300	C18—H18	0.9300
C6—C7	1.372 (3)	C19—C20	1.409 (4)
C6—H6	0.9300	C19—H19	0.9300
C7—H7	0.9300	C20—C25	1.409 (4)
C8—O1	1.221 (3)	C20—C21	1.424 (3)
C8—C9	1.486 (4)	C21—C22	1.414 (3)
C9—C10	1.384 (3)	C22—C23	1.362 (3)
C9—C14	1.384 (3)	C22—H22	0.9300
C10—C11	1.367 (4)	C23—C24	1.393 (4)
C10—H10	0.9300	C23—H23	0.9300
C11—C12	1.365 (4)	C24—C25	1.357 (4)
C11—H11	0.9300	C24—H24	0.9300
C12—C13	1.368 (4)	C25—H25	0.9300
C12—H12	0.9300	N1—N2	1.426 (3)
C13—C14	1.372 (4)		

N1—C1—C2	119.9 (3)	C13—C14—C9	120.0 (3)
N1—C1—C8	121.4 (3)	C13—C14—H14	120.0
C2—C1—C8	118.7 (2)	C9—C14—H14	120.0
C7—C2—C3	118.4 (3)	N2—C15—C16	125.9 (3)
C7—C2—C1	121.2 (3)	N2—C15—H15	117.0
C3—C2—C1	120.4 (3)	C16—C15—H15	117.0
C4—C3—C2	120.4 (3)	C17—C16—C21	119.3 (3)
C4—C3—H3	119.8	C17—C16—C15	115.7 (3)
C2—C3—H3	119.8	C21—C16—C15	124.9 (3)
C3—C4—C5	120.6 (3)	C16—C17—C18	121.5 (3)
C3—C4—H4	119.7	C16—C17—H17	119.3
C5—C4—H4	119.7	C18—C17—H17	119.3
C6—C5—C4	118.9 (3)	C19—C18—C17	120.6 (3)
C6—C5—H5	120.5	C19—C18—H18	119.7
C4—C5—H5	120.5	C17—C18—H18	119.7
C5—C6—C7	120.6 (3)	C18—C19—C20	120.7 (3)
C5—C6—H6	119.7	C18—C19—H19	119.6

C7—C6—H6	119.7	C20—C19—H19	119.6
C6—C7—C2	121.1 (3)	C25—C20—C19	120.6 (3)
C6—C7—H7	119.4	C25—C20—C21	119.6 (3)
C2—C7—H7	119.4	C19—C20—C21	119.7 (3)
O1—C8—C9	122.9 (3)	C22—C21—C20	117.2 (3)
O1—C8—C1	117.6 (3)	C22—C21—C16	124.6 (3)
C9—C8—C1	119.4 (3)	C20—C21—C16	118.2 (3)
C10—C9—C14	119.2 (3)	C23—C22—C21	121.4 (3)
C10—C9—C8	121.8 (3)	C23—C22—H22	119.3
C14—C9—C8	119.0 (3)	C21—C22—H22	119.3
C11—C10—C9	119.9 (3)	C22—C23—C24	120.9 (3)
C11—C10—H10	120.0	C22—C23—H23	119.5
C9—C10—H10	120.0	C24—C23—H23	119.5
C12—C11—C10	120.6 (4)	C25—C24—C23	119.8 (3)
C12—C11—H11	119.7	C25—C24—H24	120.1
C10—C11—H11	119.7	C23—C24—H24	120.1
C11—C12—C13	120.0 (4)	C24—C25—C20	121.1 (3)
C11—C12—H12	120.0	C24—C25—H25	119.5
C13—C12—H12	120.0	C20—C25—H25	119.5
C12—C13—C14	120.3 (4)	C1—N1—N2	110.8 (2)
C12—C13—H13	119.8	C15—N2—N1	111.5 (2)
C14—C13—H13	119.8		

Hydrogen-bond geometry (Å, º)

D—H···*A*	*D*—H	H···*A*	*D*···*A*	*D*—H···*A*
C5—H5···O1^{i}	0.93	2.49	3.355 (4)	156
C3—H3···N1	0.93	2.53	2.827 (4)	99
C14—H14···O1	0.93	2.54	2.826 (4)	98
C22—H22···N2	0.93	2.28	2.930 (4)	126

Symmetry code: (i) −*x*+1, *y*−1/2, −*z*+3/2.